POLITECNICO DI MILANO

Facoltà di Ingegneria Industriale

Corso di Laurea in
Ingegneria Meccanica

Energy Management of Hybrid Electric Vehicles:
A Comparison between Stochastic Dynamic Programming and Equivalent Consumption Minimisation Strategy

Relatore: Prof. Angelo ONORATI

Tesi di Laurea di:

Damiano BARDINI Matr. 765291

Anno Accademico 2012 – 2013

To all those who taught me
To all those who supported me
To all those who accompanied me

Abstract

The thesis deals with the issue of energy management in charge-sustaining hybrid electric vehicles, with the goal of indicating the best strategy for managing the power split in real-life conditions. Particular attention is dedicated to two local optimal energy management strategies: Stochastic Dynamic Programming (SDP) and Equivalent Consumption Minimisation Strategy (ECMS). The work draws a rigorous comparison between the two above-cited strategies, encompassing the classical aspect of fuel consumption and the more original aspect of vehicle driveability. From the comparison, SDP appears being the most appropriate energy management strategy for charge-sustaining hybrid electric vehicles by virtue of its close-to-optimal fuel consumption, of its robustness to additional constraints, and its particularly beneficial engine utilisation pattern.

Keywords: Driveability, Energy Management, Equivalent Consumption Minimisation Strategy, Hybrid Electric Vehicles, Pontryagin's Minimum Principle, Stochastic Dynamic Programming.

Sommario

La tesi tratta l'argomento della gestione dell'energia nei veicoli ibridi elettrici, con l'intento di indicare la strategia di controllo più appropriata per la gestione dell'energia in condizioni di guida realistiche. Particolare attenzione è data a due strategie di gestione dell'energia basate sull'ottimizzazione locale: la Programmazione Dinamica Stocastica (SDP) e la Strategia di Minimizzazione del Consumo Equivalente (ECMS). Il contributo principale del lavoro è costituito dalla comparazione rigorosa delle due strategie citate in precedenza, comparazione che include l'aspetto classico del consumo di carburante e l'aspetto, più originale, della guidabilità del veicolo. Dalla comparazione, la strategia SDP appare essere la soluzione più appropriata grazie ai consumi relativamente prossimi ai consumi ottimali, alla robustezza all'imposizione di vincoli relativi alla guidabilità del veicolo, ed al particolarmente favorevole profilo di utilizzo del motore termico del veicolo.

Parole chiave: Gestione dell'Energia, Guidabilità, Principio del Minimo di Pontryagin, Programmazione Dinamica Stocastica, Strategia di Minimizzazione del Consumo Equivalente, Veicoli Ibridi Elettrici.

L'autore intende indicare che un ampio estratto della tesi in italiano è presentato nell'Allegato 3.

Acknowledgments

This Master's thesis has been developed during my apprenticeship at IFP Energies nouvelles. I intend to thank the persons that offered me this great opportunity by deciding to sponsor my studies at IFP School. My gratitude especially goes to Dr. Thomas Leroy, my supervisor at IFP Energies nouvelles, and to Dr. Gilles Corde, head of the control department.
I also intend to thank Prof. Angelo Onorati, my thesis advisor, who has dutifully followed my work and has been most helpful any time I needed advice or information.
Finally, I would like to thank my alma mater, Politecnico di Milano, for providing me with a quality education and an international attitude, notwithstanding all the difficulties faced by Italian universities over the last few years.

Note to the reader

The thesis presents in detail a part of the analysis on energy management strategies carried out during my 12-months apprenticeship at IFP Energies nouvelles. In the context of the study, also a scientific article has been written and will be published later on this year. The reader interested in a more synthetic exposition of the study and of the principal results presented in the thesis is therefore addressed to the following publication:

D. Bardini and T. Leroy, "Impact of driveability constraints on local optimal energy management strategies for hybrid powertrains", *Proceedings of the 7th IFAC Symposium on Advances on Automotive Control (AAC)*, 2013.

Contents

List of Figures

List of Tables

Introduction

Concerns on fossil fuels availability in the long period and on man-induced climate modifications have raised a considerable attention on the problem of efficient fuel utilization in road transport in the last years. The issue is of particular relevance considering that vehicles, accounting for a significant part of oil consumption globally, are currently responsible of 20-25 % of CO_2 emissions into the atmosphere [1]. The situation is destined to become even more serious in the coming years, with projections of vehicles accounting for 30-50 % of global CO_2 emissions in 2050 [2].
The scientific community and the industry alike have been proposing a variety of innovations to face this challenge, coming up with new solutions in the aspects of internal combustion engine design, of alternative fuels, and of hybrid powertrain architectures.
When one considers passenger vehicles, promising results in terms of fuel economy, technical feasibility, and possibility of reaching the broad market have been obtained by hybrid electric powertrains. Such powertrains present an electric propulsion system alongside the propulsion system based on the internal combustion engine (ICE). Vehicles equipped with these powertrains are defined hybrid electric vehicles (HEV).

I.1 Why hybrid electric vehicles?

It is correct to state that the last generations of internal combustion engines equipped on passenger vehicles have reached quite satisfactory levels of peak efficiency. Spark-ignition engines, in fact, now present a peak thermal efficiency around 25 %, while compression-ignition engines reach values of peak thermal efficiency above 30 %. In this way, internal combustion engines are positioned relatively close in terms of peak efficiency to the other plants generating power from fossil fuels (notably, gas turbines and steam turbines) [3].
However, internal combustion engines equipped on vehicles seldom operate at their highest efficiency levels, located in the low engine speed and high torque area. This is due to the highly dynamic utilisation typical of road vehicles, where the vehicle speed and the torque request to the engine vary continuously and rapidly. Therefore, the on-road utilisation of the vehicle entails a significant

amount of time in which the torque requested to the engine is low, with engine efficiency values that can be lower than 10 %. The situation is worsened by the fact that engines are designed on the highest power request they need to meet, making them decidedly oversized for normal utilisation. The straightforward result is an unsatisfactory fuel consumption of the vehicle, ultimately causing significant CO_2 vehicle emissions.

Hybrid electric vehicles manage to address this issue by introducing in the powertrain an additional propulsion system, constituted in its simplest form by an electric energy storage unit, typically a battery, an electric torque actuator, and a device coupling the thermal and electric drivelines. The additional driveline allows for a greater flexibility in engine utilisation, while ensuring the fulfilment of the torque request at the wheels. In fact, in HEVs the torque request can be met by a variety of means: by the thermal propulsion system alone, by the electric propulsion system alone or by combining the torque produced by the two propulsion systems. This double-driveline architecture of the powertrain entails a series of advantages, explained in the remainder of the section.

The first, straightforward, advantage introduced by the hybrid powertrain lies in the possibility of downsizing the original internal combustion engine while keeping the maximum power output at the wheels unchanged. This is allowed by the capability of the hybrid powertrain to deliver power to the wheels from both the internal combustion engine and the motor at the same time. The main advantage brought by downsizing the engine is a significant reduction in fuel consumption, due to the higher average torque of the engine [4], [5].

Furthermore, with a hybrid powertrain it is possible to power the wheels through the electric propulsion system alone when the torque request at the wheels is low. Powertrain efficiency yielded in such cases is improved thanks to the lower sensitivity to the torque level presented by the efficiency of the electric propulsion system with respect to the thermal propulsion system. Conversely, when torque request is high, it is possible to normally use the thermal propulsion system, now working at a satisfactory efficiency level, to power the vehicle [6].

Including an electric driveline in the powertrain also permits a decoupling, partial or total according to the considered hybrid architecture, between the torque request at the wheels and the torque delivered by the thermal engine. In this way it is possible to run the engine at a torque level higher or lower than the torque needed to power the wheels, respectively storing or using some of the energy in the electric energy storage unit, which acts as an energy buffer. The

advantage in this lies in the possibility of choosing more freely the engine operating point, thus permitting to operate the engine on its optimal operating line (OOL) far more often than in the case of the pure thermal powertrain. Eventually, this yields a significant improvement in fuel consumption [7].
The advantages in fuel consumption introduced by HEVs are not limited to the improvement of engine efficiency. In fact, the introduction of the electric driveline also allows recovering part of the kinetic energy provided to the vehicle. When the torque at the wheels is negative, instead of using the dissipative brakes, it is possible to have the motor brake the vehicle by appropriately managing the motor magnetic field. Since electric motors can also operate as generator, the mechanical energy absorbed by the motor is thus transformed into electric energy and stored into the battery [8].
The last advantage in fuel consumption introduced by HEVs worth mentioning here is the Stop & Start feature, which is usually implemented effortlessly on hybrid powertrains by virtue of the powerful electric machines in the powertrain. Thanks to this feature, the engine is shut down when the vehicle is standing still and, afterwards, when the driver intends to take off, it is either turned back on or substituted by the electric motor for meeting the acceleration request. In this way, idle fuel consumption of the vehicle is practically reduced to zero [9].

Aside from the advantages in fuel consumption presented above, HEVs present also a few advantages in terms of functionality with respect to the pure thermal vehicles, thanks to the wider range of features of the powertrain.
The first to be mentioned is the possibility of cranking the engine with the motor, which allows the removal of the starter motor from the powertrain. The new cranking procedure is generally an improvement over the usual cranking process, for two reasons. First off, the electric motor in HEVs is characterised by a higher voltage with respect to the starter motor of a conventional vehicle, thus allowing a faster and smoother engine cranking. Secondly, the introduction of the electric motor usually enables the possibility of employing some improved cranking techniques, most notably the inertia cranking [10].
It is also important to highlight that the addition of a fast actuator, such as the electric motor, to the powertrain introduces a new range of opportunities to provide the driver with improved driving comfort. An immediate example of this is found in hybrid vehicles equipped with an automated manual transmission (AMT). In fact, such transmission is characterised by a torque gap

during gear shifts because at some point no gear is engaged. This torque gap is not expected by the driver and, consequently, it constitutes a nuisance in the driving experience. The hybridisation of the powertrain solves the issue: the electric motor is, in fact, able to compensate the torque gap due to gear shift, providing in this way a perfectly smooth ride [11].

The advantages exposed above obviously do not come at no cost. In fact, the hybridisation entails a significant complication in the architecture of the powertrain, which becomes bigger and more articulated. As a result, the design process takes longer and is more costly, the powertrain includes more components and its production cost is higher, and the fitting of the powertrain into the vehicle becomes tighter.
In addition, the complicated powertrain architecture requires a more articulated control strategy. In fact, the control system of the powertrain now needs to address also the power split between the thermal and the electric drivelines, an issue that is not present in purely thermal powertrains. The power repartition in the powertrain greatly affects the fuel economy of the vehicle and constitutes the central subject of the study.

I.2 The energy management problem in HEVs

As stated above, hybridisation of the powertrain poses new challenges in terms of control of the system. In fact, aside from presenting additional components to be controlled (electric motor, power electronics, electric storage unit), the hybrid powertrain also introduces the problem of energy management. Now the power request at the wheels can be fulfilled by either of the two drivelines, or by a combination of the two. A question promptly arises: which of the possible operating modes is the most convenient?
There exist some cases where the answer to the problem is pretty straightforward. For instance it is clear that, while braking, the focus of the strategy ought to be on maximizing the recovered energy in the battery, thus braking the vehicle with the motor alone. However, simple solutions prove inefficient in general utilisation of the vehicle, which requires a deeper and more rigorous analysis.
The first step in the definition of the energy management strategy lies in identifying the objectives of the hybrid powertrain. The classic objective, and

the first reason for hybridising the vehicle, is the reduction of fuel consumption. However, a variety of aspects, such as minimisation of pollutants emissions and vehicle driving comfort, can also be taken into account for the definition of the strategy. As a result, the general approach of energy management strategies consists in the minimisation of a cost function, encompassing fuel consumption and all other aspects relevant to the particular case. Considering that there exist several methods for carrying out this minimisation, different energy management strategies are yielded.

Another aspect of great relevance in the definition of the energy management strategy lies in the control of the state of charge (SOC) of the battery of the electric driveline. This control needs to take care of two aspects. First off, it is required to constantly keep the battery SOC within prescribed boundaries, in order to ensure the battery's correct and prolonged functioning [12]. Secondly, the control strategy needs to ensure the most appropriate and convenient exploitation of the energy stored in the battery. In order to expand on this aspect, it is necessary to present the two configurations that hybrid electric vehicles can assume. In the first, named charge-sustaining hybrid and usually indicated with the acronym HEV, all the energy delivered to the wheels is produced in the internal combustion engine. The battery can be recharged only by the engine or by regenerative braking and merely acts as an energy buffer. On the contrary, plug-in hybrid electric vehicles (PHEV) incorporate also the possibility of recharging the battery through the electric grid. Hence, the energy delivered to the wheels originates either from the engine or from the electric grid, with the battery doubling in function as energy buffer and energy reservoir. Given the diversities in the two hybrid configurations, the energy management needs to adapt the control on the SOC to the appropriate case. In fact, in charge-sustaining hybrids, the control strategy needs to ensure that the SOC level when the key is turned off is sufficient for permitting utilisation of the electric driveline at next key-on. Conversely, in plug-in hybrids, the strategy is generally aimed at depleting the battery almost completely before the vehicle is connected to the electric grid for recharging.

Synthesizing the concepts expressed above, the energy management problem consists in the minimisation of a cost function while ensuring a given guidance to the SOC level. This is a classical constrained optimisation problem, a well-

known problem in the optimal control domain that can be solved with several approaches.
This treatise intends to present the most common of such approaches and to draw a comparison between the viable options for charge-sustaining vehicles, proposing in this way what is thought to be the most suitable energy management strategy for today's hybrid vehicles. The analysis assumes an even greater significance when one considers, as it will be shown later on in the work, that the energy management strategies currently equipped on hybrid powertrains present several shortcomings, hampering the diffusion of hybrid vehicles.
As a consequence, the ultimate goal of the study is to identify an energy management strategy that is able to yield satisfactory results in terms of fuel consumption, that manages the SOC level in an appropriate fashion, that can be implemented on an actual vehicle, and that is compatible with the requirements of the mass market.

I.3 Organisation of the study

The thesis proposes to analyse the problem presented above with the following organisation:

- In Chapter 1, the considered vehicle for the study is presented and its most important specifications are detailed. Then, the models for the vehicle dynamics and for the vehicle components are explained and validated. In the last part of the chapter, the sample of driving cycles employed for the analysis is discussed;

- In Chapter 2, the theoretical basis of the study is illustrated. The goal and the positioning of the energy manager in the system are explained and the energy management problem is defined in rigorous terms. Then, the energy management strategies aimed at solving the problem are presented and classified according to their characteristics. A brief explanation of the theory underlying each strategy is provided and strategies' advantages and disadvantages are discussed;

- In Chapter 3, the focus is shifted on the local optimal energy management strategies, which are the most appropriate solution for the

considered energy management problem. The calibration procedure of these strategies is explained and the impact of the calibration parameters is illustrated. Then, simulation results are presented and a few conclusions regarding strategies' fuel economy are drawn. The chapter is concluded by a justification of simulation results by means of a powertrain efficiency analysis;

- In Chapter 4, the issue of vehicle driveability is introduced and its impact on energy management strategies is discussed. A few driveability parameters are presented in order of importance and their effect on simulation results is illustrated. The most important driveability aspects that are discussed are 3: the minimum dwell time, the engine utilisation, and the engine noise. Then, a conclusion regarding the driveability performance of the local optimal strategies is drawn;

- In Chapter 5, the study is concluded and the most appropriate energy management strategy is suggested. The chapter presents a summary of the study, a conclusion pointing out the reasons that back the choice of the most appropriate strategy, and the future perspectives of research in the field.

Chapter 1

Vehicle specifications and modelling

The conclusions in the study were obtained by means of simulation on the Matlab platform. It is therefore good practice to present a few relevant details about the vehicle, its modelling, and the simulation procedure.

1.1 Vehicle architecture and components

The considered vehicle for the study is a Renault Scenic. The powertrain consists of a parallel hybrid electric powertrain. There are two drivelines to the wheels: the first is the conventional thermal driveline, constituted by the engine, the clutch, the gearbox, and the differential. The second is the electric driveline, constituted by the battery, the power electronics, the electric motor, a fixed coupling gearing, and the differential. The two drivelines are disposed in parallel and are connected by means of a coupling gearing. Thanks to this disposition, a range of functioning modes is available: the power request at the wheels can be fulfilled by the thermal driveline alone, by the electric driveline alone, or jointly by the two drivelines, splitting the power demand between them.
A scheme of the powertrain architecture is reported in Figure 1.1 below.

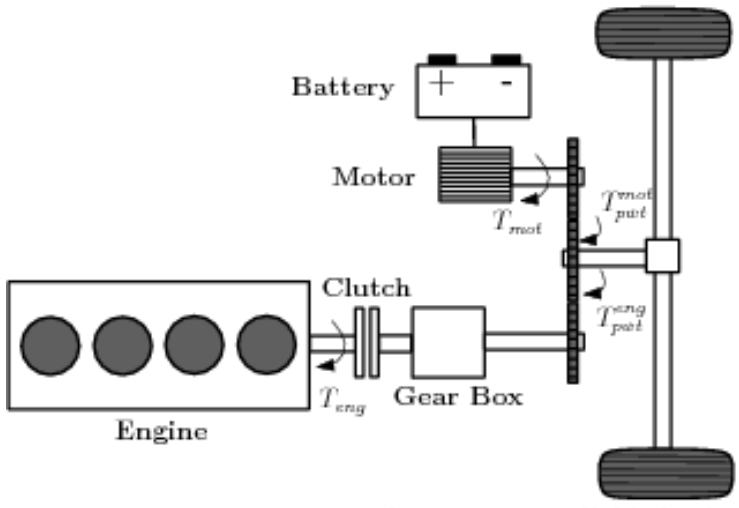

Figure 1.1 – Powertrain architecture (parallel hybrid)

As the coupling between the electric driveline and the thermal driveline is realized after the gearbox, the architecture is more specifically identified as double shaft parallel hybrid or, equivalently, post-transmission parallel hybrid [13]. The coupling device is a fixed gearing, which transfers the torque from the motor shaft to the shaft exiting from the gearbox. Such a coupling implies that the torque delivered to the wheels is simply the sum of the torque produced by the engine and the torque produced by the motor, multiplied times the transmission ratio and the transmission efficiency of the respective path to the wheels.
The engine delivers power to the wheels via the 6 gears automated manual transmission and the differential. The motor is connected to the wheels via the fixed ratio gearing and the differential. The engine can be disconnected from the wheels by means of the clutch interposed between the engine itself and the gearbox. Conversely, the motor is connected to the wheels at all times, being there no decoupling device on its path to the wheels.
The vehicle is equipped with a four-cylinder, 2.0 L turbocharged spark ignited engine (model Renault F4Rt), delivering a peak power of 150 kW at 5000 rpm. The electric machine is a 42 kW electric motor.
The basic vehicle information is summarized in Table 1.1 below. Extended vehicle and powertrain specifications can be found in Annex 1.

Table 1.1 – Vehicle information

Engine	4 cylinders, 2.0 L, 150 kW / 5000 rpm
Motor	42 kW
Transmission	Automated manual transmission
Battery	NiMH, 5 Ah
Vehicle mass	1930 kg

It is important to stress the limited capacity of the battery, 5 Ah. In reality, the exploitable capacity of the battery is even lower, considering that the manufacturer suggests employing the battery only in the range of state of charge comprised between 30 % and 70 %, for battery durability and efficiency reasons. Such a limited battery capacity enables the fully electric propulsion of the vehicle only for very limited periods of time, covering at most a few kilometres at low speeds.
Finally, it is noteworthy to highlight that the vehicle is a charge-sustaining hybrid and, therefore, does not present any possibility of recharging the battery through the electric grid. Moreover, it is possible to add that the dimensioning of the powertrain components is the one characteristic of charge-sustaining hybrids. In fact, the powertrain presents a small, low-capacity battery, a relatively powerful engine and a low hybridisation ratio. This last parameter is

defined as the ratio of the motor power over the total powertrain power [14], as in (1.1) below:

$$HR = \frac{P_{mot,max}}{P_{pwt,max}} \tag{1.1}$$

where $P_{mot,max}$ is the peak power of the motor and $P_{pwt,max}$ is the peak power of the whole powertrain. The hybridisation ratio for the considered powertrain is 0.22, a usual value for charge-sustaining hybrids[1]. As a result, the conclusions drawn in the study can be generalised to the great majority of charge-sustaining parallel hybrids.

1.2 Powertrain modelling

The model consists of a backward model [15], taking as input the speed profile of a given driving cycle and simulating the powertrain behaviour along it. There are several model outputs of interest in the study: SOC trajectory, engine state pattern, engine utilisation points, etc. However, the most significant model output is the integral fuel consumption of the vehicle along the cycle.
Additionally, it is relevant to highlight that the model neglects transient operation of the powertrain, splitting the driving cycle into samples of 1 second each along which the speed and acceleration are considered to be constant.

The section intends to synthetically present the model employed in the study and is structured as follows. First, vehicle operation is analysed in terms of energy, drawing an energy balance. Then, the focus is shifted on the powertrain components, whose models are illustrated. Finally, the model validation process is explained.
For a more systematic analysis on hybrid powertrain modelling, the reader is invited to refer to [16].

1.2.1 Vehicle energy balance

The first step in the analysis consists in defining the vehicle mass. In the simplest approach, the vehicle is considered as a point mass and only its static mass is taken into account. In the study, a more refined approach is followed, employing an equivalent mass that takes into account also the inertia of rotating

[1] For comparison, the last generation of Toyota Prius presents a hybridisation ratio of 0.27, while the Honda Civic Hybrid presents a hybridisation ratio of 0.21.

parts of the vehicle, most prominently the wheels. The equivalent mass of the vehicle is then expressed as

$$m_{eq} = m + 4 \cdot \frac{J_{wheel}}{{r_{wheel}}^2} \tag{1.2}$$

where m is the static mass of the vehicle, J_{wheel} is the moment of inertia of each wheel, and r_{wheel} is the wheel radius.
It is then possible to write the equilibrium of forces of the vehicle

$$m_{eq} \cdot \frac{dv}{dt} = F_{inertia} = F_{traction} - F_{aero} - F_{rolling} - F_{slope} \tag{1.3}$$

where v is the vehicle speed, $F_{inertia}$ the inertia force needed to accelerate or decelerate the vehicle, $F_{traction}$ the force produced (or absorbed) by the powertrain that is delivered to the wheel, F_{aero} the aerodynamic resistive force, $F_{rolling}$ the rolling friction resistive force, and F_{slope} the force due to the slope of the road. The forces F_{aero} and $F_{rolling}$ are necessarily positive, being resistive forces and opposing the movement in any direction. On the contrary, the other forces in the equation can either be positive or negative. $F_{inertia}$ is positive when the vehicle is accelerating and negative when the vehicle is decelerating. $F_{traction}$ is positive when the powertrain is providing power to the wheels and negative when the powertrain is absorbing power from the wheels[2]. F_{slope} is positive when the vehicle is moving uphill, negative when the vehicle is moving downhill.
The aerodynamic resistive force F_{aero} is modelled as

$$F_{aero} = \frac{1}{2} \cdot \rho_{air} \cdot A_f \cdot c_d \cdot v^2 \tag{1.4}$$

ρ_{air} being the air density, A_f being the vehicle frontal area, and c_d being the aerodynamic drag coefficient, a parameter that expresses the aerodynamic efficiency of the vehicle design.
The employed model of the rolling resistive force $F_{rolling}$ is

$$F_{rolling} = f_r\left(v, p_{tyre,} \dots\right) \cdot m \cdot g \cdot cos(\vartheta) \tag{1.5}$$

where g is the gravity acceleration and ϑ is the slope of the road. Parameter f_r is the rolling friction coefficient, which is recognized to depend on many

[2] An example of powertrain absorbing power from the wheels is during fuel cut-off in a purely thermal powertrain or during regenerative braking in a purely electric powertrain.

parameters of the vehicle, among which the vehicle speed, the tyres pressure p_{tyre}, and the road condition. An experimental characterization of the rolling friction coefficient f_r is presented in Figure 1.2 below.

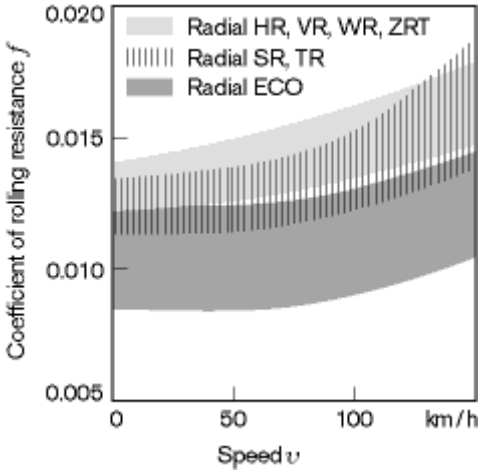

Figure 1.2 – Impact of speed on the rolling friction coefficient for different tyres typologies [17]

In order to represent the dependence of the tyres rolling friction coefficient on vehicle speed, in this study f_r is modelled as

$$f_r = f_{r,1} + f_{r,2} \cdot v \tag{1.6}$$

$f_{r,1}$ and $f_{r,2}$ being two coefficients provided by the manufacturer.
Moving back to the description of forces in (1.3), the slope force F_{slope} is the horizontal component of vehicle weight

$$F_{slope} = m \cdot g \cdot sin(\vartheta) \tag{1.7}$$

For a better comprehension of the backward model employed in the study, it is helpful to rearrange (1.3) as follows

$$F_{traction} = F_{inertia} + F_{aero} + F_{rolling} + F_{slope} \tag{1.8}$$

All terms on the right hand side of equation (1.8) are known once the vehicle characteristics, the road slope and the speed of the vehicle are known. Therefore, provided that the speed profile of the considered driving cycle and the road slope are inputs to the model, the force $F_{traction}$ required to move the vehicle can be computed at all times along the driving cycle.

Nevertheless, the required traction force does not represent a straightforward request for the powertrain, which instead outputs torque. It is then necessary to convert $F_{traction}$ into torque

$$T_{pwt} = F_{traction} \cdot r_{wheel} \tag{1.9}$$

where T_{pwt} is the torque delivered to the wheels. As a result, T_{pwt} is known once the speed of the vehicle and the road slope are known. Hence, T_{pwt} constitutes an input to the energy management strategy, which must ensure that the torque produced in the powertrain is able to satisfy the torque request at the wheel[3].

Moving back to the equilibrium of forces of the vehicle, it is possible to show that the equality holds also for powers. In fact, multiplying all the terms in (1.8) times the vehicle speed v yields

$$P_{traction} = P_{inertia} + P_{aero} + P_{rolling} + P_{slope} \tag{1.10}$$

where the forces of (1.8) have become the equivalent power terms. Integrating (1.10) over the duration of the driving cycle, the energy balance equation is derived

$$E_{traction} = E_{kinetic} + E_{aero} + E_{rolling} + E_{potential} \tag{1.11}$$

Note that the integral of the inertial power $P_{inertia}$ is, by definition, the kinetic energy $E_{kinetic}$ and the integral of the power due to the road slope P_{slope} is, by definition, the potential energy $E_{potential}$.

Grouping the energy term given by the aerodynamic resistance and the term given by the rolling resistance into the energy term $E_{resistive}$, as follows

$$E_{resistive} = E_{aero} + E_{rolling} \tag{1.12}$$

the energy balance can be rewritten as in (1.13)

$$E_{traction} = E_{kinetic} + E_{resistive} + E_{potential} \tag{1.13}$$

[3] The situation here described applies to the simulation case, where the vehicle speed profile is known. As for reality, the situation is different. In fact, the driver adjusts the vehicle speed by acting on the accelerator pedal. A cartography translates the pedal position into the torque request at the wheel, whose value is then passed on to the energy management strategy.

The conclusion that can be drawn from (1.13) is, essentially, that the energy produced by the powertrain ($E_{traction}$) is used in three ways: to accelerate the vehicle ($E_{kinetic}$), to win the resistive forces ($E_{resistive}$), and to win the gravity force ($E_{potential}$).
The energy $E_{resistive}$, used to win the resistive forces, is dissipated, being the aerodynamic force and the rolling friction force non conservative. Conversely, gravity is a conservative force, thus the potential energy $E_{potential}$ is recuperated by the vehicle when moving downhill.
As for the kinetic energy $E_{kinetic}$, the matter is less straightforward. The powertrain, in order to accelerate the vehicle, provides it with kinetic energy. Part of this energy is used to win the resistive forces and to win the gravity force; nevertheless, another part of this energy has to be dissipated by the mechanical brakes in order to brake the vehicle when the driver requests it. As a result, in conventional powertrains only a limited part of the kinetic energy is conserved in the form of potential energy, the rest being dissipated by resistive forces and by the mechanical brakes. On the contrary, in hybrid powertrains, the quantity of kinetic energy that is conserved is higher, thanks to the possibility of braking the engine with the motor, producing in this way electric energy that is stored in the battery (regenerative braking function, which was presented in the Introduction).

1.2.2 Powertrain components

WHEELS AND MECHANICAL BRAKES

The wheels constitute the connection between the vehicle and the road, delivering the torque produced by the powertrain to the ground.
Here the wheels are modelled as perfectly rigid elements, of non-negligible dimensions and possessing a non-negligible moment of inertia. Furthermore, the wheels are assumed to function in perfect rolling conditions, meaning that all the torque provided to the drive axle is delivered to the road.
The rotating speed of the wheels (and, consequently, of the drive axle) is linked to the vehicle speed, according to the straightforward relationship

$$\omega_{wheel} = \frac{v}{r_{wheel}} \tag{1.14}$$

The mechanical brakes are simply modelled by means of the negative torque they provide to the wheels, T_{brake}. This value is smaller or equal than zero at all times and is limited to a finite value, as in (1.15)

$$T_{brake,limit} \leq T_{brake} \leq 0 \tag{1.15}$$

where $T_{brake,limit}$ is the maximum braking torque of the mechanical brakes.
It is now possible to write the equilibrium of the torques at the wheel, valid at all times:

$$T_{pwt} = T_{pwt}^{eng} + T_{pwt}^{mot} + T_{brake} \tag{1.16}$$

where T_{pwt}^{eng} and T_{pwt}^{mot} are the torque delivered to the wheels by the engine and by the motor, respectively. The torque equilibrium above highlights how there are only three organs in the vehicle capable of determining the torque delivered to the wheels: the engine, the motor, and the brakes.
In Paragraph 1.2.1, it was explained how the torque at the wheels T_{pwt}, first introduced in (1.9), constitutes an input to the energy management strategy. Equation (1.16) gives a hint about the primary task of the energy management strategy: selecting the values of T_{pwt}^{eng}, T_{pwt}^{mot}, and T_{brake} so that the request at the wheels T_{pwt} is fulfilled.

GEARINGS

The torque needed at the wheel from the engine and from the motor, defined in (1.16), and the drive axle rotating speed, defined in (1.14), are propagated to the prime movers through the gearings on the driveline.
The gearings are modelled through the lossy model presented in (1.17):

$$\begin{cases} \omega_{out} = \dfrac{\omega_{in}}{i_g} \\ T_{out} = \eta_g \cdot i_g \cdot T_{in} \end{cases} \tag{1.17}$$

where ω_{in} and ω_{out} are the rotating speeds on the input and output shafts, T_{in} and T_{out} are the input and output torques to the gearing, r_g is the reduction ratio of the gearing, and η_g is its efficiency. The input shaft is identified as the one delivering power, expressed in the following terms:

$$P_{in} = T_{in} \cdot \omega_{in} > 0 \tag{1.18}$$

P_{in} being the power of the input shaft.
In (1.17), the ratio of input and output speeds is fixed by the kinematic constraint imposed by the gears coupling. Consequently, the whole power loss is accounted for in the torque relation.

TRANSMISSIONS

There are three transmissions in the vehicle architecture presented in Figure 1.1: two fixed ratio transmissions, the differential and the transmission connecting the electric driveline with the thermal driveline, and a variable ratio transmission, the gearbox.
The fixed ratio transmissions are modelled as in (1.17).
Also the gearbox model follows (1.17), with the difference of being able to switch dynamically the values of the reduction ratio i_g and of the efficiency η_g. Consequently, there are six values of i_g and six values of η_g, reproducing the six gears of the transmission, as in (1.19):

$$\begin{cases} \omega_{out,m} = \dfrac{\omega_{in}}{i_{g,m}} \\ T_{out,m} = \eta_{g,m} \cdot i_{g,m} \cdot T_{in} \end{cases} \tag{1.19}$$

m being the considered gear number, comprised between 1 and 6.
According to the current gear engaged, the corresponding value of ω_{out} and T_{out} is used.

In the study, the gear shift law is imposed through the same heuristic rule for all strategies. This was done with the idea in mind of carrying out a fair comparison between the different energy management strategies. In fact, in this way, the differences in the results will be due only to the different power split operated by the strategies, and not to a different gear shift pattern.
The heuristic rule used for managing the gearshifts is illustrated in Annex 2.

INTERNAL COMBUSTION ENGINE

As previously stated, the internal combustion engine considered in the study is the Renault F4Rt, a four-cylinder, turbocharged spark-ignited engine characterised by a displacement of 2.0 L and a peak power of 150 kW.

The inputs to the model of the engine, for each time step in the driving cycle, are the rotating speed of the engine and the torque request to the engine. The rotating speed of the engine is defined once the vehicle speed and the engaged gear at the considered time step are known, as demonstrated by (1.14) and (1.19). The torque request to the engine is, instead, the output of the energy management strategy. The output of the model of the engine is the fuel flow, which is then used to compute the integral fuel consumption along the driving cycle.
The internal combustion engine is modelled through the map presented in Figure 1.3, defining for each value of torque and rotating speed the fuel flow into the engine. It is important to highlight how the considered map is defined for steady-state operating conditions, while fuel consumption for transient operation of the engine is not considered. The map was obtained through experimental characterisation of the engine at the test bench.

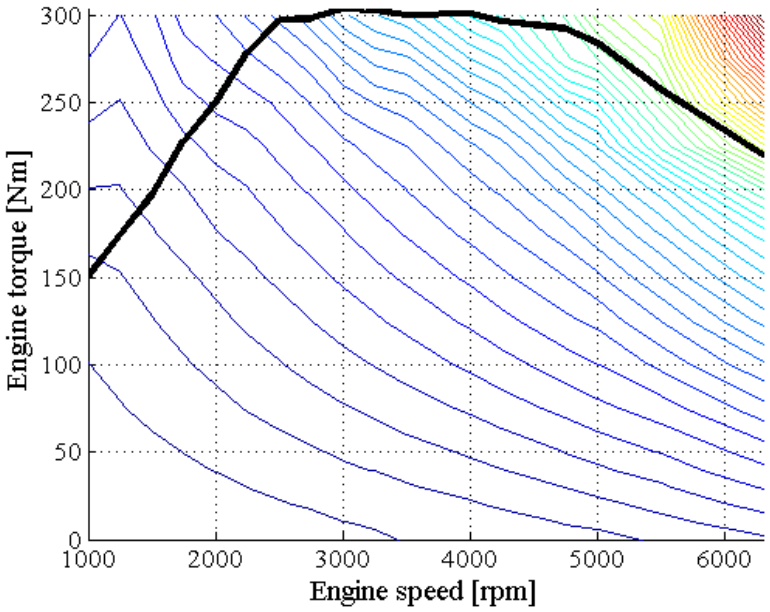

Figure 1.3 – Fuel flow map of the internal combustion engine

The map in Figure 1.3 is presented without scale for obvious confidentiality reasons. Anyway, fuel flow is the lowest where the line is blue, in the bottom-left area, and the highest where the line is red, in the top-right area. The engine torque limit is represented by the bold black line.
This map constitutes a key element in the powertrain model but does not help to understand how efficiently the engine is being operated. In order to better interpret the choices made by the energy management strategy, the map of brake specific fuel consumption (BSFC) is derived. BSFC is defined as the ratio

between the fuel flow and the brake power of the engine, i.e. the power provided by the engine on the wheel axle:

$$BSFC = \frac{Q_{fuel}}{P_b} \tag{1.20}$$

with Q_{fuel} the fuel flow into the engine and P_b the brake power of the engine.
The interest for BSFC primarily lies in its inverse proportionality to fuel conversion efficiency (also referred to as overall engine efficiency). In fact, it is possible to prove [18] that (1.20) can be rearranged as follows

$$BSFC = \frac{1}{\eta_f \cdot LHV} \tag{1.21}$$

with η_f being the fuel conversion efficiency and LHV the lower heating value of the fuel.
Thanks to its inverse relationship to the fuel conversion efficiency, the BMEP map presented in Figure 1.4 consists of an immediate visual aid for understanding how efficiently the engine is operating. Therefore, the BSFC maps is of great help for explaining the decisions of the energy management strategies.

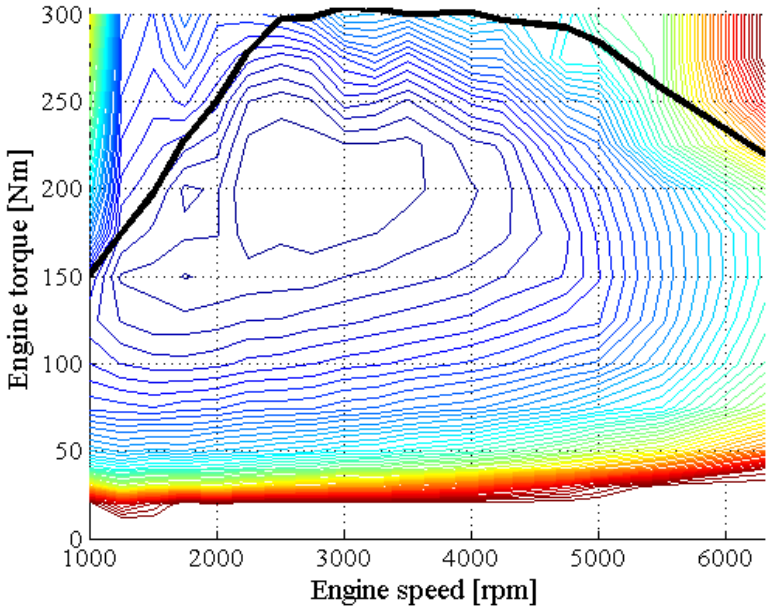

Figure 1.4 – Brake specific fuel consumption map of the internal combustion engine

Also in this map the scale of values is not presented for confidentiality reasons. However, the highest efficiency area is located in correspondence of the lowest BSFC area, pictured in blue and corresponding to low speed and high torque values. Conversely, the lowest efficiency area is located in correspondence of the highest BSFC area, pictured in red and corresponding to the low torque utilisation of the engine.
In addition, it is worth mentioning how the limits in engine torque were enforced in the model. At any instant of time, the torque request to the engine is checked against the maximum torque limit, represented in Figures 1.3 and 1.4 by the black bold line, and the minimum torque limit, not visible in the two maps. If the required torque exceeds one limit, its value is then saturated to the torque limit. In this way, the feasibility of the engine operating point is ensured, but it might be possible that the prescribed driving cycle is not followed. Anyway, such a situation does not constitute a major issue for the study, considering that it occurs very seldom thanks to the high torque deliverable by the engine and that it affects all the energy management strategies alike, thus not impacting the fairness of the comparison.
Finally, it is good practice to spend a few words about the engine idle condition. First off, the model of the powertrain does not include a clutch model but simply considers the clutch disconnected when the gearbox is in neutral gear (gear number 0) and considers the clutch connected when any other gear is engaged. When any gear but neutral is engaged, the engine speed is derived from the vehicle speed and the engine torque is set by the energy management strategy. When the neutral gear is engaged, the engine is considered being in idle condition. The idle condition consists in engine speed equal to 750 rpm and zero torque. Since the fuel consumption for this operating point was not identified in the experimental characterization of the engine, its value is assumed being equal to the closest engine operating point which can be found in the map of Figure 1.3, namely engine speed equal to 1000 rpm and zero torque.

ELECTRIC MOTOR

The model of the electric motor is, all in all, analogous to the model of the engine. That is to say, also the electric motor has been modelled by means of a map, obtained through experimental characterisation. The employed map, presented in Figure 1.5, receives as inputs the speed of the motor, known as long as the vehicle speed is known, and the torque demand to the motor, which is also set by the energy management strategy. The output of the map consists of the electric power produced or received by the electric motor, which is the power absorbed from the battery in case the motor is producing power and is the power passed to the battery in case the motor is receiving power.

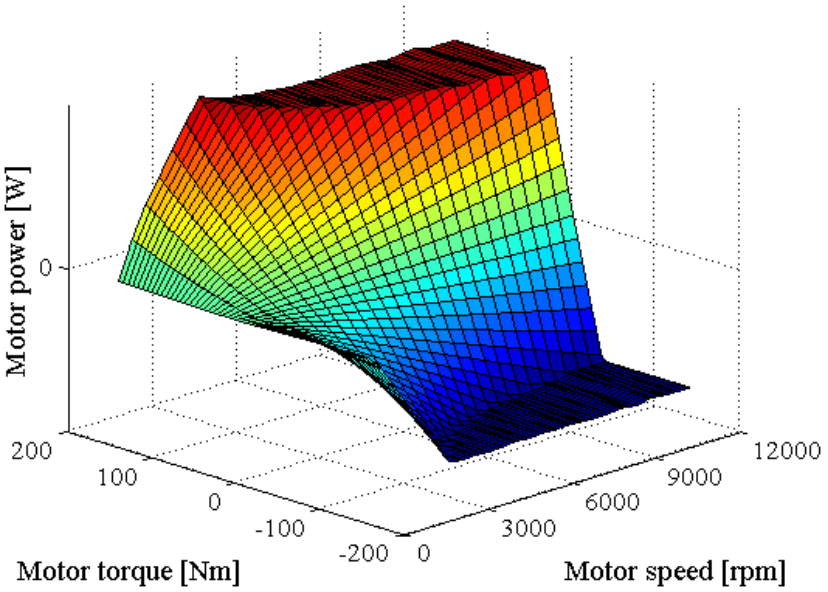

Figure 1.5 – Electric power map of the electric motor

Also in this map the scale of power is not displayed for confidentiality reasons.
The adopted convention for the study is that a positive motor power indicates that the motor is producing power, while a negative motor power indicates that the motor is receiving power[4].
The efficiency of the electric motor η_{mot} is obtained by relating the electric power of the motor P_{elec}, obtained through the map pictured in Figure 1.5, and the mechanical power of the motor P_{mech}, defined as

$$P_{mech} = T_{mot} \cdot \omega_{mot} \tag{1.22}$$

where T_{mot} is the torque of the motor and ω_{mot} is the rotating speed of the motor.
The relation between the electric power of the motor and the mechanical power of the motor, from which the motor efficiency η_{mot} can be derived, changes according to whether power is being produced or absorbed by the motor, as in (1.23).

[4] Considering that the backward motion of the vehicle is not modelled in the study, motor speed is positive (or zero) at all times. Hence, to positive motor power corresponds a positive motor torque and to negative motor power corresponds a negative motor torque. Consequently, a positive motor torque indicates that the motor is producing power, a negative motor torque indicates that the motor is receiving power.

$$\begin{cases} P_{elec} = P_{mech} \cdot \eta_{mot} & \text{for} \quad T_{mot} < 0 \\ P_{elec} = 0 & \text{for} \quad T_{mot} = 0 \\ P_{elec} = \dfrac{P_{mech}}{\eta_{mot}} & \text{for} \quad T_{mot} > 0 \end{cases} \tag{1.23}$$

Similarly to what happened for the limits in the internal combustion engine, torque request values exceeding the prescribed motor limits are saturated to the respective limit values.

BATTERY

Another part of the vehicle model assuming a great importance is the battery model, necessary because of the need to compute the state of charge of the battery at any time along the driving cycle. The knowledge of the SOC is fundamental since, as it was explained in the introduction, sustaining the SOC level along the driving cycle is one of the basic requirements to the energy management strategy.
The composition of the battery model starts with the definition of the state of charge at time k, as follows

$$x_k = -\frac{\int_0^k I_{batt}(t)dt}{Q_{batt}} \tag{1.24}$$

with I_{batt} being the current of the battery and Q_{batt} the capacity of the battery. The convention on the sign of the current was made so that the current is positive when the battery is being discharged.
In principle, the battery capacity Q_{batt} is dependent on several parameters, namely the value of the current and the ageing of the battery, but it is here assumed to be constant and a design parameter.
The SOC profile is computed stepwise over the driving cycle, starting from the initial value of the SOC, which needs to be an input to the model. Considering the charge-sustaining nature of the hybrid vehicle considered, the initial SOC and the target SOC in the study are the same, and equal to 50 %.
The open circuit voltage of the battery V_{oc}, i.e. the voltage of the battery when not connected to any load, can be expressed as a function of the SOC. Likewise, the internal resistances, R_{disch} and R_{ch} for discharging and charging conditions respectively, are expressed as a function of the SOC alone[5]:

[5] In reality, the three parameters presented here also depend on the battery temperature. Nevertheless, this dependence is here assumed to be negligible.

$$\begin{cases} V_{oc} = g_1(x) \\ R_{disch} = g_2(x) \\ R_{ch} = g_3(x) \end{cases} \tag{1.25}$$

The functions g_1, g_2, and g_3 are defined through experimental characterization, associating to each value of the SOC the corresponding value of the voltage or of the resistance.
Once these values are computed, the current in the battery I_{batt} can be computed according to (1.26) [19].

$$\begin{cases} I_{batt} = \dfrac{V_{oc}}{2 \cdot R_{ch}} - \sqrt{\dfrac{|V_{oc}^2 - 4 \cdot P_{elec} \cdot R_{ch}|}{4 \cdot {R_{ch}}^2}} & \text{for} \quad P_{elec} < 0 \\ I_{batt} = 0 & \text{for} \quad P_{elec} = 0 \\ I_{batt} = \dfrac{V_{oc}}{2 \cdot R_{disch}} - \sqrt{\dfrac{|V_{oc}^2 - 4 \cdot P_{elec} \cdot R_{disch}|}{4 \cdot {R_{disch}}^2}} & \text{for} \quad P_{elec} > 0 \end{cases} \tag{1.26}$$

The value of the battery resistance can be either R_{disch} or R_{ch}, respectively when the battery is being discharged and when it is being recharged.
In case the battery is being recharged, it is also necessary to take into account the faradaic efficiency of the battery, accounting for charge losses due to unproductive reactions. The current of the battery is then defined as follows

$$\begin{cases} I_{batt,2} = I_{batt} \cdot \eta_{faradaic} & \text{for} \quad I_{batt} < 0 \\ I_{batt,2} = 0 & \text{for} \quad I_{batt} = 0 \\ I_{batt,2} = I_{batt} & \text{for} \quad I_{batt} > 0 \end{cases} \tag{1.27}$$

Then, adapting (1.24) to the discrete nature of the model, the value of the SOC for the following instant of time $k + 1$ is computed:

$$x_{k+1} = x_k - \frac{I_{batt,2} \cdot \Delta t}{Q_{batt}} \tag{1.28}$$

Aside from ensuring a sufficient final value of the SOC, the energy management strategy needs to maintain the battery SOC level within given boundaries at all times, in order to prevent the battery from ageing too rapidly and in order to make it operate at good efficiency levels. This imposition is enforced in the model by a system of flags which prevents the energy management strategy from choosing the torque splits that cause an excursion out of the prescribed boundaries.

1.2.3 Model validation

As explained previously, the model of the vehicle was built in the Matlab environment. The modelled powertrain is well known at IFP Energies nouvelles and has been used also for previous studies. In the framework of these previous studies, a Simulink model of the powertrain was developed and validated against the experimental results obtained at the test bench. Consequently, the validation strategy for the presented Matlab model consists in comparing its behaviour to the Simulink model.
One may wonder why a new Matlab model has been developed, when a Simulink model of the powertrain was already available. There are two main reasons for this. First off, the implementation of the Stochastic Dynamic Programming strategy requires, as it will be better explained in Chapter 2, the off-line generation of torque split maps. This process, involving a recursive optimisation, is practically impossible to implement in Simulink, while Matlab proves easily suitable for such an application. Secondly, simulations in the study are carried out on a sample of 100 random driving cycles. While possible with both environments, launching automatically the simulation on multiple cycles is more smoothly implemented in Matlab.

The validation procedure consists in comparing step by step the results of the two models for different utilisation cases on a relevant driving cycle, which is here the WLTC cycle (Worldwide harmonized Light duty Test Cycle) [20].
In the first comparison, the two models are employed only with the internal combustion engine enabled, meaning that the models are reproducing the behaviour of a pure thermal vehicle. The intent for this test is to validate the part of the model reproducing the thermal driveline.
The results of the comparison are presented in Figures 1.6 and 1.7 below.

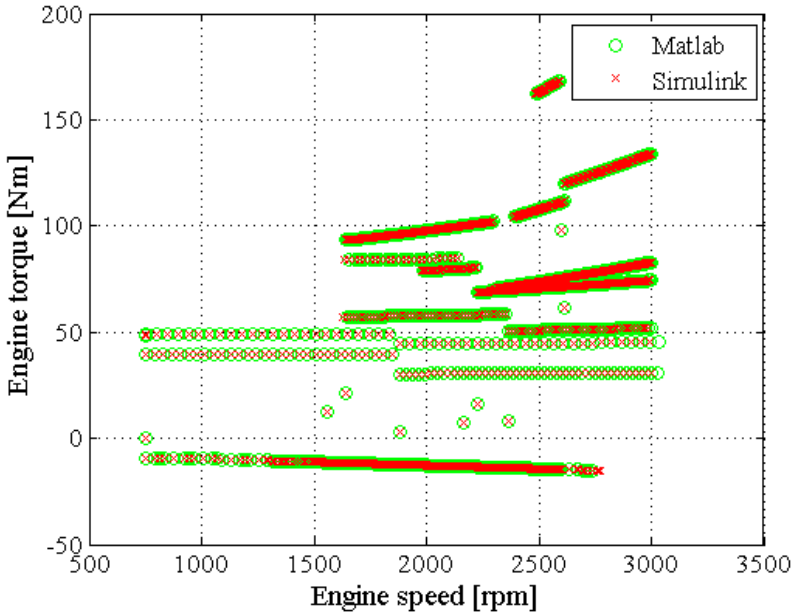

Figure 1.6 – Engine operating points comparison for the two models – pure thermal vehicle

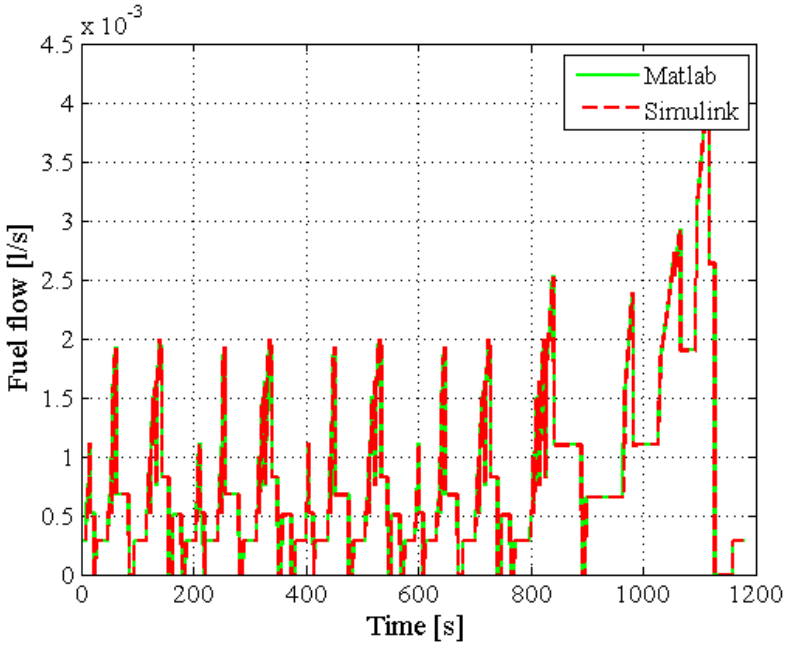

Figure 1.7 – Fuel flow comparison for the two models – pure thermal vehicle

The engine operating points along the cycle are practically the same between the two strategies. Consequently, also the fuel flow into the engine is the same, fact

that is reflected in the fuel consumption results, 7.403 l/100 km for the Simulink model and 7.406 l/100 km for the Matlab model.
Thanks to these results, the thermal part of the Matlab model is considered to be validated.
Then, the two electric parts are compared. Both models are run in the zero-emissions vehicle mode (ZEV), meaning that the power to the wheels is provided only by the electric driveline.
The result presented in Figure 1.8 regards the SOC profile for the two models. Due to the limited capacity of the battery, both models are not able to power the vehicle along the whole driving cycle in the ZEV mode. So, the vehicle will not be able to follow the entire driving cycle. The comparison is nonetheless legitimate since both models should respond in the same way to the case of inability of following the driving cycle.

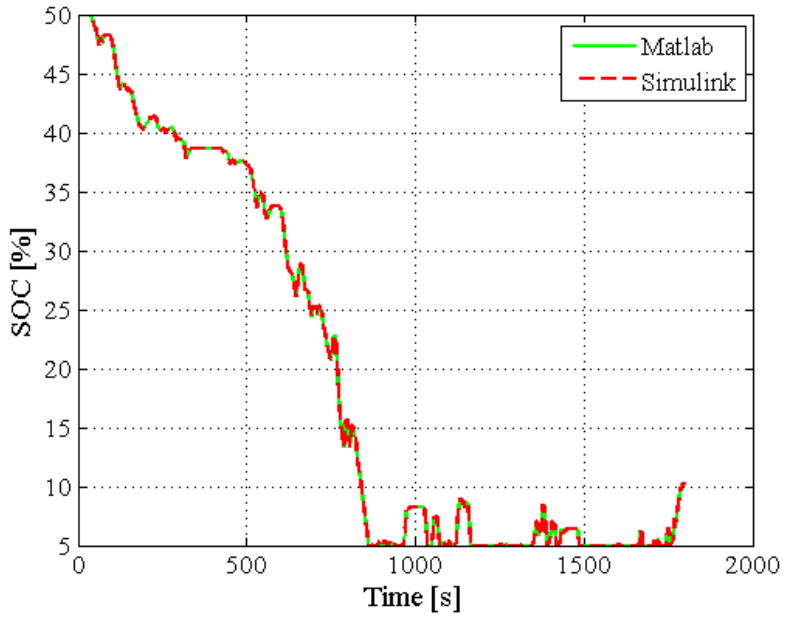

Figure 1.8 – Comparison of the state of charge for the two models – full-electric vehicle

Figure 1.8 shows that the profile of the SOC for the two models is exactly the same. Therefore, also the electric driveline of the Matlab model is validated.
Finally, the two full models, reproducing the entire hybrid architecture, are compared. The energy management strategy employed is the same for the two models and yields the optimal results for the given driving cycle.

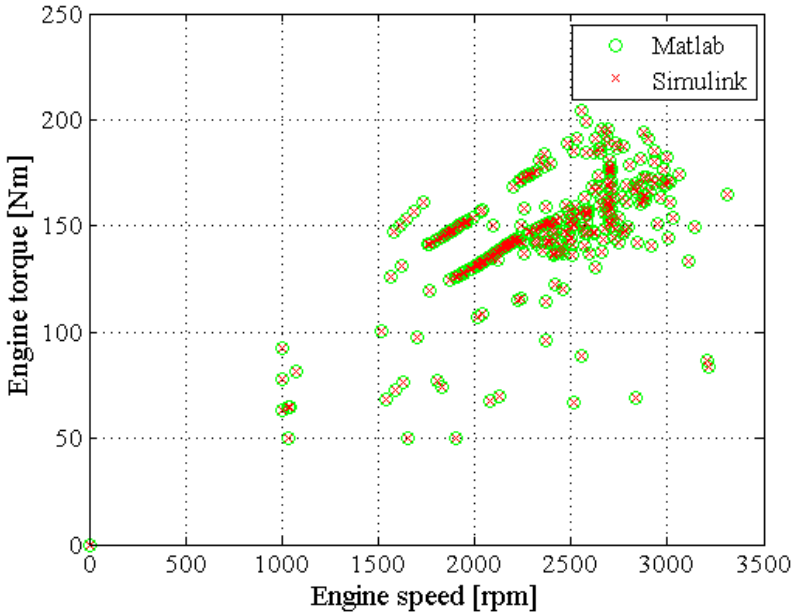

Figure 1.9 – Engine operating points comparison for the two models – hybrid vehicle

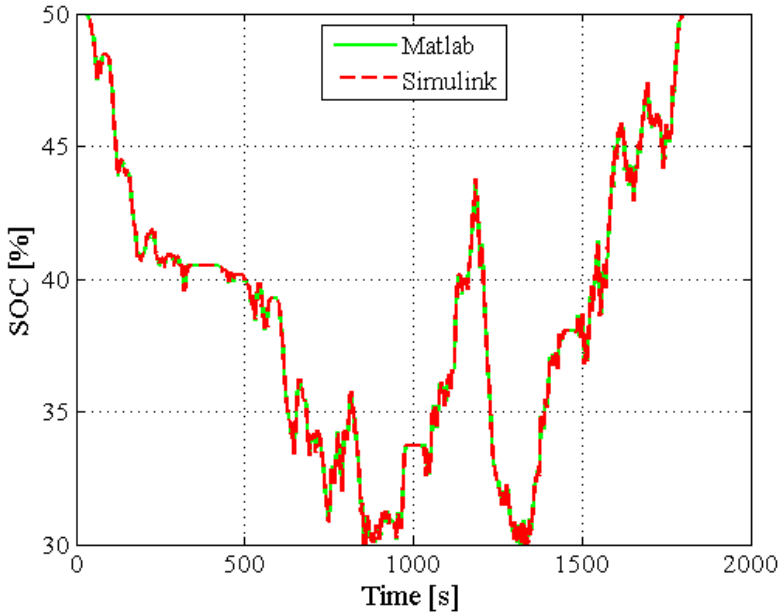

Figure 1.10 – State of charge comparison for the two models – hybrid vehicle

Figures 1.9 and 1.10 present the results of the comparison, showing a match between the two models that is essentially the same as the one for the two drivelines considered independently, illustrated in Figures 1.6 and 1.8.
Also the fuel consumption results highlight the proximity of the two models. In fact, the results are really close: 4.855 l/100 km for the Matlab model and 4.845 l/100 km for the Simulink model. As a consequence, the complete Matlab model of the hybrid vehicle is considered validated.

1.3 The driving cycles

In order to provide realistic results, a reliable model alone is not sufficient. In fact, it is also necessary to perform the simulation over a sample of cycles that captures well real-world driving conditions and that represents the wildly different driving patters which can be followed by an actual vehicle. With this goal in mind, simulations in the study are run on a sample of 100 randomly generated cycles, representing different driving conditions (urban, suburban and mixed).
The sample was chosen to include this many cycles with the objective of yielding dependable results. In fact, the big statistical sample makes the impact of possible aberrations in the results very limited. In addition, considering that the main goal of the study lies in the comparison of different energy management strategies, the size of the sample makes less relevant particular affinities or disaffinities of one strategy towards one cycle type. As a consequence, the results obtained with this sample of cycles are considered to be representative of the actual utilisation of a real vehicle.
The random driving cycles were generated using an algorithm that has been developed specifically for the project. The basic functioning of the algorithm is explained in the remainder of the section.

The random cycles are generated by employing a statistical database constituted by 32 reference driving cycles. This sample of driving cycles includes some regulatory driving cycles (NEDC, WLTC, FTP75, JC08, ARTEMIS and others[6]) and some real-world driving cycles that were recorded for other projects at IFP Energies nouvelles.

[6] For further information on the mentioned driving cycles, the reader is invited to refer to [67].

The first assumption for the development of the algorithm consists in modelling the driving cycles as a Markov chain [21]. This means that the following state of the driving cycle, in terms of speed and acceleration, is function of the current state, as in (1.29):

$$\begin{cases} v_{k+1} = v_k + a_k \cdot \Delta t \\ a_{k+1} \sim P(a_{k+1} | a_k, v_k) \end{cases} \tag{1.29}$$

where a is the vehicle acceleration, k is the current time step, $k+1$ is the next time step, and Δt is the time step length.

The next value of the speed is known as soon as the current speed and acceleration of the vehicle are known. Conversely, the next value of the acceleration is not deterministically known but, according to the theory of Markov chains, can be expressed in probabilistic terms depending on current speed and acceleration. Then, through the analysis of cycles in the database, an experimental probability density function for the next value of acceleration is defined for each value of current speed and acceleration. The experimental probability density functions are then fitted with normal distributions, in order to produce continuous curves.

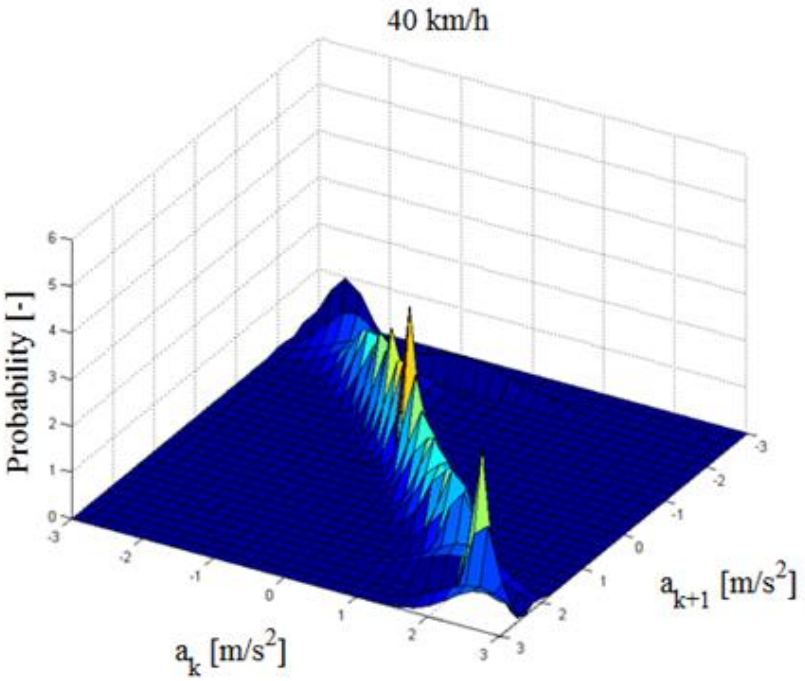

Figure 1.11 – Probability density function for next value of acceleration (for a current speed of 40 km/h and multiple current acceleration values)

An example of probability density function, for one current speed value and multiple current acceleration values, is presented in Figure 1.11.
It is interesting to notice that the greatest share of probability is clustered around the diagonal in Figure 1.11. This is because it is likely that the next value of acceleration will not be very different from the current one.
A particular situation is represented by the case when the vehicle is not moving. In this case, two binomial probability density functions were defined, using the database of cycles previously described. The first probability density function identifies the probability of turning off the key of the vehicle and ending the cycle in the following time step. The second, instead, identifies the probability of vehicle take-off in the following time step. When the vehicle takes off, the first acceleration value is defined by means of a log-normal distribution, which proves more appropriate for approximating the first acceleration data than the normal distribution, employed for all other situations.
In order to generate realistic driving cycles, the algorithm also enforces some heuristic rules preventing unrealistic behaviour. Most notably, if no heuristic rule is imposed, the generated cycles sometimes present long periods of time at low speeds ($\leq$ 5 km/h) and present decelerations up to 1 km/h and, then, acceleration without the stop of the vehicle. In order to avoid such unrealistic behaviour, a simple rule is imposed. The acceleration, in the area between 0 km/h and 5 km/h, is forced to increase or decrease monotonically until the vehicle reaches zero speed or surpasses the 5 km/h threshold.
The sample of driving cycles is then randomly generated by employing the normal and log-normal probability density functions to define the acceleration values, by employing the two binomial probability density functions to address the behaviour when the vehicle is stopped, and by using the heuristic rule to prevent unrealistic behaviour. Then, a further automatic selection is made, discarding the driving cycles that do not meet some particular criteria, aimed at ensuring that the generated cycle is representative of realistic vehicle utilisation.

In order to provide the reader with an idea of how the random driving cycles employed in the study look like, three examples of random driving cycles are illustrated in figures below. All three driving cycles were generated using the algorithm presented in the section.

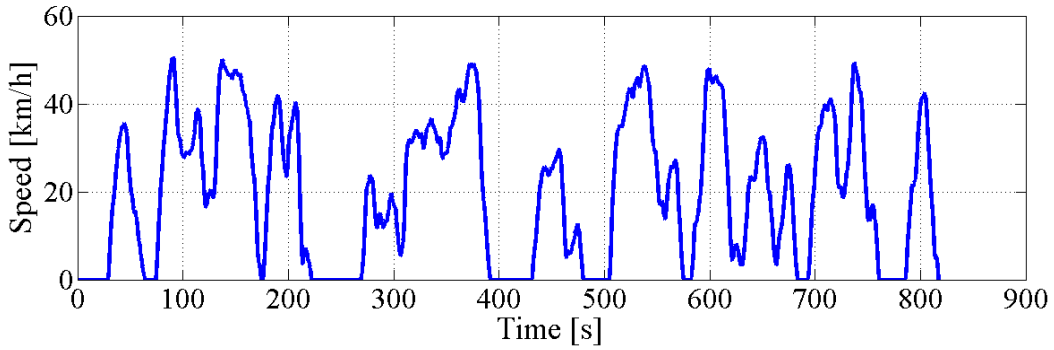

Figure 1.12 – Randomly generated urban cycle

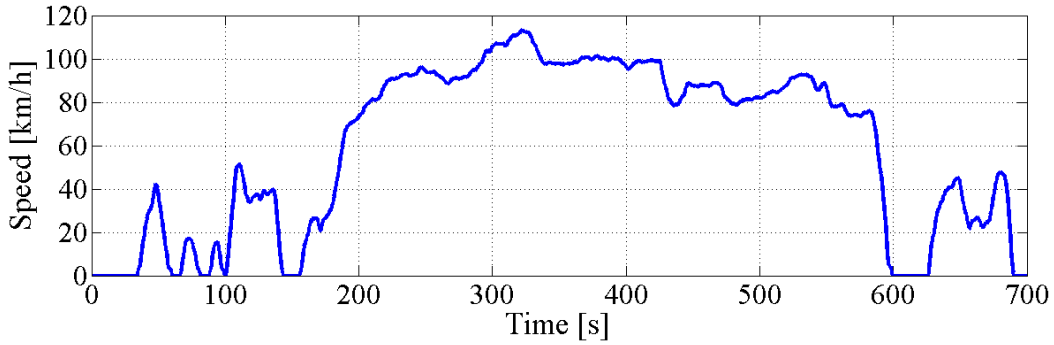

Figure 1.13 – Randomly generated suburban cycle

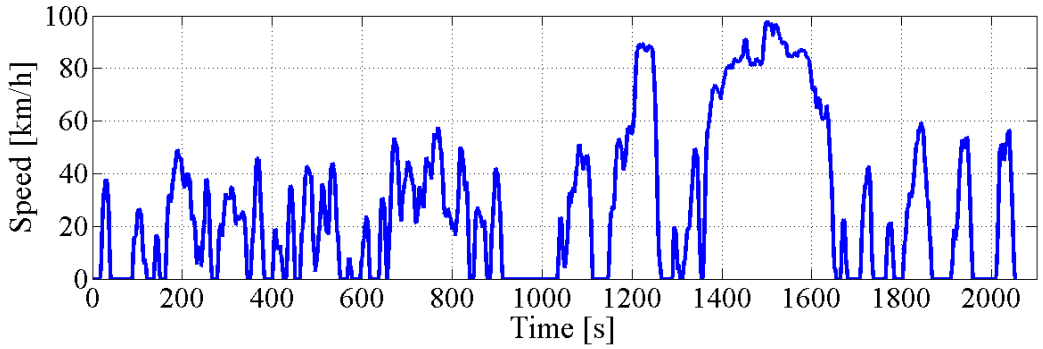

Figure 1.14 – Randomly generated mixed cycle

The cycles presented in Figures 1.12 through 1.14 appear to be representative of a real driving situation, showing a dynamic and rugged profile. The speed is continuously evolving and never stays constant, exactly like as in a real vehicle. In addition, it is interesting to note how the same algorithm, employing the same cycle database, is able to output very different driving cycles, in terms of speed profile and in terms of cycle duration.

As a result, it is possible to state that the sample of 100 random driving cycles employed in the study constitutes a realistic and varied benchmark for the simulation of the energy management strategies.

1.4 Conclusion

In the chapter, the hybrid vehicle considered in the study was introduced, presenting its double shaft parallel architecture and detailing the specifications of its most important components. Then, a few details regarding the model of the vehicle were illustrated, starting from the vehicle energy balance and following with the modelling of the different powertrain components. In the ensuing part, the Matlab model of the vehicle was validated against a Simulink model, which had been previously validated against experimental data from the powertrain. Finally, some hints about the random cycles generating algorithm were given and a few random driving cycles were presented.
To conclude the chapter, it is important to highlight one point about the level of detail of the model. In fact all models, being approximations of reality, comport a certain degree of inaccuracy. The presented model is not any different, being relatively simple and relying on several approximations. Yet, validation shows that the produced results are realistic and appropriate for the purposes of the study. In addition, the simplicity of the model entails significant gains in terms of computational time, which are quite relevant considering that several energy management configurations are simulated and each configuration is tested over one hundred cycles. As a result, the short simulation time for one driving cycle, on average around 15 seconds, proves being a notable advantage in the study.
It is then possible to state that the presented model has proven being sufficiently quick and accurate to support the research project here illustrated.

Chapter 2

Energy management in HEVs

In the introduction, the problem of addressing the power split in hybrid electric vehicles was introduced. Several control strategies aimed at addressing the issue have been proposed in the last years; some have found application on actual vehicles, some others are still at their conceptual level. This chapter proposes to synthetically illustrate the most relevant strategies that have been developed in the field, pointing out advantages and flaws of each of them.
The discussion is centred on the case of parallel hybrids, architecture of the vehicle which has been introduced in Chapter 1. Nevertheless, similar considerations apply also to the other hybrid architectures.
It is also intended to remind the reader that, in the study, the gear shift law is fixed and known along the entire driving cycle. Hence, the engine and motor speeds are known. As a result, determining the engine or motor torque is equivalent to determining the engine or motor power, with the consequence that the terms power split and torque split are used equivalently in the section.

2.1 HEV control architecture

Before starting to discuss the possible choices in terms of energy management strategy, it is good practice to introduce what the energy management strategy does and where it is positioned in the overall control architecture of the vehicle.
It is generally possible to identify three levels of control in HEVs, here presented from the lowest to the highest level:

- The *low level* or *component level control*, which controls the single components of the powertrain, in order to make sure that they will respond as dictated by the driver (or by the higher level controllers). For instance, the control loop for the fuel quantity injected in a gasoline engine is to be included in the low level control category;

- The *energy management control*, which is in charge of choosing the powertrain operating mode and the engine and motor operating points. This choice must ensure the fulfilment of the torque request at the

wheels, while minimising the operating cost of the vehicle. The analysis of the energy management control constitutes the subject of the chapter;

- The *supervisory control*, whose function is to decide when to employ the energy management controller for determining the powertrain behaviour and when to employ other strategies. In fact, during vehicle utilisation, it is possible to encounter some particular conditions requiring to override the set points given by the energy management controller. An example for such case is the limp home mode, where the focus for the set points choice is not anymore on the energy optimisation but on the necessity of ensuring the vehicle operation.

Figure 2.1 below schematically illustrates the architecture of the control system for a hybrid vehicle, showing the positioning of the three levels of control presented above in the overall control architecture.

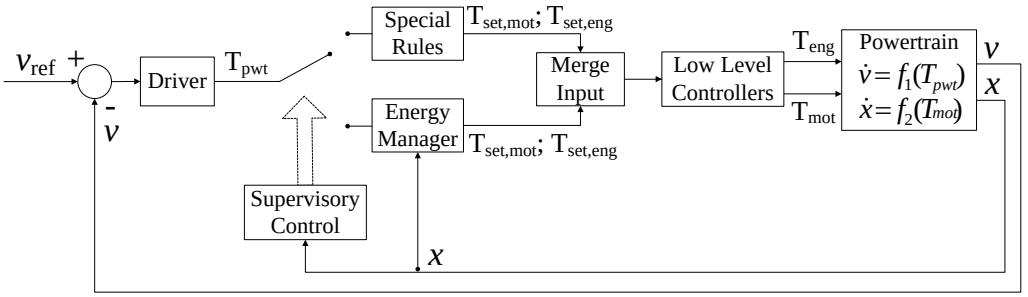

Figure 2.1 – Architecture of the powertrain controller

The driver acts on the accelerator pedal in order to follow a desired profile of velocity (v_{ref}), passing in this way to the powertrain a torque request to be met (T_{pwt})[7]. The supervisory control, based upon some states of the powertrain (here only the state associated to the battery state of charge (x) is represented for simplicity), switches between the energy manager and the particular case rules. These two strategies generate set points for the torque request to the thermal engine ($T_{set,eng}$) and to the electric motor ($T_{set,mot}$). Then, the set points for the active strategy are passed on to the low level controllers, which put the commands into action, thus producing torque from the engine (T_{eng}) and from the electric motor (T_{mot}). The internal dynamics of the system will then

[7] Figure 2.1 describes the actual control architecture of the vehicle. The vehicle model employed in the study, instead, neglects driver impact and derives the torque request T_{pwt} directly from the prescribed speed profile of the vehicle.

determine the vehicle dynamics and the output states of the controller, which are in this example the actual vehicle velocity (v) and the state of charge of the battery (x). Many other parameters identifying the state of the system can be used as feedbacks in the control architecture. However, only two parameters were represented in Figure 2.1 for the clarity of the representation.
Purely thermal powertrains do not need to include the two top layers of control, the supervisory control and the energy management, as in thermal powertrains the driver's request can be accomplished only by means of the internal combustion engine or of the mechanical brakes. Therefore, there are no degrees of freedom in the selection of how to accomplish the driver's request. Instead, the driver's intentions about the vehicle behaviour, expressed by the accelerator and brake pedals positions, are passed directly to the low level controllers which put into action the driver's wish.
On the contrary, the incorporation of an electric driveline into the powertrain introduces several degrees of freedom in the way the driver's request can be accomplished, as it was presented in the introduction. Therefore, these additional degrees of freedom need to be addressed by adding an energy management controller to the system. The more complicated system also commands the addition of a supervisory control, aimed at ensuring the functioning of the vehicle even in case of technical problems.

2.2 The energy management problem

2.2.1 Degrees of freedom

Adding an electric driveline to the system comports the introduction of two new degrees of freedom in powertrain operation. On the one hand, it is now possible to employ the powertrain in a variety of operating modes, resulting from the possibility of transferring torque to the wheels with either of the two parallel drivelines. On the other hand, when both drivelines are providing torque to the wheels, it is possible to alter the power split between the two drivelines.
Focusing on the first of the two degrees of freedom introduced above, the powertrain operating modes, and following the approach of [16], it is possible to identify a set of control variables which define the state of the powertrain:

- The power split ratio PS, defined as the ratio between the power being produced or absorbed by the motor and the total power of the powertrain:

$$PS = \frac{P_{mot}}{P_{pwt}} = \frac{P_{mot}}{P_{mot} + P_{eng}} \tag{2.1}$$

where P_{mot} is the power of the motor, P_{eng} is the power of the engine, and P_{pwt} is the total power of the powertrain. The ratio PS is defined for each instant of time, employing the instantaneous value of the power of components, which can be either positive (prime mover producing power) or negative (prime mover absorbing power);

- The engine state e_{on}, a Boolean variable distinguishing when the engine is turned on ($e_{on} = 1$) from when the engine is turned off ($e_{on} = 0$);

- The clutch state c_{on}, another Boolean variable distinguishing the cases of clutch engaged (engine connected to the transmission - $c_{on} = 1$) and clutch disengaged (engine not connected to the transmission - $c_{on} = 0$).

A variety of operating modes originates from the combination of the three parameters presented above, depending also on the torque request at the wheels. Table 2.1 below summarizes them.

Table 2.1 – Possible operating modes for parallel hybrid vehicles

Operating mode	$\mathbf{T_{pwt}}$	***PS***	$\mathbf{e_{on}}$	$\mathbf{c_{on}}$
Powertrain inactive	= 0	-	0	0
Fully electric (1)	> 0	1	0	0
Fully electric (2)	> 0	1	0	1
Fully thermal	> 0	0	1	1
Power assist	> 0	∈ (0, 1)	1	1
Battery recharge (1)	> 0	< 0	1	1
Regenerative braking (1)	< 0	1	0	0
Regenerative braking (2)	< 0	1	0	1
Battery recharge (2)	< 0	> 0	1	1

The table reports, for completeness purposes, all the possible combinations of the parameters previously presented, even if some operating modes will not prove very common when considering the real powertrain utilisation. For instance, the fully electric (2) operating mode is not of great interest unless it is needed to deplete the battery so urgently that an additional load, the engine brake, needs to be added to the normal road load.

It is now possible to present the two duties of the energy management strategy. The first duty consists in deciding, for each instant of time, what is the most convenient powertrain operating mode. The second duty consists in determining

the engine and the motor operating points, when they are not imposed by the operating mode. In fact, when the parameter PS presented above is fixed, the motor and the engine torque are determined by the torque request at the wheels. Conversely, when the parameter PS is not fixed (power assist mode and the two battery recharge modes), the motor and engine torque need to be optimised.
Inferring from what stated above, it would appear as if the control strategy outputs two results, the operating mode and the power split. This is not correct as the energy management strategy outputs only one value; the reason for this is that such output is able to address both the power repartition and the powertrain operating mode questions.
In order to explain what stated above, it is first necessary to recall the equation expressing the balance of torques at the wheel, equation (1.16). Considering that the torque balance is valid for any generic instant of time k, (1.16) can be rewritten as in (2.2).

$$T_{pwt,k} = T_{pwt,k}^{eng} + T_{pwt,k}^{mot} + T_{brake,k} \tag{2.2}$$

The torque provided by the brakes, T_{brake}, is known by making a few reasonable assumptions about the control strategy. In fact, it is reasonable to think that the brakes are used only if the braking torque provided by the motor, and, in case, by the engine, is not sufficient to match the required negative torque at the wheels. Then, the mechanical brakes will be activated and will provide the additional braking torque necessary to satisfy the torque request at the wheels. As a result, it is reasonable to assume that T_{brake} is different from zero only in regenerative braking (1) mode or in regenerative braking (2) mode and that its value in such cases is known.
The cases of regenerative braking are not very interesting under an energy management perspective, considering that in such conditions the optimal behaviour of the powertrain is easily defined and, therefore, there is no need to employ a sophisticated control strategy. Consequently, the analysis is reduced to other cases than the regenerative braking, which are far more interesting for the analysis of the energy management of the powertrain. In such other cases, (2.2) becomes

$$T_{pwt,k} = T_{pwt,k}^{eng} + T_{pwt,k}^{mot} \tag{2.3}$$

since, as explained before, T_{brake} is different from zero only in the two regenerative braking cases.
Expression (2.3) can be reformulated as

$$T_{pwt,k} = T_{eng,k} \cdot i_{tr,th,k} \cdot \eta_{tr,th,k} + T_{mot,k} \cdot i_{tr,el} \cdot \eta_{tr,el} \tag{2.4}$$

where T_{eng} is the torque produced by the engine, T_{mot} is the torque produced by the motor, $i_{tr,th}$ and $\eta_{tr,th}$ are the reduction ratio and the efficiency of the transmissions between the engine and the wheel (the gearbox and the differential), and $i_{tr,el}$ and $\eta_{tr,el}$ are the reduction ratio and the efficiency of the transmissions between the motor and the wheel (the coupling gearing and the differential). The reduction ratio and efficiency of the electric driveline are fixed, while the reduction ratio and efficiency of the thermal driveline vary according to the gear changes in the gearbox. Therefore, the reduction ratio and efficiency of the thermal driveline depend on time, justifying the presence of index k in their expression in (2.4).
Parameter T_{pwt} is an input to the control strategy both in the real case, as shown in Section 2.1, and in simulation, as shown in Paragraph 1.2.1. Furthermore, the geometry and the efficiency of all transmissions in the powertrain are design parameters, and the gear shift law is imposed. As a result, the only unknowns in (2.4) are T_{eng} and T_{mot}. That is to say, once either T_{eng} or T_{mot} is defined also the other torque is univocally defined.
The analysis above was centred on the torque balance in the powertrain. It is straightforward that the same applies to power as well since, for the well-known relationship (2.5), power is proportional to torque with the rotating speed of the considered shaft being the proportionality coefficient:

$$P = T \cdot \omega \tag{2.5}$$

In the powertrain, the rotating speed of all shafts is known if the vehicle velocity and the gear shift law are known. In fact, once the rotating speed of the wheel is computed, as in (1.14), all other shafts' speeds can be computed through the reduction ratios of the transmissions.
Multiplying all the elements in (2.3) times the rotating speed of the wheel ω_{wheel}, the power balance at the wheel is obtained:

$$P_{pwt,k} = P_{pwt,k}^{eng} + P_{pwt,k}^{mot} \tag{2.6}$$

where P_{pwt} is the power required at the wheel, P_{pwt}^{eng} is the power at the wheel provided by the internal combustion engine, and P_{pwt}^{mot} is the power at the wheel provided by the electric motor.
Similarly to what was done previously for the torque, (2.6) can be reformulated as:

$$P_{pwt,k} = P_{eng,k} \cdot \eta_{tr,th,k} + P_{mot,k} \cdot \eta_{tr,el} \tag{2.7}$$

P_{eng} being the power produced by the engine and P_{mot} being the power produced by the motor.
As shown before, the power request at the wheels P_{pwt} is known, and the efficiencies are design parameters. As a result, once one of the two power values P_{eng} and P_{mot} is determined, also the other power is known. Equivalently, once either T_{eng} or T_{mot} is defined, also all powers in (2.7) are defined. Then, it is possible to determine the power split ratio PS and the engine state (assuming to turn the engine off in case of $P_{eng} = 0$). Thanks to these information, and to the knowledge of the torque request at the wheels, the powertrain operating mode can be determined as shown by Table 2.1[8].
To sum up, the section has proven that the powertrain operating mode and all powers and torques in the powertrain are defined when either T_{eng} or T_{mot} is defined. Consequently, it is now clear how the control strategy needs to output one single parameter to define both the powertrain operating mode and the power split.

2.2.2 Definition of the optimal control problem

Figure 2.1 showed the positioning of the energy management controller in the hybrid powertrain control architecture. The energy management controller illustrated there was a simplification, aimed at explaining the general functioning of the energy management strategy. In order to proceed with the analysis, it is necessary to redefine the energy manager block and its inputs, adapting it to a more realistic scheme.
In said figure, the energy manager block used to have two inputs, an external one, the torque request at the wheels T_{pwt}, and a powertrain state, the battery state of charge *x*. There were also two outputs, the set point for the engine torque $T_{set,eng}$ and the set point for the motor torque $T_{set,mot}$.
Paragraph 2.2.1 has given a proof of how, once one of the two torques is defined, also the other is univocally defined. Therefore, the number of outputs of the energy management strategy is reduced to one, here named u.
As for the external input, for convenience reasons the torque request at the wheels T_{pwt} is split into two inputs, the vehicle speed v and the vehicle

[8] Possible ambiguity might arise from the cases where the choice of the powertrain operating mode is not solely dictated by the torque request T_{pwt}, by the power split ratio PS, and by the engine state e_{on}, as in some cases a choice regarding the state of the clutch needs to be done as well. If, when the engine is on, it is straightforward that the clutch will be connected, when the engine is off the clutch might be either connected or disconnected. Nevertheless, since the cases of engine off and clutch connected are of little practical use, it is reasonable to impose that, when the control strategy commands the engine to be off, the clutch is disconnected.

acceleration *a*, which is easily derived from the speed information. Equations (1.2) through (1.9) prove how these terms are equivalent.
As for the powertrain state, in Figure 2.1 only one state was used as a feedback for the energy manager for simplicity, but it was said that more states could be added. This is the case, and the powertrain states employed as inputs to the energy management strategy are then two: the state of charge of the battery *x* and the engine state e_{on}.
The basic scheme of the redefined energy management controller is pictured in Figure 2.2 below.

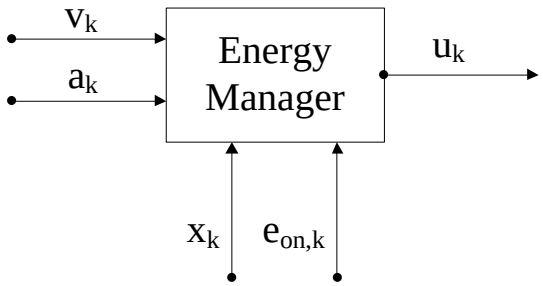

Figure 2.2 – Black box representation of the energy management controller

Now that the inputs and outputs have been clarified, the question revolves around what is contained in the box of Figure 2.2. This is the subject of the remainder of the chapter.

As reminded before, only one control variable is needed to define the powertrain operating mode and its power split. In the presented study, the selected control variable *u* is the engine torque T_{eng}[9].

$$u_k = T_{eng,k} \tag{2.8}$$

The choice of the engine torque over the motor torque is arbitrary as, once one of the two parameters is set, also the other is determined, according to what was demonstrated in the previous paragraph.
For convenience, the four inputs to the energy management strategy are recalled for convenience in Table 2.2 below. Also their name is changed as, using more appropriate control jargon, they are addressed as the states of the system.

[9] It would be more appropriate to refer to the engine torque set point as the output of the energy management strategy. Anyway, considering that the dynamics of the low level controllers are not of interest for the study, the engine torque set point and the actual engine torque are assumed to be the same. Reasonably, this is also the case for the electric motor.

Table 2.2 – States of the system

Symbol	State of the vehicle
x_k	State of charge (SOC)
v_k	Vehicle speed
a_k	Vehicle acceleration
$e_{on,k}$	Engine state:

It is useful to remark a distinction between these system states, which was hinted previously. Speed and acceleration consist of external states, independent from control strategy decisions. Instead, battery SOC and engine state constitute internal states, as their evolution depends on control strategy decisions and they identify the current condition of the powertrain.
In order to make the notation lighter, it is possible to group the states of the system into a vector. So let $\boldsymbol{X_k}$ be the vector grouping the states of the system presented above, as in (2.9).

$$\boldsymbol{X_k} = \begin{Bmatrix} x_k \\ v_k \\ a_k \\ e_{on,k} \end{Bmatrix} \tag{2.9}$$

The model for dynamics of the SOC was presented in Paragraph 1.2.2, in the part dealing with the battery model. Since SOC dynamics have a particular relevance in the definition of the energy management strategy, notation (2.10) is introduced for representing SOC dynamics in a compact form.

$$x_{\boldsymbol{k+1}} = f(x_k, u_k) \tag{2.10}$$

As for the other internal state, Paragraph 2.2.1 has explained how the engine state e_{on} is determined.
It is then possible to see that the evolution of the values of internal states x and e_{on} is determined by the current values of internal states themselves, by the values of external states v and a, and by the control variable u. As a result, the dynamics of the states can be expressed as in (2.11), indicating that the following state of the system depends on the current state and on the current control decision.

$$\boldsymbol{X_{k+1}} = F(\boldsymbol{X_k}, u_k) \tag{2.11}$$

The system states identify the functioning of a physical system and, therefore, have to comply with the physical limits of such system. For instance, the SOC

of the battery is imposed to respect some given boundaries, for ensuring durability and efficiency of the battery. Or, similarly, the torque request at the wheels should not exceed the powertrain limits, in order to avoid damage to the components of the powertrain.
The expression summarizing all the physical constraints in the system, valid at all times, is presented below:

$$G(\boldsymbol{X_k}, u_k) \leq 0 \tag{2.12}$$

The constraints are imposed as hard constraints, meaning that the values of the control variable that cause the infringement of the system constraints are simply discarded and not made available among the possible values of the control variable[10].
Similarly to the case of system states, also the control variable identifies an aspect of a physical system, in this case the engine torque. As a result, also the control variable u needs to respect some constraints. For instance, the value of u should never exceed the maximum engine torque. Or, similarly, the value of u should not cause a torque request to the motor exceeding its limits. Such constraints are expressed formally as in (2.13):

$$u_k \in U_k \tag{2.13}$$

where U_k is the set of values of the control variable that, at the k^{th} instant of time, ensures that the constraints associated to the control variable are respected.
An additional condition is imposed by the charge-sustaining nature of the hybrid vehicle considered. Such architecture imposes that the value of the SOC of the battery, when the cycle is finished and the key is turned off, must be high enough to allow operation of the electric motor at the beginning of the following driving cycle. This final condition can be implemented as an inequality in the energy management control strategy, imposing that the final value of the SOC is higher than a given threshold, or as an equality, setting a target value for the SOC at the end of the cycle. In the study both formulations are employed, since some energy management strategies require one formulation and other strategies require the other formulation. However, for the definition of the control problem, the second formulation is generally preferred.
As a result, the condition on the final value of the SOC writes

$$x_N = \overline{x} \tag{2.14}$$

[10] The concept of hard constraint is opposed to that of soft constraint, which indicates a constraint imposed through a penalty in the cost function of the system.

where x_N denotes the SOC at the end of the driving cycle, whose last time step is indicated with N, and $\overline{x}$ is the desired final value of the SOC. The chosen value of $\overline{x}$ is 50 % throughout the study.

Aside from ensuring that the system's constraints are met, the energy management strategy presents another key duty, which was briefly described in the introduction: the minimisation of the operating cost of the powertrain.
Therefore, the next step in the analysis consists in defining a cost function for the powertrain. In the classical approach, the energy management strategy focuses on the minimisation of fuel consumption alone, with the cost function equal to the fuel flow alone. More recent approaches have explored the possibility of addressing other aspects of the powertrain, integrating them in the cost function. As a result, new strategies have been introduced with the intent of reducing emissions in petrol hybrid powertrains [22], reducing NOx emissions in diesel hybrid powertrains [23], improving vehicle driveability [24], [25], and extending battery lifetime [26], [27].
The approach followed in this study is twofold. First, a classical cost function based on fuel consumption alone is introduced. Then, a more realistic cost function, which limits the number of engine events along the driving cycle, is introduced. The two cost functions have different utilisations, which will be explained later on in the chapter.
The first cost function, based on fuel consumption alone, writes

$$C_1(\boldsymbol{X_k}, u_k) = Q_{fuel}(\boldsymbol{X_k}, u_k) \tag{2.15}$$

where Q_{fuel} is the fuel flow entering the engine.
The second cost function, aimed both at minimising fuel consumption and at reducing the number of engine events, writes

$$C_2(\boldsymbol{X_k}, u_k) = Q_{fuel}(\boldsymbol{X_k}, u_k) + \gamma \cdot \left(e_{on,k+1} - e_{on,k}\right)^2 \tag{2.16}$$

where γ is a weighing coefficient determining the magnitude of the cost for an engine event.
Once the cost function is defined, the duty of the energy management strategy is to find the control law that minimises the cost function along the driving cycle. Expressing what stated above in formal fashion:

$$u^* = \arg\min \left[\sum_{k=1}^{N} C(\boldsymbol{X_k}, u_k) \right] \tag{2.17}$$

where C is the considered cost function which can either be C_1 or C_2. The control law u^* yielded by the optimisation presents the star symbol to denote its optimality. In principle, the control law u^* is constituted by the sequence of optimal control commands, as in (2.18):

$$u^* = \begin{Bmatrix} u_1^* \\ u_2^* \\ \vdots \\ u_k^* \\ \vdots \\ u_N^* \end{Bmatrix} \tag{2.18}$$

where u_k^* is the value of the control variable that minimises the cost function at time instant *k*, while complying with system constraints (2.12), (2.13) and (2.14).

To sum up, the task of the energy manager is to solve the minimisation problem (2.17), subject to the system dynamics (2.11) and to the constraints of (2.12), (2.13) and (2.14). The complete optimal control problem can be then formulated by joining all the elements:

$$\begin{aligned} u^* &= \arg\min_{u \in U} \left[\sum_{k=1}^{N} C(\boldsymbol{X_k}, u_k) \right] \\ \text{subject to } &\begin{cases} \boldsymbol{X_{k+1}} = F(\boldsymbol{X_k}, u_k) \\ G(\boldsymbol{X_k}, u_k) \leq 0 \\ x_N = \overline{x} \end{cases} \end{aligned} \tag{2.19}$$

2.3 The energy management strategies

The problem defined in (2.19) is a classical constrained optimisation problem. Optimal control theory has developed several methodologies apt to resolve the problem, with the result of different strategies that can be used to manage the energy flow in hybrid electric vehicles. This section proposes to provide an overview on the existing energy management strategies, also setting a theoretical basis for the ensuing part of the study.

Following the classification proposed in [28], it is possible to identify three typologies of energy management strategies:

- *Heuristic strategies*. Heuristic strategies are composed by a set of cascaded rules defining how the powertrain should respond to each situation. Hence, these strategies do not contain any explicit optimisation[11]. Such strategies rely only on present or past information and can be thus implemented on-line, meaning that the strategy can determine the torque split while the vehicle is being employed. All of the manufacturers currently rely on heuristic strategies for the energy management in production hybrid vehicles;

- *Global optimisation strategies***.** Global optimisation strategies solve the control problem as a whole, along the entire driving cycle. This comports one advantage and one drawback: the advantage is that these strategies yield the optimal solution for the control problem, thanks to the knowledge of the entire driving cycle beforehand. The drawback is that such strategies cannot be implemented on actual vehicles due to the need for knowledge of future information[12]. As a result, global optimisation strategies cannot manage the optimisation of the torque split in an actual vehicle and can only be implemented in simulation, from which their denomination of off-line strategies. The most widespread global optimisation strategies are the Pontryagin's Minimum Principle (PMP) and the Dynamic Programming (DP);

- *Local optimisation strategies.* Local optimisation strategies reduce the global optimisation problem into a succession of local optimisation problems. Since the control problem is not solved as a whole on the entire driving cycle, there is no need for future information and the strategy can be implemented on-line on an actual vehicle. Anyway, the optimality of the local solution granted by the strategy does not imply in any way the optimality of the global

[11] That is to say, the problem (2.19) is solved informally, trying to find a strategy that complies with the constraints and reduces fuel consumption as much as possible. A proper, mathematical resolution of (2.19) is not carried out in heuristic strategies.

[12] In some cases it is possible to have partial future information on the driving cycle (for instance by using a GPS system). As a result, it is possible to imagine employing an adapted version of the global optimisation strategy for the energy management of the powertrain. Anyway, the development of such mixed strategies is still at its embryonic level and they are yet to prove their effectiveness in actual situations.

solution. So, the solution of the control problem yielded by local optimisation strategies will be suboptimal with respect to the one yielded by global optimisation strategies. The local optimisation strategies that have received the greatest attention in HEV applications are the Equivalent Consumption Minimisation Principle (ECMS) and the Stochastic Dynamic Programming (SDP).

Another aspect, already mentioned, which deserves a further explanation is the distinction between off-line and on-line energy management strategies:

- *Off-line strategies*. Off-line strategies are strategies which cannot determine the power split during vehicle operation. Due to their need for future information or to their computational requirements, such strategies can only be implemented in simulation and are unsuited for application on-vehicle. Global optimisation strategies are off-line strategies;

- *On-line strategies*. On-line strategies are able to determine the power split during vehicle operation and are compatible with application on-vehicle. Such strategies, generally characterised by low computational requirements, do not employ any future information. Due to the lack of future information, on-line strategies are not able to fulfil exactly the final condition on the SOC (2.14), thus needing a tolerance on the requirement for the final SOC value. Heuristic strategies and local optimisation strategies are on-line strategies.

Since the study intends to determine which control strategy is the most appropriate for application on actual hybrid vehicles, the focus is primarily on on-line strategies. However, results from off-line strategies will also prove useful for comparison purposes.
In the remainder of the chapter, a selection of the energy management strategies that received the greatest attention in the last years is presented. An introduction to the theoretical basis of each strategy is provided and strategy's advantages and disadvantages are discussed.

2.3.1 Heuristic strategies

Heuristic strategies generally consist of a set of rules detailing the behaviour of the powertrain in any given condition, hence their alternative denomination of rule-based controllers. The set of rules usually presents a structure composed of if-else conditions, as in the simple rule based controller presented below.

- If the lower SOC limit is reached, then:
  - Engine is on
  - $P_{eng} = \max(P_{eng,opt}, P_{pwt})$
  - $P_{eng} \leq P_{eng,max}$
  - $P_{mot} = P_{pwt} - P_{eng}$
- If the upper SOC limit is reached, then
  - Engine is off if $P_{pwt} \leq P_{eng,min}$
    - $P_{eng} = 0$
    - $P_{mot} = P_{pwt}$
  - Engine is on if $P_{eng,min} < P_{pwt} < P_{eng,max}$
    - $P_{eng} = P_{pwt}$
    - $P_{mot} = 0$
  - Engine is on if $P_{pwt} \geq P_{eng,max}$
    - $P_{eng} = P_{eng,max}$
    - $P_{mot} = P_{pwt} - P_{eng}$
- In any case:
  - If $a \geq a_{max}$ then $P_{eng} = P_{eng,max}$
  - If $P_{pwt} < 0$ then regenerative braking is active
  - $P_{batt,ch} \leq P_{batt,ch,max}$
  - $P_{batt,disch} \leq P_{batt,disch,max}$

Figure 2.3 – An example of heuristic energy management strategy [29]

The heuristic strategy presented above uses the same denomination for the variables already employed in the chapter. However, there are still a few values

needing definition: $P_{eng,opt}$ is the power yielded in the most efficient operating area of the engine, $P_{eng,max}$ and $P_{eng,min}$ are the maximum and minimum power that can be produced by the engine, a_{max} is the maximum value of the acceleration allowable by the powertrain, $P_{batt,ch}$ and $P_{batt,disch}$ are the power passing through the battery during charge and discharge, $P_{batt,ch,max}$ and $P_{batt,disch,max}$ are their respective limits.
In order to make the strategy easier to read, the transmission efficiencies are omitted from the heuristic strategy presented in Figure 2.3.
The rule-based strategy presented above is quite simplistic and sets conditions only on the battery SOC. Many other vehicle parameters can be employed to define the powertrain behaviour and, in real applications, parameters are often combined within the same strategy, possibly using a fuzzy logic approach (for instance, refer to [30], [31], and [32]).
Most heuristic strategies are created with the goal in mind of reducing fuel consumption to the greatest degree. As a result, the rules defining the strategy are usually directed at employing the engine in its high efficiency area and at exploiting the regenerative braking as much as possible. Anyway, such goals are not achieved by means of a mathematical optimisation but rely on the engineering sense and on the intuition of the developer.
The development of heuristic strategies is generally articulated into two steps: at first, the relevant rules for the control of the powertrain are defined. Then, the calibration of the thresholds in the strategy follows. Calibration of the strategy is usually carried out by means of simulations on a vehicle model but, usually, also encompasses work on the test bench and on test vehicles.

The main advantage of heuristic strategies lies in their simplicity. In fact, such strategies are fairly easy to understand and are very well suited for implementation on actual vehicles, thanks to their low requirement of computational resources and their natural adaptability to on-line applications [33]. This reason, joined with a good reliability and satisfactory results of fuel consumption [34], has permitted heuristic strategies to monopolize the scene of production vehicles. In fact, at the moment, every hybrid electric vehicle in the market uses a heuristic strategy for the energy management of the vehicle.
Notwithstanding their widespread utilisation, heuristic energy management strategies present several important issues. First off, it takes a long amount of time and significant investments in qualified workforce to develop the strategy, owing to the long rules definition and calibration processes. The situation is worsened by the fact that strategy definition needs being repeated for every new hybrid powertrain, as heuristic strategies cannot be transferred on different powertrains. In addition, the same calibration has proven being inadequate for

all driving conditions, posing some questions about robustness of heuristic strategies [35]. Finally, even if fuel consumption obtained with heuristic strategies is generally satisfactory, it has been shown how heuristic strategies present a structural disadvantage in terms of fuel consumption with respect to strategies deriving from a mathematical optimisation [36].

2.3.2 Pontryagin's Minimum Principle

Pontryagin's Minimum Principle, proposed by the Russian mathematician Lev Pontryagin in 1958 and presented in [37], provides a set of conditions necessary to ensure the optimality of control law u^*, solution of the constrained optimisation problem (2.19).
The basis of Pontryagin's Minimum Principle lies in the definition of the Hamiltonian function of the system. The Hamiltonian consists in a redefinition of the cost function presented in (2.15), which now includes also a control term apt to grant the respect of final condition (2.14). The Hamiltonian then writes

$$H(\boldsymbol{X_k}, u_k, \lambda_k) = C_1(\boldsymbol{X_k}, u_k) + \lambda_k \cdot f(x_k, u_k) \tag{2.20}$$

where λ_k is an optimisation variable, defined the co-state or adjoint state of the system. The reader is reminded that function $f(x_k, u_k)$ represents the dynamics of the battery SOC, as shown in (2.10).
The optimal control problem formulated in (2.19) presents only one final condition, expressed in (2.14); as a result only one optimisation variable is needed and λ_k is a scalar value. The Pontryagin's Minimum Principle, however, is also able to handle optimal control problems presenting multiple conditions, at any point along the cycle. In such cases, λ_k would be a vector and the multiplied function would represent the dynamics of all the states on which the conditions are imposed.
Returning to the constrained optimisation problem, Pontryagin's Minimum Principle states that the necessary condition of optimality for solution u^* of problem (2.19), constituted by the sequence of the control variables u_k^*, is the compliance to the following conditions, at any instant of time *k* along the cycle:

1. It minimises the Hamiltonian function, presented in (2.20):

$$u_k^* = \arg \min_{u_k \in U_k} [H(\boldsymbol{X_k}, u_k, \lambda_k)] \tag{2.21}$$

2. The co-state λ satisfies the dynamic equation:

$$\dot{\lambda} = -\left.\frac{\partial H}{\partial x}\right|_{u_k^*, x_k} \tag{2.22}$$

3. The final condition (2.14) is respected;

4. The system's dynamics (2.11) and the instantaneous constraints (2.12) and (2.13) are respected.

As state above, Pontryagin's Minimum Principle provides a necessary condition of optimality, but not a sufficient condition. In principle, it is possible to have multiple control laws u^* complying with the four points illustrated above, while the optimal control law must be one by definition. Nevertheless, this problem can be addressed easily by comparing the total cost yielded by each control law u^* complying with the Pontryagin's Minimum Principle conditions. The control law yielding the minimum total cost is then the optimal control law.
In order to apply it to the strategy under consideration, (1.28) can be rearranged as follows:

$$\Delta x = -\frac{I_{batt,2} \cdot \Delta t}{Q_{batt}} \tag{2.23}$$

Equation (2.23) captures the dynamics of the SOC and is a particular declination of the general notation $f(x_k, u_k)$, introduced in (2.10).
Substituting the terms in (2.20), it is possible to obtain the reformulated Hamiltonian function:

$$H(\boldsymbol{X_k}, u_k, \lambda_k) = C_1(\boldsymbol{X_k}, u_k) - \lambda_k \cdot \frac{I_{batt,2} \cdot \Delta t}{Q_{batt}} \tag{2.24}$$

Applying the dynamic equation to the reformulated Hamiltonian function of (2.24), the following is yielded:

$$\dot{\lambda} = -\left.\frac{\partial H}{\partial x}\right|_{u_k^*, x_k} = 0 \tag{2.25}$$

since no element in H of (2.24) explicitly depends on the SOC [16]. The straightforward result is that the co-state λ is constant along the driving cycle.
In the PMP strategy implemented for the study, this co-state value, in principle different for every driving cycle, is found by means of a dichotomy that stops when the co-state value grants the respect of final condition (2.14). It is clear

that, in order to find the value of the co-state able to ensure that final condition (2.14) is respected, the driving cycle profile of the vehicle has to be known per advance. As a result, the utilisation of Pontryagin's Minimum Principle yields an inherently off-line energy management strategy.

A widespread attention has been given to the application of Pontryagin's Minimum Principle to the energy management problem in hybrids, with many adaptations described in the literature (for instance [38], [39], and [40]). The PMP strategy is generally employed as a benchmark apt to identify the optimal results that can be yielded by the hybrid vehicle. Practical implementations on vehicles are out of question because of the impossibility of having detailed knowledge about the driving cycle in advance in actual applications. Some studies [41], [42] have shown how it is possible to derive real-time energy management controllers from the PMP strategy. However, such strategies, whose robustness to different driving cycles is yet to be proven, were unable to gain widespread interest in the scientific community and to find an adaptation on a real vehicle.

2.3.3 Dynamic Programming

Dynamic programming [43], [44], introduced by mathematician Richard Bellman, is a method employed to solve complex optimisation problems in a stepwise fashion.
The cornerstone of the strategy is Bellman's principle of optimality, which reads:

> *"An optimal policy has the property that whatever the initial state and initial decision are, the remaining decisions must constitute an optimal policy with regard to the state resulting from the first decision."* [44]

To reformulate what written above, Bellman's principle of optimality basically states that the optimal solution of a subset of a problem, from one of its intermediate steps to the end, is the terminal part of the optimal solution for the full problem. This has a major impact on the resolution of the optimisation problem since the evaluation of all the possible paths from the initial state to the final state, a time consuming and resource intensive task, becomes unnecessary. In fact, the solution can be obtained with much fewer evaluations by just working backwards from the end point.
Considering the already discretized system of (2.11), the integral cost for a generic control law u along the entire driving cycle writes

$$J_u(0) = C_1(\boldsymbol{X_N}) + \sum_{k=0}^{N-1} C_1(\boldsymbol{X_k}, u_k) \tag{2.26}$$

where C_1 is the cost function that was presented in (2.15) and N indicates the last time step in the considered cycle.
The cost-to-go, i.e. the cost of the tail of the problem, is similarly defined:

$$J_u(\tau) = C_1(\boldsymbol{X_N}) + \sum_{k=\tau}^{N-1} C_1(\boldsymbol{X_k}, u_k) \tag{2.27}$$

with τ being a generic instant of time in the driving cycle:

$$0 \leq \tau < N \tag{2.28}$$

It is possible to notice that (2.27) is a generalisation of (2.26), since the two equations are the same if τ is equal to 0.
The optimal cost function J^* is the one that minimises the cost:

$$J^*(\tau) = \min_u J_u(\tau) \tag{2.29}$$

As a result, the optimal control law u^* is the one that yields the optimal cost function:

$$J_{u^*}(\tau) = J^*(\tau) \tag{2.30}$$

The final SOC value is an imposition to the strategy, as it was shown in (2.14). Here, its respect is granted by simply plugging it into equation (2.27). Having set the value of SOC at $\tau = N$, the SOC profile necessary to yield such value is then computed backwards from the last time step.
Similarly, the initial SOC value is an input, and so a constraint, to the strategy. Its enforcement is granted by modifying the cost of the solution in case the constraint is not respected:

$$C_1(\boldsymbol{X_0}, u_0) = \begin{cases} 0 & for\ x_0 = x_{initial} \\ \infty & for\ x_0 \neq x_{initial} \end{cases} \tag{2.31}$$

where $x_{initial}$ is the prescribed initial value of the SOC and x_0 is the initial value of the SOC yielded with the considered control law.
As explained before, Bellman's principle of optimality states that the optimal control strategy obtained through the minimisation of (2.27) is optimal also for

the corresponding tail sub-problem of (2.26). Then, the optimal control law can be found by proceeding backwards from the final instant of time N:

$$u_\tau^* = \arg \min_{u_\tau \in U_\tau} [J_u(\tau)] \quad \text{for } \tau = \{N-1, N-2, \dots, \tau, \tau-1, \dots, 1, 0\} \tag{2.32}$$

At each time step τ, the cost associated to every possible control choice u_τ is computed. The optimal control variable u_τ^* is the one that yields the lower cost. When optimising the next point $\tau - 1$, which corresponds to the previous time step since the algorithm is moving backwards, it will not be necessary to evaluate all the possible control laws between the considered time step $\tau - 1$ and the end of the cycle. In fact, Bellman's principle grants that the optimal control law computed at time step τ is optimal also for the case of step $\tau - 1$, save for the single time step between $\tau - 1$ and τ. Therefore, the only control value to optimise is the one between time steps $\tau - 1$ and τ.
The control law defined at the last step of the iteration $\tau = 0$ (the initial time step of the driving cycle) consists of the optimal control law of the problem:

$$u^* = u_0^* \tag{2.33}$$

and the corresponding cost $J^*(0)$ is the optimal cost for the considered problem. In order to verify the optimal cost and the respect of the SOC constraints, a final forward evaluation of the control strategy is carried out by running the model employing u^* as the control law.

The very structure of the Dynamic Programming algorithm, with the optimisation being carried out backwards, makes the strategy evidently non-causal. The driving cycle needs to be known per advance and, consequently, the strategy is unfit for on-line applications. In addition, Dynamic Programming algorithms are very resource intensive, thus being generally slower than algorithms based on Pontryagin's Minimum Principle.
Nevertheless, Dynamic Programming enjoys a quite widespread popularity in energy management applications, serving mainly as a benchmark for the powertrain architecture or for other strategies [45], [46], [47]. Some studies have proposed the utilisation of Dynamic Programming for deriving rule-based control strategies [48], [47]. However, similarly to the case of on-line controllers derived from Pontryagin's Minimum Principle, also these controllers have not yet found a great attention in the scientific community or a vehicle implementation owing to doubts regarding their robustness to different driving cycles.

2.3.4 Equivalent Consumption Minimisation Strategy

The Equivalent Consumption Minimisation Strategy, introduced in [40], [49], is an on-line energy management strategy for HEVs, which provides a solution to problem (2.19) without requiring any future driving profile knowledge.
As stated by the very name of the strategy, its foundation lies in the definition of an equivalent consumption, as follows. When charge-sustaining applications are considered, the battery is functioning merely as an energy buffer. In fact, all energy passing through it is generated by means of burning fuel in the internal combustion engine. During vehicle operation, the electric driveline can power the vehicle and energy from the battery can be used, but then it will be necessary to replenish the battery later on by producing an excess of energy in the internal combustion engine. As a result, the battery can be seen as a reversible fuel tank and an equivalent fuel flow can be formulated:

$$Q_{equivalent} = Q_{fuel} + Q_{batt} = Q_{fuel} + \frac{s}{LHV} \cdot P_{batt} \tag{2.34}$$

The parameter $Q_{equivalent}$ is the equivalent fuel flow of the powertrain, Q_{fuel} is the already presented fuel flow into the engine, and Q_{batt} is the equivalent fuel flow for the battery. LHV is the lower heating value of the fuel, P_{batt} is the power produced or absorbed by the battery, and s is the so called equivalence factor, a weighing parameter employed to convert electric energy into its fuel mass flow equivalent [38].
When the internal combustion engine is using fuel and P_{batt} is greater than zero, both the thermal driveline and the electric driveline are using energy to power the vehicle. The energy of the electric driveline was stored previously (or will be compensated later on) in the battery by burning fuel in the internal combustion engine. Hence, it is clear that the equivalent fuel flow being used at this moment is higher than the simple fuel flow into the engine. Conversely, when P_{elec} is smaller than zero, the battery is storing energy that will be used later and, so, the equivalent fuel consumption is lower than the actual fuel consumption[13].
As a result, the strategy optimizes the equivalent fuel consumption rather than the actual fuel consumption, meaning that the focus is not on engine functioning alone but rather on the whole powertrain operation.
Since ECMS is an on-line control strategy and is conceived for being implemented on actual vehicles, the cost function selected for the application is not anymore (2.15), constituted by the fuel flow alone. Instead, expression

[13] Dissimilarly from actual fuel consumption, equivalent fuel consumption can be negative when the powertrain operates in regenerative braking mode. The physical interpretation of this situation is the following: the vehicle is not employing any fuel but, instead, is storing energy in the battery, energy which will help reducing the actual fuel consumption later on.

(2.16) is preferred by virtue of its ability to impose a limit on the number of engine events. This constitutes a first, basic driveability consideration aimed at improving the driving experience of the vehicle. In addition, being able to control the number of engine events is also convenient for comparison purposes, as it will be explained later on.
As a result, the cost function for the ECMS strategy writes

$$C_{ecms}(\boldsymbol{X_k}, u_k) = Q_{fuel}(\boldsymbol{X_k}, u_k) + \psi \cdot \left(e_{on,k+1} - e_{on,k}\right)^2 \tag{2.35}$$

where ψ is a proportionality coefficient used to weigh the cost of each engine event, similar to γ of (2.16) but specific to the ECMS strategy.
Substituting the fuel flow Q_{fuel} in (2.34) with the cost defined in (2.35), the Hamiltonian of the system is yielded:

$$H(\boldsymbol{X_k}, u_k, s_k) = C_{ecms}(\boldsymbol{X_k}, u_k) + \frac{s_k}{LHV} \cdot P_{batt}(\boldsymbol{X_k}, u_k) \tag{2.36}$$

The working principle of the strategy is straightforward: at each instant of time, the energy management strategy selects the control variable that yields the minimum value of the Hamiltonian, as in (2.37).

$$u_k^* = \arg\min_{u \in U}[H(\boldsymbol{X_k}, u_k, s_k)] \tag{2.37}$$

It goes without words that the selection of the value for the control variable is confined to the values of u_k that ensure the respect of constraints (2.12) and (2.13).
Under some assumptions, it is possible to prove [39] that the Hamiltonian defined in the ECMS strategy (2.36), excluding the term of the cost function limiting the number of engine events, and the Hamiltonian defined in the PMP strategy (2.24) are equivalent. Yet, the PMP strategy yields an off-line controller while the ECMS strategy yields and on-line controller. The reason for this is to be found in the different equivalence terms, λ for the PMP strategy and s_k for the ECMS strategy. It has been shown previously that λ is determined by means of imposing the final condition (2.14) and that this requires knowledge of the future vehicle speed profile, thus yielding an inherently off-line strategy. Conversely, in order for ECMS to be an on-line strategy, s_k has to be determined in an alternative way, not relying on information about future driving conditions.
Several techniques aimed at determining s_k have been proposed since the introduction of the ECMS strategy. A first, simplistic approach was setting s_k equal to one at all times and for any driving cycle [50]. This strategy is definitely perfectible as the constant equivalent factor does not prove effective

in limiting fuel consumption and ensuring SOC sustainability for all driving cycles. Therefore, strategies for adapting the value of s_k on-line were created. Among the most relevant examples, it is possible to mention pattern recognition techniques [51], adaptation on current driving conditions [52], telemetry (T-ECMS) [42], and short-horizon forecast of future driving conditions (A-ECMS) [53].

The strategy adopted in this study is analogous to the one presented in [38]. A proportional controller[14] is employed for adjusting on-line the value of the equivalence factor s_k on the basis of the distance of the current value of SOC from the desired value of the SOC at the end of the cycle:

$$s_k = s_0 - k_p \cdot (x_k - \overline{x}) \tag{2.38}$$

where k_p is the gain of the proportional controller and s_0 is the initial value of the equivalence factor. This value, common to all driving cycles, in theory should be as close as possible to the optimal value of the equivalence factor along the driving cycle, in order to yield a value of s_k that only slightly differs from the optimal equivalence parameter. In the presented work, the value of s_0 is determined, off-line, as the average optimal value of the equivalence factor for a relevant sample of reference driving cycles. Anyway, simulations have shown that a great deal of precision is unnecessary in determining the value of s_0, as the results present no significant difference unless the value of s_0 is completely mistaken.

The proportional controller in (2.38) ensures the charge sustainability of the operation by adapting on-line the value of s_k, thus impacting the relative convenience of thermal and electric operation. In fact, when SOC is below its target level $\overline{x}$, the value of the equivalence factor s_k is increased, according to (2.38). In this way electric energy ends up having a higher relative cost in (2.36). The final result is that the powertrain uses more the internal combustion engine to power the vehicle, thus enabling the SOC level to rise. When, instead, the value of the SOC is above its target level, the exact opposite situation verifies: the value of s_k is reduced, electric energy is made cheaper, and the powertrain employs more the electric driveline for powering the wheels, with the result of reducing the SOC level.

This adaptation of the value of s_k proves effective in ensuring the sustainability of the battery SOC and very easy to implement in an on-line platform,

[14] A proportional controller was chosen over a proportional-integral controller, more widespread for ECMS applications, in order to make the tuning of the strategy easier and quicker. However, simulations carried out in the context of this study show that the impact of the addition of the integral term to the controller on results of fuel consumption is greatly limited.

considering that the resources required for implementing the controller (2.38) are greatly limited.

The ECMS strategy has enjoyed a great deal of attention among researchers since it was first introduced. A significant number of studies was carried out on the subject, and many different implementations of the strategy have been proposed, as shortly discussed above and more thoroughly presented in [54]. Several research teams, both from academia and industry, have also moved on to the experimental testing of the strategy [55], [56], [57].
The conclusion deriving from this important research effort is that the ECMS strategy yields satisfactory results of fuel consumption, not far from the optimal results, smoothly ensures self-sustainability of operation, and can be implemented in an on-line platform fairly easily.
Nevertheless, there are still a few open questions regarding the strategy. In fact, due to the unresolved issue of adapting multiple equivalent factors on-line, the ECMS strategy cannot accept additional states to control other than the state of charge of the battery. And, as first presented by this study, the ECMS strategy appears to struggle when some real world driveability constraints are added to the energy management strategy.

2.3.5 Stochastic Dynamic Programming

As it was discussed in Paragraph 2.3.3, Dynamic Programming is an effective strategy for finding the optimal solution of a problem, but its application to the energy management of HEVs is hampered by its inherently off-line nature. A new strategy was developed from Dynamic Programming for obtaining optimal results in on-line applications: Stochastic Dynamic Programming. In fact, Stochastic Dynamic Programming, thanks to the utilisation of statistical information, manages the power split without needing the knowledge of the future driving speed profile. Nevertheless, the solution can be still considered optimal, but in probabilistic terms, as it will be explained further on in the treatise. An introduction to Stochastic Dynamic Programming can be found in [43].
The cornerstone of the strategy lies in modelling the driving cycle as a Markov chain, similarly to what presented in Section 1.3. Recalling equation (1.29), this means that the next vehicle state, in terms of velocity and acceleration, is

expressed as a function of the current vehicle state. If the next value of velocity is known deterministically thanks to the kinematic relation in (1.29), the next value of acceleration is not known exactly but can be expressed in probabilistic terms as a function of current vehicle speed and acceleration.
This approach entails game-shifting consequences on the resolution of the constrained optimisation problem in (2.19), since it allows removing the time dimension from it. As a result, the problem can be reported from a global optimisation to a local optimisation, in this way enabling an on-line implementation of the energy management strategy.
Similarly to the case of the ECMS strategy, the cost function employed assumes the shape of expression (2.16). This is done in order to contain the number of engine events along the driving cycle, providing an improved comfort to the driver, and in order to be able to compare the different strategies with the same number of engine events. Therefore, the cost function for the SDP strategy writes

$$C_{sdp}(\boldsymbol{X_k}, u_k) = Q_{fuel}(\boldsymbol{X_k}, u_k) + \beta \cdot \left(e_{on,k+1} - e_{on,k}\right)^2 \tag{2.39}$$

Equation (2.39) is analogous to (2.35) and (2.16), the only difference being the proportionality coefficient for engine events, which is here named β and is specific to the SDP strategy.
The optimal control variable u^* is found by solving the stochastic shortest path problem in (2.40):

$$\begin{aligned} u^*(\boldsymbol{X_k}) = \arg\min_{u \in U} \mathbb{E}\Bigg[& \sum_{n=1}^{\infty} C_{sdp}(\boldsymbol{X_n}, u^*) \\ & + \alpha \cdot (x_k - \overline{x})^2 \cdot P(V_{on,k+1} = 0) \Bigg] \end{aligned} \tag{2.40}$$

where α is a proportionality coefficient and V_{on} is the indicator of the position of the car key[15].

[15] V_{on} equal to 1 means that the car key is turned on and the vehicle is ready to move. Conversely, V_{on} equal to 0 means that the car key is turned off, the vehicle is stopped, the powertrain is off and the driving cycle is concluded.

Analysing (2.40), it is possible to see that the stochastic shortest path problem consists of a minimisation problem, therefore not dissimilar from the minimisation problems solved in other strategies.
However, there are a few key differences. In fact, the strategy is not minimising the actual cost associated with the different power splits, as for the previous strategies. It is, instead, minimising the expected cost, i.e. the cost associated to each state of the vehicle, in terms of speed and acceleration, multiplied times its probability of verifying. In addition, this minimisation is not focusing on present system conditions only, but is carried out over an infinite horizon, starting from current system conditions $\boldsymbol{X_k}$.
Considering that, with the removal of time dependence, constraint (2.14) is lost, an additional term regarding the SOC level is added to the function to minimise. This term is employed to grant the self-sustainability of the powertrain operation, by means of introducing an additional cost in case the current SOC is distant from the desired value of the final SOC. The importance of this cost is determined by the proportionality coefficient α, which, therefore, defines how tight is the control on the SOC. It is important to note that also this term is a probabilistic cost, since one of the multipliers is the probability of turning off the car key in the next time step [58]. In fact, it is in the strategy's interest to have a SOC close to the target SOC only if it is likely that the driving cycle is at its end. On the contrary, imposing a constraint on the SOC level while it is impossible that the driving cycle will terminate in a short time is unnecessary and can penalise the final results of fuel consumption yielded by the strategy.
The utilisation of the expected cost in the strategy marks a clear difference with the case of Dynamic Programming. There, the actual cost was minimised and, consequently, the optimal control law was yielded. The results yielded by the SDP strategy are not optimal in the strictest sense, but are optimal in probabilistic terms. In other words, if the state of the vehicle evolves in its most likely way, the SDP strategy outputs the optimal control law. Clearly, this is not always the case, and the results obtained by employing the SDP strategy are generally worse than the optimal results.

An introduction to the theoretical basis of the SDP strategy has been presented. As for the practical implementation of SDP as the energy management strategy, it is carried out with the following steps:

1. As it was done for the random cycles generation in Section 1.3, a sample of reference driving cycles is analysed and a series of probability distribution functions for the next value of acceleration, depending on current velocity and acceleration, is generated;
2. The state variables presented in Table 2.2 are properly discretized into a finite number of values:

$$\begin{aligned} x &= \{x_1, x_2, \dots, x_{Nx}\}^T \\ v &= \{v_1, v_2, \dots, v_{Nv}\}^T \\ a &= \{a_1, a_2, \dots, a_{Na}\}^T \\ e_{on} &= \{e_{on,1}, e_{on,2}\}^T \end{aligned} \tag{2.41}$$

3. All the possible combinations of the state variables are grouped into a four dimensional matrix;
4. Problem (2.40) is solved for all the possible combinations of the state variables in the matrix. The resolution is carried out off-line and recursively, using a policy iteration method [59] and arresting when the reduction in the cost obtained with the new iteration is below a given threshold. The result is a time-invariant four dimensional map, having as inputs the discretised system states presented in (2.41), x, v, a, e_{on}, and as output the value of the optimal control variable u^*. An excerpt of the control map, since four dimensional maps cannot be easily represented in figure, is presented in Figure 2.4 below;
5. The control strategy is implemented on-line by using the four dimensional map generated in point 4. During vehicle utilisation, the map, according to the current state of the system, dictates the most convenient value of the engine torque, managing in this way the torque repartition in the powertrain in an on-line fashion.

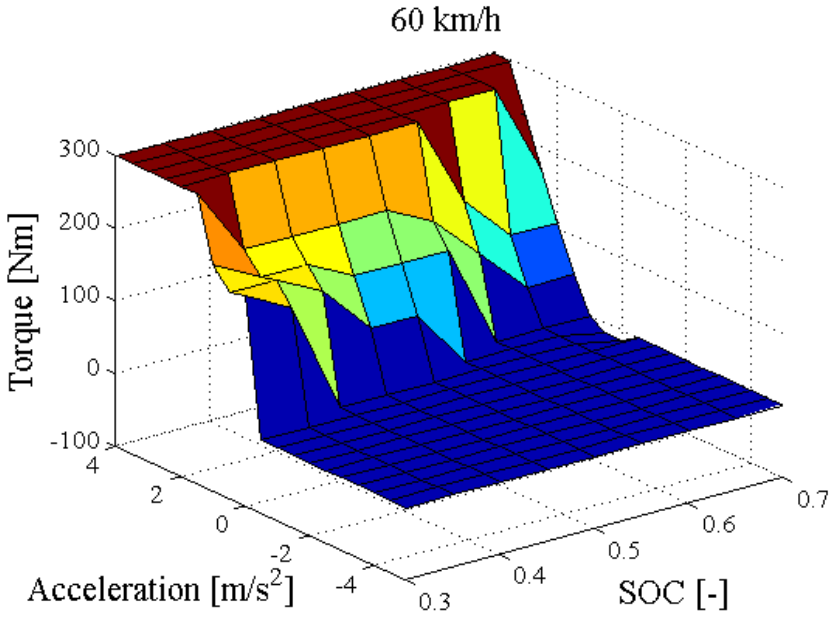

Figure 2.4 – Control map for fixed values of speed (60 km/h) and engine state (engine on) and multiple values of SOC and acceleration

The SDP strategy proves being an effective solution for energy management in HEVs, yet it has only received a limited interest in the scientific community thus far, especially if compared to the ECMS strategy. A strong development to the strategy has been carried out at the University of Michigan [58], [60], [61], [62]. Lately, a few other players have shown interest in the strategy: IFP Energies nouvelles [63], the University of Minnesota [64], and Renault S.A.S. [65].

The first results regarding the strategy are fairly encouraging: the strategy can be smoothly implemented on-line, it yields a fuel consumption not far from the optimal values, it ensures the SOC self-sustainability [63], it allows a very easy addition of other control states and constraints [61], and it naturally presents a good behaviour towards vehicle drivability issues, as introduced in [24], [25], and expanded in the following chapters of this work.

The main difficulty for the strategy at the moment lies in its adaptation to the limited Powertrain Control Module (PCM) hardware available on production vehicles. In fact, the four dimensional map output by the strategy cannot be implemented on a production vehicle PCM for obvious reasons of lack of memory capacity. A first solution proposed to obviate this problem consists in the utilisation of Artificial Neural Networks (ANN) to implement the strategy on-line in the vehicle [63]. Another viable solution could be the interpolation,

with mathematical formulas, of regular parts of the map or the identification of a set of rules starting from the map produced by the SDP strategy. In this way an on-line strategy is produced, which can be smoothly equipped on a production vehicle. This strategy would ensure satisfactory fuel consumption, in principle better than heuristic strategies, and would be robust to all driving conditions, differently from rule-based strategies derived from the PMP and DP strategies. Anyway, the developments in this direction are just starting to move their first steps.

2.4 Conclusion

The chapter has introduced the problem of energy management in hybrid electric vehicles. The architecture of the control system equipped on HEVs and its basic functioning were first illustrated. Then the powertrain operating mode and the power split, two additional degrees of freedom due to the incorporation of the electric driveline to the powertrain, were presented. It was explained how these two degrees of freedom reduce to one since the power split manages to identify also the powertrain operating mode. Successively, the optimal control problem was defined in rigorous terms.

In the ensuing part, the control strategies providing a solution to the optimal control problem were illustrated, marking a distinction between strategies not containing any explicit optimisation but relying on a set of rules based on intuition and experience (heuristic strategies) and strategies operating an optimisation of the cost function. Among the latter, two families were identified: the global optimisation strategies and the local optimisation strategies. The former produce the optimal results of fuel consumption but require the knowledge of the driving cycle per advance, yielding a strategy that is inherently non-causal and is implementable only in off-line applications. Notable examples of such strategies are the Pontryagin's Minimum Principle and the Dynamic Programming. The local optimisation strategies, instead, do not require any knowledge regarding future driving conditions and are thus causal strategies that can be implemented in on-line applications with ease. Examples particularly worth mentioning in this family of strategies are the Equivalent Consumption Minimisation Principle and the Stochastic Dynamic Programming.

Chapter 3

Strategies calibration and fuel consumption results

In Chapter 2, the most widespread energy management strategies were presented. A distinction was made between on-line and off-line energy management strategies, explaining how only the former are suited for in-vehicle application. The study proposes to identify the most suitable energy management strategy to equip on actual vehicles; as a result, the focus is on on-line strategies. Considering that heuristic strategies, owing to their structural limitations explained in Paragraph 2.3.1, do not constitute an optimal solution to the energy management problem, attention in the analysis will be then laid upon local optimal energy management strategies: Stochastic Dynamic Programming and Equivalent Consumption Minimisation Strategy.
In this chapter, the process of calibration of the two strategies mentioned above is illustrated. Then, results yielded by the optimal calibration of the two strategies are analysed and compared to the optimal results yielded by an off-line strategy based on Pontryagin's Minimum Principle. In the last part of the chapter, the results of fuel consumption, for all strategies, are interpreted by means of a powertrain efficiency analysis.

3.1 Methodology

The goal of the chapter consists in comparing in a rigorous and fair way the energy management strategies previously presented, in order to understand how they manage the energy in the powertrain and how efficient is their operation. As stated previously, the core of the analysis is the comparison of local optimal strategies: Stochastic Dynamic Programming and Equivalent Consumption Minimisation Strategy. However, also a strategy based on Pontryagin's Minimum Principle, even if inherently off-line, is included in the comparison in order to provide a baseline for fuel consumption results. In fact, thanks to the optimal results yielded by PMP, it will be possible to assess how suboptimal results yielded by the two local optimal strategies are.

The three strategies are simulated using the vehicle model of Chapter 1 on 100 driving cycles, randomly generated as described in Section 1.3 and representing different driving conditions (urban, suburban, and mixed). This sample of random driving cycles, which constitutes a clear distinction from the classical approach of employing one single reference driving cycle, was selected in order to test the energy management strategies on realistic and varied conditions. In addition, the wildly different driving cycles in the sample also allow verifying the robustness of the controller to very different driving conditions. The number of driving cycles, 100, was chosen to be quite high with the idea in mind to obtain reliable results from the statistical standpoint and to make possible aberrations in single cycles less significant.

In order to carry out a fair comparison, local optimal strategies are imposed to present the same number of engine events. In fact, it is straightforward that a strategy allowing many engine events tends to be more efficient than a strategy imposing a limited number of engine events, as it is less constrained and, consequently, more optimal. The number of engine events was then limited to 2 per minute, a value that appears being appropriate for ensuring a sufficient comfort to the driver.

Final condition (2.14) cannot be strictly enforced in on-line strategies as the entire driving cycle is not known beforehand. As a result, on-line strategies will yield a variety of SOC values at the end of the driving cycle, in the vicinity of the target SOC but generally different from it. In order to have an equal comparison energy-wise, fuel consumption results are adjusted to compensate for a final SOC value different from the target SOC. The adjustment is carried out with an interpolation employing different values for the final SOC to find the equivalent fuel consumption if the SOC were equal to its target value.

Finally, it is reminded that the initial SOC value and the target SOC value are equal to 50 % throughout the whole study.

3.2 Calibration of the local optimal energy management strategies

Local optimal energy management strategies perform an instantaneous optimisation of the cost function, trading off fuel consumption with the requirement of SOC sustainability and the limitation of engine events.

In order to determine the relative importance of these three goals, two proportionality parameters were introduced for each strategy, one to insure the SOC sustainability and the other to limit the number of engine events. In the SDP strategy the two parameters were, respectively, α (2.40) and β (2.39). In the ECMS strategy these two parameters were k_p (2.38) and ψ (2.35).

A proper calibration of these parameters is required in order to grant a satisfactory behaviour of the energy management strategy. The calibration process is carried out by means of simulation of the strategies over the sample of 100 random driving cycles, following a fairly simple methodology. A threshold of acceptability for the results of final SOC and of number of engine events is defined; then, the selected calibration is the one that minimizes fuel consumption while complying with the imposed threshold.

3.2.1 Calibration of the SDP strategy

CALIBRATION OF PARAMETER α (SOC sustainability)

Parameter α, introduced in (2.40), is the proportionality parameter determining how tightly the value of the SOC is controlled. Its impact is shown by Figures 3.1 and 3.2 below, representing the SOC profiles yielded by different values of α on the same driving cycle.

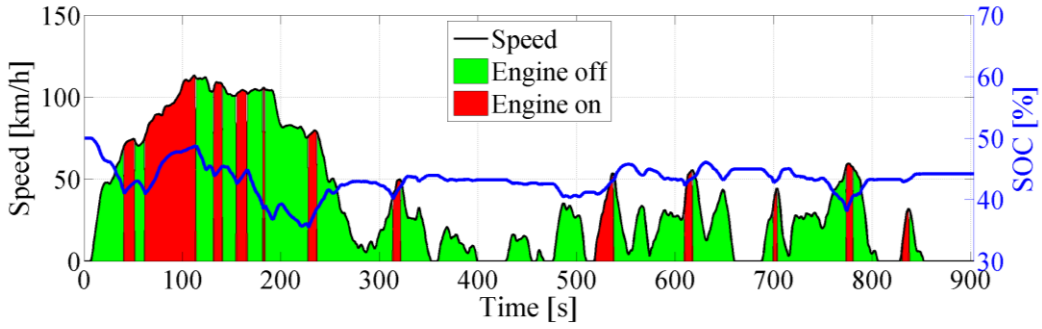

Figure 3.1 – SOC profile over a random driving cycle for a value of α = 10

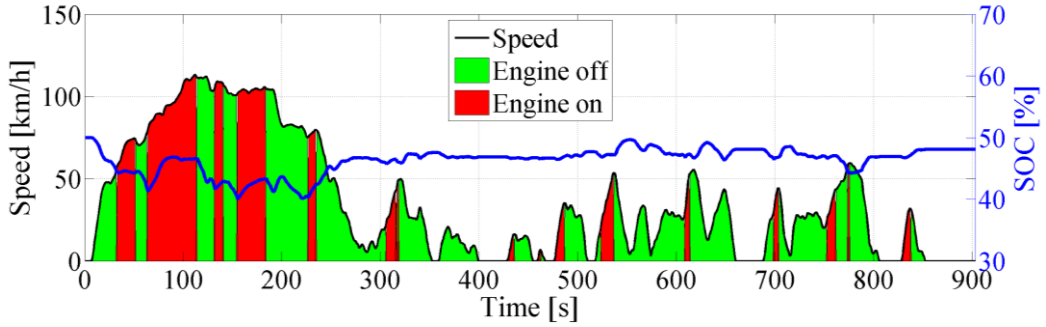

Figure 3.2 – SOC profile over a random driving cycle for a value of $\alpha = 80$

Parameter α has a significant impact on the profile of the battery SOC: the greater α of Figure 3.2, in fact, ensures a tighter control on the SOC with respect to the α of Figure 3.1. As a result, the greater α allows for smaller SOC excursions along the driving cycle and yields a final SOC closer to 50 %.

The requirements for selecting the value of α are twofold. First off, the final value of the SOC should not be too low, in order to grant the possibility of employing the electric driveline at the beginning of the following driving cycle. It is quite difficult to define univocally a threshold below which a final SOC is too low, considering that the concept of acceptable final SOC depends on the utilisation of the vehicle at the beginning of the following driving cycle. In the study, a minimum final SOC of 40 % is required for each of the 100 random driving cycles, in order to grant charge sustaining operation of the hybrid powertrain with sufficient robustness.

The second requirement for selecting the value of α is that the SOC should always be contained in the acceptable window [30 % – 70 %], defined by the battery manufacturer to ensure durability and efficient operation of the battery[16]. This second requirement proves being practically unaffected by the value of α, as when the value of SOC is far from the target SOC the quadratic term in (2.40) proves being dominant over the value of α. As a result, any value of α, as long as different from 0, manages to comply with the request of the SOC level never exceeding its prescribed boundaries in any of the 100 random driving cycles.

The impact of α on fuel consumption, number of engine events, and final value of the SOC is analysed. In order to consider the impact of parameter α alone, the

[16] This constraint can also be implemented by adding a rule on top of the strategy. Anyway, the comparison that is being carried out in this chapter intends to compare the strategies in their original form, without adding further rules on top of them. Hence, the respect of the prescribed SOC window must be granted by the strategy alone.

analysis is carried out by keeping parameter β constant and equal to 0.001. The average results of the simulation of SDP over 100 random driving cycles for five different values of α ($\alpha = 10, 20, 30, 40, 50$) are thus presented in Figure 3.3.

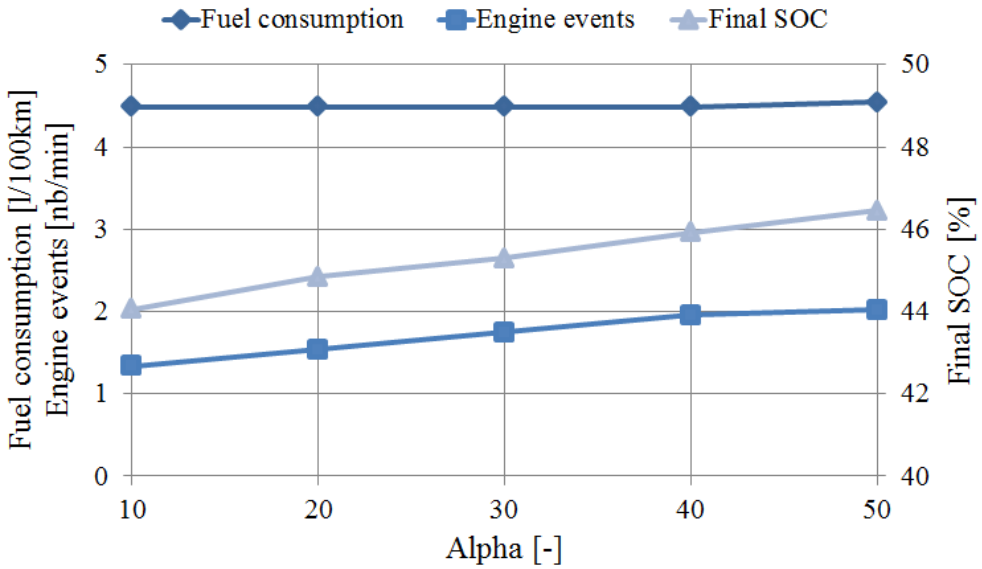

Figure 3.3 – Impact of α on fuel consumption, engine events and final value of the SOC

As expected, the value of α has a significant impact on the average final value of the SOC. Similarly to what was pointed out earlier, for greater values of parameter α, the final SOC is closer to the target SOC. Nevertheless, all presented values of alpha yield fairly high average values of final SOC, all above 44 %.

Secondly, it is possible to notice that greater values of α cause an increase in the number of engine events. The explanation can be found by analysing (2.40): considering that parameter β is constant, when α is big the relative cost of an engine event is reduced, with respect to the cost associated to the control of the SOC. As a result, when α is big, the strategy tends to give place to more engine events.

As regards fuel consumption, the results reported in Figure 3.3 would make one believe that the value of α does not have a noticeable impact on it. This is not the case, as it can be understood by joining the information coming from the trends of fuel consumption and of engine events. In fact, it is reasonable to think that, if the strategy with $\alpha = 10$ were to have the same number of engine events

as the strategy with $\alpha = 50$, then its result of fuel consumption would be significantly better than the one presented in Figure 3.3, as the strategy would be less constrained and more optimal. As a result, it is reasonable to say that a greater value of α would yield worse results in terms of fuel consumption, in case the number of engine events were kept constant[17].

The results presented in Figure 3.3 are helpful to understand the impact of parameter α on the strategy but are not really useful for the calibration procedure, being the values of α too sparse. Figure 3.4 below presents the results for a finer grid of α values, concentrated around the value of α that yielded the most interesting results in Figure 3.3, i.e. $\alpha = 10$, by virtue of its result of fuel consumption achieved with the greatest constraint on the number of engine events.

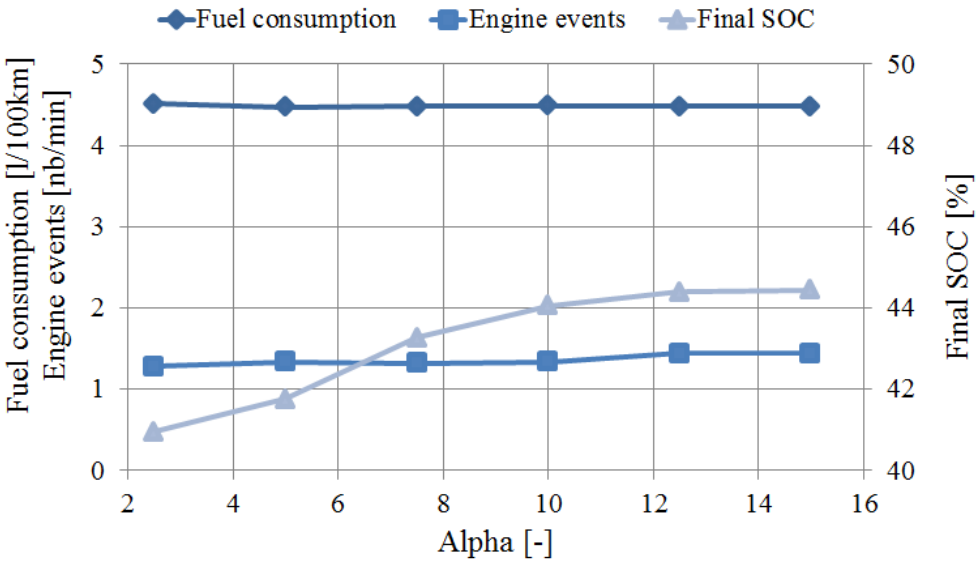

Figure 3.4 – Results of the impact of α in the neighbourhood of $\alpha = 10$

Results of Figure 3.4 show how small variations in the value of parameter α have a really limited impact on the results of fuel consumption and engine

[17] It is practically impossible to provide evidence in support of this reasoning for the SDP strategy. In fact, it is in theory possible to alter the value of β in order to keep the number of engine events constant for the different values of α. Yet, this is unfeasible in reality as it would require generating many SDP maps to find the right value of engine events, eventually demanding an incongruous amount of time for the analysis.
A proof to this conclusion is instead presented further on, while discussing the calibration of parameter k_p in the ECMS strategy.

events. Therefore, the fine tuning of the parameter can neglect such drivers and focus instead on the final value of the SOC.

The value of α is chosen so that to ensure the charge sustainability of the operation for all possible utilisation of the vehicle. As a result, the average value of the final SOC presented in Figure 3.4, even if interesting for understanding the impact of parameter α on the strategy, is not the most appropriate aspect to take into account for the calibration procedure. Instead, the calibration of α is carried out by analysing the final SOC for each of the 100 random cycles, which are a sample of all possible utilisations of the vehicle. The value of α is then chosen as the minimum α ensuring that the final SOC is bigger or equal than 40 % for all the 100 random driving cycles.

The value of α chosen in this way is 10. The terminal values of the SOC for the 100 random driving cycles for the selected value of α are presented in Figure 3.5 below.

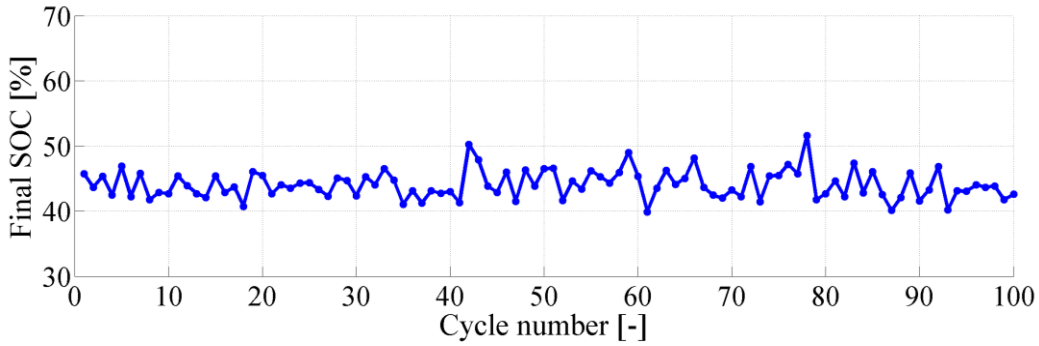

Figure 3.5 – Terminal values of the SOC for the 100 random driving cycles - $\alpha = 10$

CALIBRATION OF PARAMETER β (engine events)

As previously explained, the limitation of the number of engine events along the driving cycle consists of a first, basic driveability consideration to provide the driver with a pleasant driving experience. This limitation is carried out by tuning parameter β.

Parameter β, introduced in (2.39), is the proportionality parameter determining the importance of the cost attributed to an engine event. A high value of β entails a high cost for an engine event in cost function (2.39), eventually

yielding few engine events along the driving cycle. The impact of β is exemplified by Figures 3.6 and 3.7 below, which present the engine state along the same random driving cycle for the SDP strategy with the same value of α ($\alpha = 10$) and different values of β.

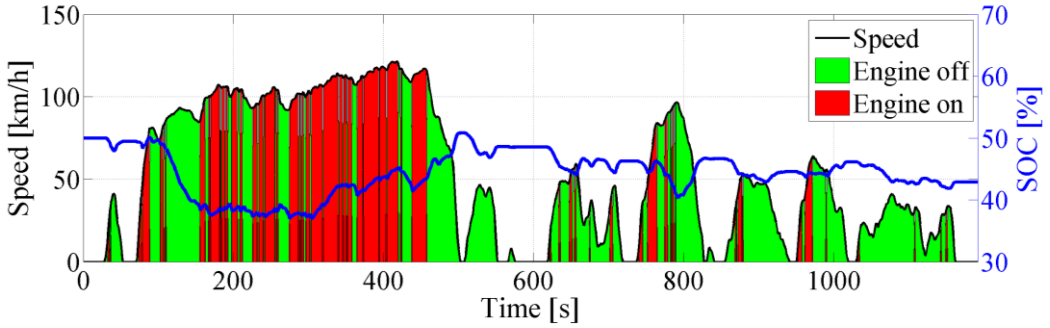

Figure 3.6 – Engine state over a random driving cycle for $\beta = 0$

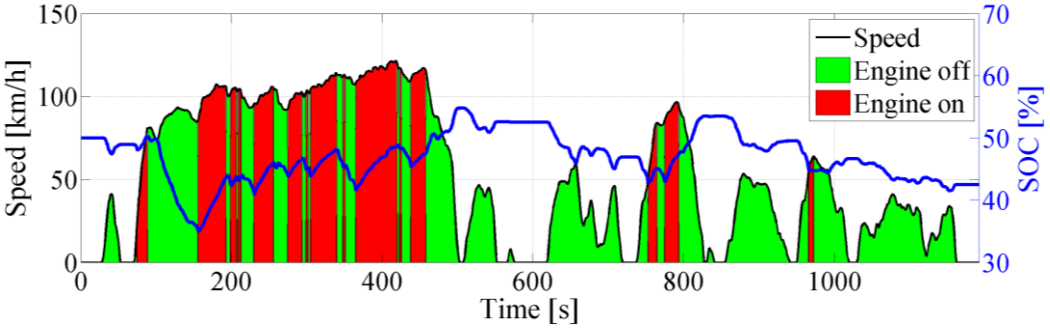

Figure 3.7 – Engine state over a random driving cycle for $\beta = 0.001$

The difference in engine utilisation is evident. When β is equal to 0, there is a huge number of engine events along the driving cycle, with the engine often changing state a few seconds after a previous change. This behaviour would easily result in being annoying for the driver, due to the continuous engine crankings and to the unsteady noise coming from the engine. The situation is improved by increasing the value of parameter β, as shown in Figure 3.7. In fact, using a value of β equal to 0.001, the number of engine events along the driving cycle is significantly reduced and the steadier pattern of utilisation of the engine translates into a more comfortable driving experience for the driver.

Therefore, in order to improve the driveability of the vehicle, calibration of parameter β is done so that the average number of engine events over 100 random driving cycles does not exceed the threshold of 2 events/minute. The

choice of this threshold is arbitrary and, consequently, up for discussion. Such value was chosen here since it appears being reasonable for granting a smooth ride. However, further insights regarding engine events and driveability in Chapter 4 will provide a more realistic approach to the problem.

Similarly to what was done for the analysis on parameter α, the impact of parameter β on fuel consumption, number of engine events and final value of the SOC is analysed. The value of α is fixed ($\alpha = 10$), while different values of beta are tested ($\beta = 0$, 0.00005, 0.0001, 0.00025, 0.0005, 0.00075, 0.001). The results of simulation over 100 random driving cycles are presented in Figure 3.8 below.

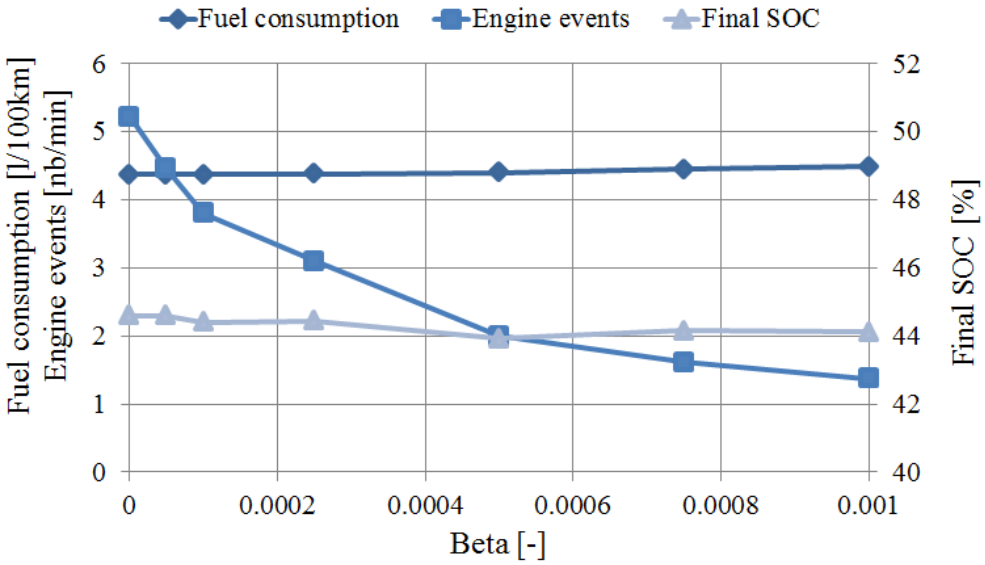

Figure 3.8 – Impact of β on fuel consumption, engine events and final value of the SOC

As expected, parameter β has a strong impact on the average number of engine events, with high values of β greatly reducing the number of engine events along the driving cycle. Fuel consumption shows an increase, even if limited in magnitude, for greater values of β, owing to the increased constraints on the strategy due to the limit on the number of engine events. The value of the final SOC sees a slight decrease for greater values of β due to the lower relative importance of the term associated to SOC control in (2.40).

Calibration of parameter β is done by setting a limit on the average number of engine events (here equal to 2 events/minute) and, then, by selecting the smallest value of β complying with such limit, in order to keep the results of

fuel consumption as low as possible. The final SOC value is non-influential in the choice as its variations due to the different values of β are negligible.
Following the guidelines explained above, the value of parameter β selected for the SDP strategy is $\beta = 0.0005$.
Concerning the impact of parameter β and, consequently, of the number of engine events on fuel consumption, it is interesting to analyse the results presented by Figure 3.9, relating fuel consumption and number of engine events.

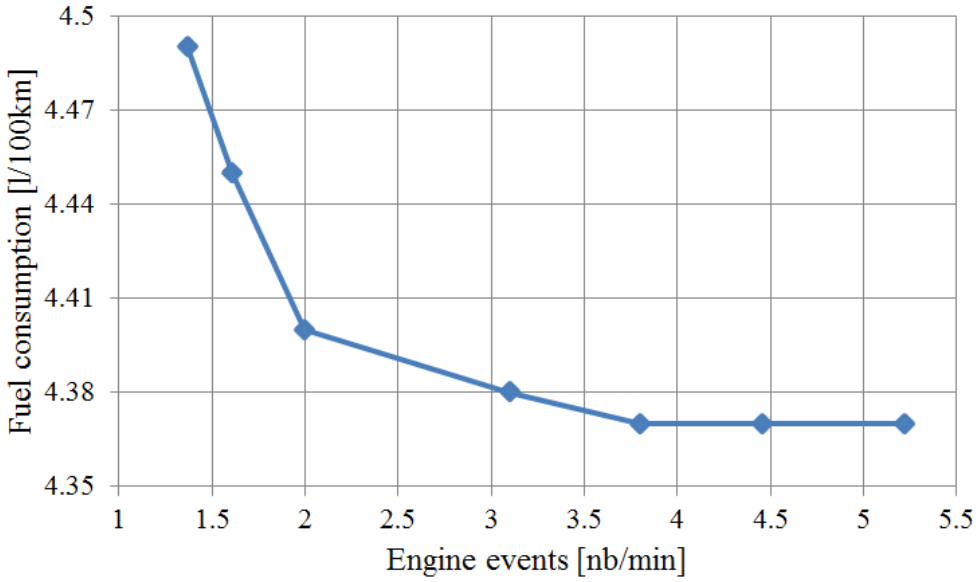

Figure 3.9 – Impact of the number of engine events on fuel consumption

Aside from the general trend of decreasing fuel consumption for an increasing number of engine events, the interest of Figure 3.9 lies in the different slopes presented by the curve. As a matter of fact, if imposing a limit on the number of engine events up to 2 events/minute yields slightly higher fuel consumption, further reductions in the limit of engine events cause a strong increase in fuel consumption. This pattern is very interesting for fine tuning the β parameter. In fact, if the selected threshold for the number of engine events is located in the area presenting a steep variation of fuel consumption, then a small increase in this threshold could yield a significant decrease in fuel consumption. Conversely, if the threshold is placed in the flatter zone, then it would be possible to increase the driver's comfort by reducing the average number of engine events per minute without penalizing fuel consumption excessively.

It is therefore generally advisable to avoid operating in the flat area in the right part of Figure 3.9 and, instead, to lower the limit on the number of engine events until the steep slope area is reached. Anyway, this re-calibration does not apply to the case under analysis as the limit value of engine events is already placed at the point of inflexion between the two different slopes of the curve.

3.2.2 Calibration of the ECMS strategy

CALIBRATION OF PARAMETER k_p (SOC sustainability)

Parameter k_p, introduced in (2.38), is employed in the ECMS strategy to control the SOC value along the driving cycle, assuming a function analogous to the one of parameter α in the SDP strategy.
The impact of different values of parameter k_p is illustrated in Figures 3.10 and 3.11 below, presenting the SOC profile over a random driving cycle for two different values of k_p. Parameter ψ, used to limit the number of engine events, is kept constant and equal to 0.0005.
Similarly to parameter α, parameter k_p has two major impacts on the evolution of the battery SOC. In fact, when k_p is equal to 1, there are quite huge oscillations in the SOC value along the driving cycle and the final SOC is relatively far from 50 %, the target SOC value. Conversely, when the selected value of k_p is 5, oscillations of the value of SOC are much more contained and the final SOC is very close to the target SOC.

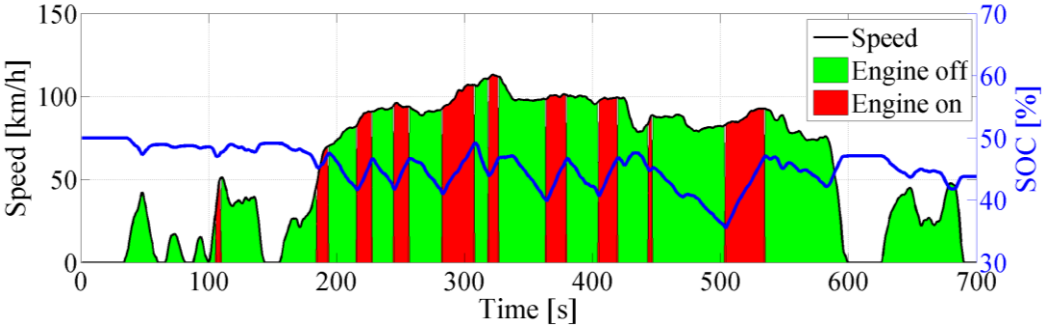

Figure 3.10 – SOC profile over a random driving cycle for a value of k_p = 1

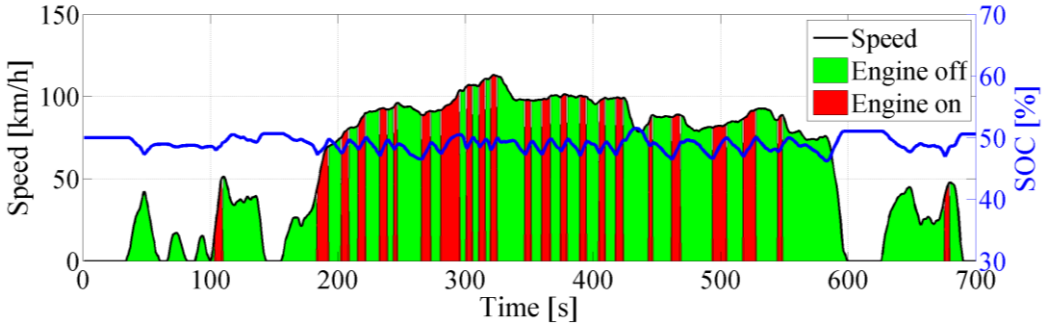

Figure 3.11 – SOC profile over a random driving cycle for a value of k_p = 5

The requirements needing to be fulfilled by the calibration of parameter k_p of the ECMS strategy are two. On the one side, the final SOC value should not be too far from the target value, in order to ensure charge sustainability of the powertrain operation. Therefore, it is required that the final SOC for each of the 100 random driving cycles is equal or greater than 40 %. On the other side, the SOC level should always be within the prescribed SOC window [30 % - 70 %].
Unsurprisingly, these are the same requirements that in the SDP strategy were fulfilled by means of tuning parameter α. Yet, there is one major difference between the two strategies. If in the SDP strategy the respect of the SOC boundaries was achieved with any value of α different from 0, the same cannot be said for the ECMS case. As a result, the value of k_p should be high enough to grant that the SOC value will never exceed the prescribed boundaries.
An example of insufficient value of k_p is shown in Figure 3.12 below.

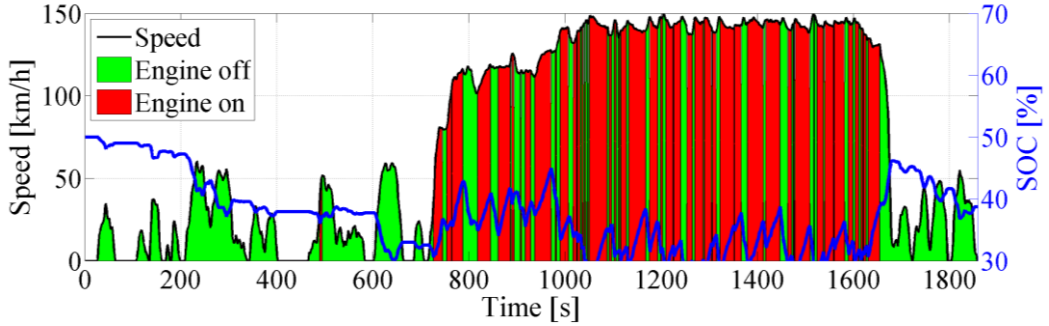

Figure 3.12 – SOC profile over a random driving cycle for a value of k_p = 0.3

Figure 3.12 shows how a value of k_p equal to 0.3 is not sufficient for granting the respect of the lower SOC boundary along the presented driving cycle. Such

high speed cycle proves particularly challenging for the control strategy which, however, needs to be robust to any type of vehicle utilisation.
Consequently, the minimum acceptable value of the k_p parameter has to be chosen by analysing the behaviour of the control strategy on the most extreme driving cycle. In particular, the greatest challenges are posed by driving cycles presenting long periods of time at high speeds, like as the driving cycle depicted in Figure 3.12. In addition, it is good practice to allow a safety margin while choosing the minimum value of k_p. In fact, as shown in Paragraph 3.2.1, when the constraint of a limited number of engine events along the driving cycle is imposed, the control on the SOC profile is reduced because of the different relative importance assumed by terms in the cost function.
For the case under consideration, the minimum acceptable value for parameter k_p, chosen following the guidelines above, is 1.
The impact of parameter k_p on fuel consumption, engine events, and final SOC is studied by simulating the ECMS strategy over the sample of 100 random driving cycles. Five different values of k_p are considered (k_p = 1, 2, 3, 4, 5), while ψ is constant ($\psi = 0.0005$). The results of the analysis are presented in Figure 3.13 below.

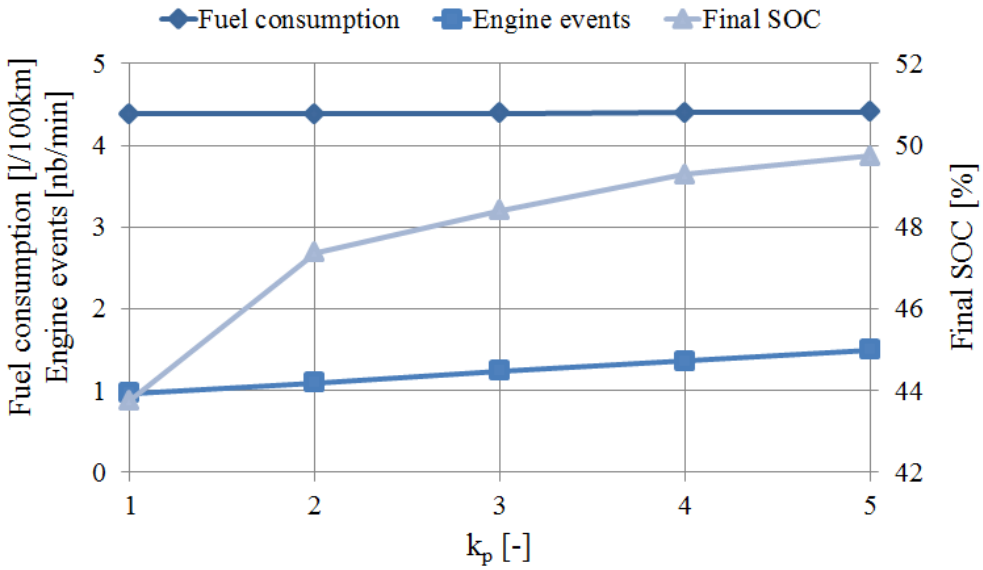

Figure 3.13 – Impact of k_p on fuel consumption, engine events and final value of the SOC

The most relevant impact of parameter k_p is, reasonably enough, on the final value of the battery SOC, with the terminal SOC being closer to the target value

of 50 % when k_p assumes a greater value. Nevertheless, the final SOC for all the considered values of k_p is quite high, being in any case above 44 %.
Also the number of engine events is similarly affected, seeing an increase for higher values of k_p. This is promptly explained by analysing (2.36) and (2.38): when the SOC is below its target value, a high value of k_p yields, on average, relatively high values of s_k. As a consequence, the term associated to the control on the SOC will tend to have a greater relevance in the Hamiltonian with respect to the cost term, which also contains the cost attributed to engine events.
Conversely, fuel consumption is practically unaffected by the variations in the value of k_p. Again, this result should be analysed together with the result of the number of engine events: if all the cases were to have the same number of engine events, it is reasonable to think that the cases with higher k_p would present a higher fuel consumption, due to the more constrained situation with respect to the one illustrated in Figure 3.13. The proof for this reasoning is provided by Figure 3.14, which presents the results of fuel consumption and of final SOC for the different values of k_p employed above, with the values of ψ adapted so that to have a constant average number of engine events, 2 events/minute, for all cases.

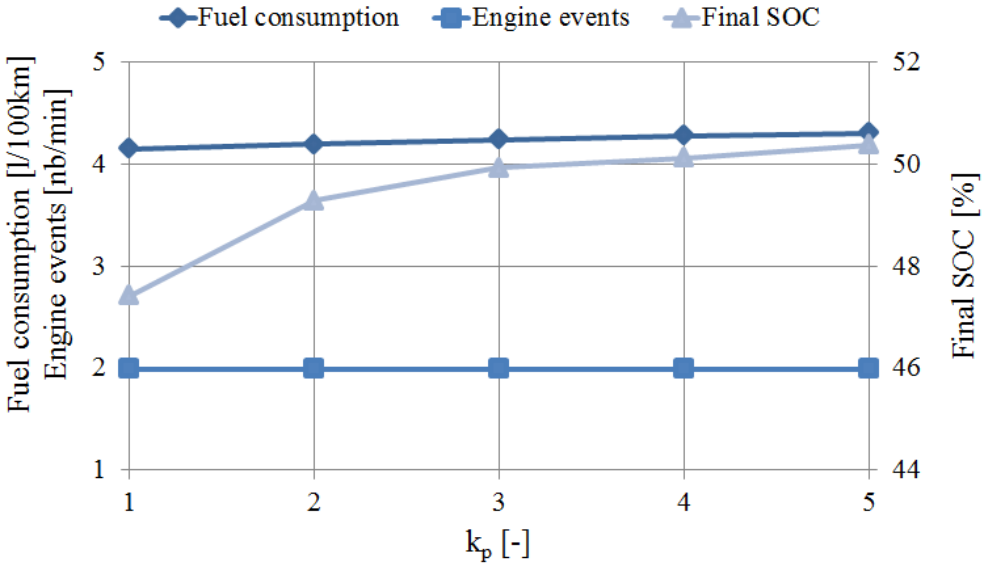

Figure 3.14 – Impact of k_p on fuel consumption and final value of the SOC – Number of engine events is kept constant

As expected, it is now possible to observe an increase in the value of fuel consumption for higher values of k_p, even if limited in magnitude. Anyway, this

trend of fuel consumption is enough to indicate that the optimal choice for calibration is the smallest value of k_p complying with the requirements of terminal SOC and SOC not exceeding the prescribed boundaries.
It was previously stated that all the values of k_p greater or equal to 1 comply with the constraint imposing to have a SOC level within the prescribed boundaries. Also the requirement of having a terminal SOC greater than 40 % for each of the 100 random driving cycles is satisfied by all values of k_p greater or equal to 1, as demonstrated by Figure 3.15, presenting the values of terminal SOC for k_p equal to 1.
As a result, the chosen value of parameter k_p for calibration of the ECMS strategy is 1.

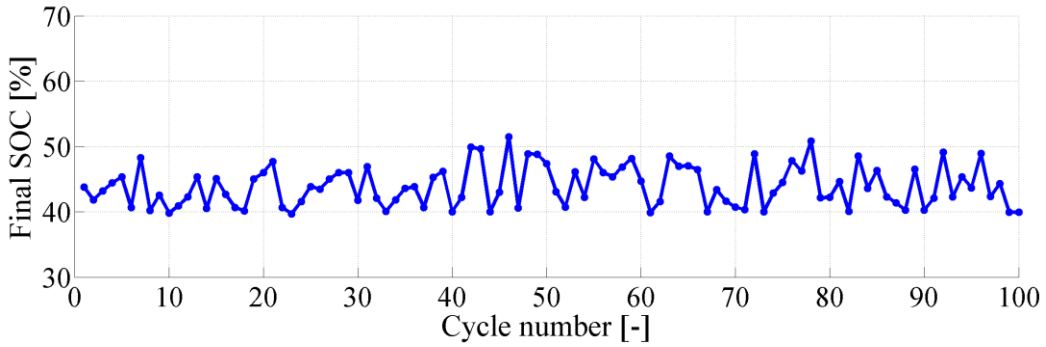

Figure 3.15 – Terminal values of the SOC for the 100 random driving cycles - $k_p = 1$

CALIBRATION OF PARAMETER ψ (engine events)

Parameter ψ, presented in (2.35), is the parameter weighing the cost of engine events in the ECMS strategy. Its function is equivalent to the function parameter β has in the SDP strategy, namely to limit the number of engine events along the driving cycle by imposing a cost for turning on or shutting down the engine.
The study proposes to carry out a fair comparison between the local optimal energy management strategies. In order to do so, it is necessary to impose that both SDP and ECMS present the same number of engine events along each of the 100 random driving cycles in the sample. Since a limit on the number of engine events was imposed on the SDP strategy in Paragraph 3.2.1, and the parameter β was calibrated accordingly, it is now unnecessary to perform the calibration for parameter ψ. In fact, once the value of parameter β is selected,

the value of parameter ψ is univocally defined as the value ensuring the ECMS strategy to yield the same number of engine events as the SDP strategy along the considered driving cycle.

However, it is of sure interest to analyse the impact of parameter ψ on the results of fuel consumption, number of engine events, and final value of the SOC. The results, illustrated in Figure 3.16 and obtained from simulation on the sample of 100 random driving cycles, are for values of ψ varying ($\psi = 0$, 0.00005, 0.0001, 0.00025, 0.0005, 0.00075, 0.001) and k_p constant ($k_p = 1$).

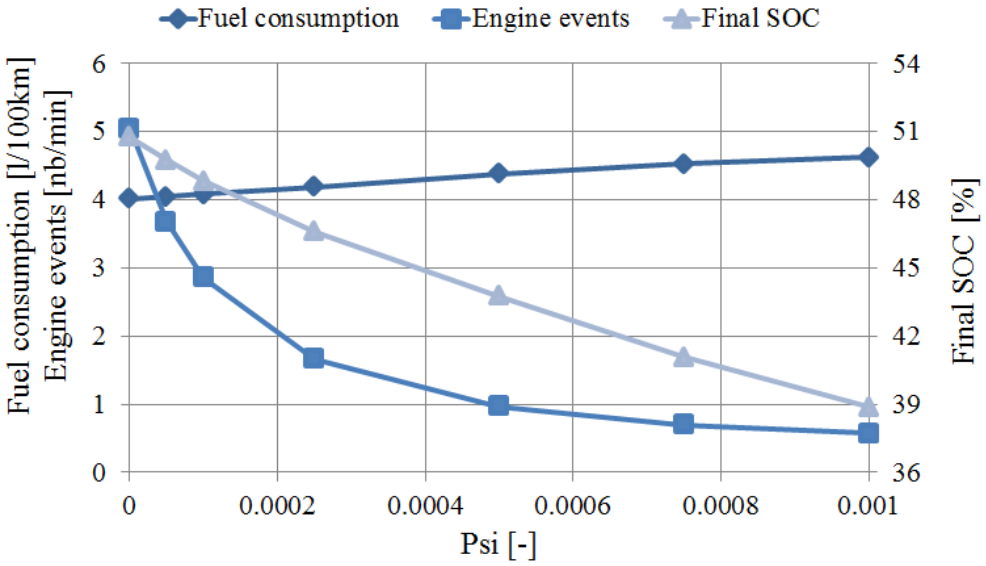

Figure 3.16 – Impact of ψ on fuel consumption, engine events and final value of the SOC

As expected, parameter ψ has a strong impact on the number of engine events, which decrease when ψ increases. It is also interesting to compare the response of SDP and ECMS to variations of the proportionality coefficient associated to the number of engine events, especially considering that tested values of ψ are the same as tested values of β. Both strategies present a similar number of engine events when β and ψ are 0. On the contrary, for greater values of the proportionality coefficient, the number of engine events yielded by the ECMS strategy is significantly lower than the number yielded by the SDP strategy. As a result, a greater sensitivity towards the proportionality coefficient is noted for the ECMS strategy.

This greater sensitivity is confirmed by results of fuel consumption. Fuel consumption shows an increase for both strategies when the proportionality

coefficient β or ψ is increased, but the increase presented by the ECMS strategy is decidedly more important.
It is also interesting to note the profile followed by the terminal value of the SOC: an increase in the value of ψ determines a significant increase in the distance of the terminal SOC from its goal value, 50 %. This is due to the fact that a high value of ψ results in being dominant over the value of s_k, shifting in this way the importance in the Hamiltonian (2.36) towards the limitation of the number of engine events rather than on the control of the SOC. It is also interesting to point out how the SDP strategy does not present such a pronounced sensitivity towards parameter β, as it was presented in Figure 3.8. The reason for this different behaviour lies in the different formulation of the functions to minimise for the two strategies. The ECMS strategy minimises Hamiltonian (2.36), where all targets of optimisation (fuel consumption, number of engine events, final value of the SOC) are active and competing at all times. On the contrary, the SDP strategy minimises a probabilistic cost in (2.40). The introduction of probabilities in the function to minimise, especially the probability of turning off the vehicle key, manages to separate pretty effectively the times at which the different targets of optimisation are dominant. The ensuing result is that the parameter associated to the limitation of engine events does not have a significant impact on the results of the terminal SOC.
To conclude the analysis, it is possible to state that calibration of parameter ψ in the ECMS strategy has a greater impact on the behaviour of the strategy rather than calibration of parameter β in the SDP strategy. As a result, it is of particular importance to select the most appropriate value of ψ in the ECMS strategy, as this parameter significantly affects all results of the strategy. On the contrary, the choice of parameter β in the SDP strategy can be done more freely, by virtue of the greater robustness of results to variations of β.

3.3 Simulation results and analysis

3.3.1 Simulation results

In this section, performances of the control strategies are assessed through simulation over the sample of 100 random driving cycles. The strategies are evaluated on results for fuel consumption, average number of engine events, and final SOC.

The focus of the study is on local optimal energy management strategies. Therefore, the results of SDP and ECMS strategies, tuned as described in Section 3.2, constitute the central part of the analysis. However, also the results of other strategies are presented here for comparison purposes.
First off, the result for the purely thermal vehicle is shown, in order to provide an indication regarding the gains in fuel consumption brought by the hybridisation of the powertrain.
Then, the results yielded with the PMP strategy are presented. Due to the guarantee of optimality associated with the PMP strategy, these results will be employed as a baseline in the study, pointing out the distance of results of local optimal strategies from optimal results.
In addition, also the results for the unconstrained SDP and ECMS strategies are presented. These strategies are defined unconstrained as they do not incorporate any limit on the number of engine events (parameters β and ψ equal to 0). In this way, it is possible to distinguish in the results of fuel consumption the impact of the constraint on the number of engine events from the sub-optimality inherent to local-optimal strategies[18].
The results yielded by the different strategies simulated over the sample of 100 random driving cycles are then presented in Table 3.1 below.

Table 3.1 – Results for simulation over 100 random driving cycles of the different energy management strategies

Strategy name	Fuel consumption [l/100km]	Engine events [nb/min]	Final SOC [%]	Gain /pure thermal [%]
Pure thermal	9.35	-	-	-
PMP	3.97	5.14	50	57.5
SDP unconstrained	4.37	5.22	44.59	53.3
SDP	4.4	2	43.93	52.9
ECMS unconstrained	4.02	5.05	50.78	57
ECMS	4.15	1.99	47.43	55.6

The first thing it is possible to notice is that the hybridisation of the powertrain is able to greatly impact fuel consumption, with gains above 50 % independently

[18] With sub-optimality inherent to the strategy it is intended to indicate the sub-optimality in the choice of engine torque and in the management of engine state operated by the local optimal strategy.

from the employed control strategy. This is mainly due to the fact that the considered internal combustion engine consists of a high power engine, which operates in highly inefficient areas during normal operation due to the limited power required to move the vehicle in most driving conditions. The introduction of the electric driveline allows modifying the engine operating points, with the subsequent increase in engine operating efficiency leading to the improved fuel consumption results presented above.

Comparing now the different energy management strategies, the best results are, of course, obtained with the PMP strategy, which yields the optimal solution to the problem.

The local optimal strategy presenting the best results of fuel consumption is the ECMS strategy, which yields a fuel consumption that is about 6 % lower than the one yielded by the SDP strategy, when the limit on the number of engine events is enforced[19]. In addition, the ECMS strategy proves its efficiency by yielding results that are particularly close to the optimal ones, especially when the unconstrained ECMS strategy is considered.

It is also interesting to analyse the impact of the limit on the number of engine events, by comparing the constrained and unconstrained cases (SDP and SDP unconstrained, ECMS and ECMS unconstrained). The change in fuel consumption due to the limitation of the number of engine events for the SDP strategy is hardly noticeable. This indicates that the distance from the optimal results of fuel consumption in the SDP strategy is mainly due to the sub-optimality inherent to the strategy itself, rather than to the constraint on the number of engine events. On the contrary, the fuel consumption results yielded by the ECMS strategy present a greater sensitivity to the imposition of a limit on the number of engine events. Consequently, it is correct to state that the distance from the optimal results of fuel consumption in the ECMS strategy is mainly due to the imposition of a limit on the number of engine events rather than on the sub-optimality inherent to the ECMS strategy. It is therefore possible to conclude that ECMS is a particularly efficient but sensitive strategy, while SDP is less efficient but certainly more robust.

Finally, it is possible to notice how the calibration procedure illustrated in Section 3.2 yields a value of the average final SOC that is closer to 50 % for the

[19] Even if the difference in fuel consumption results between the SDP and ECMS strategies appears being limited, it is important to point out how a difference of 6 % can translate into significant savings for the customer. In addition, the implementation of either local optimal strategy in the vehicle does not require any particular additional hardware, thus the switch from a strategy to the other can be done “for free”.

ECMS strategy with respect to the SDP strategy. Anyway, this does not constitute a preferential factor in the choice of the energy management strategy, as the control on the SOC is a constraint rather than a result to optimise, and compliance with the minimum final SOC and with the SOC boundaries along the cycle is ensured by both strategies.

3.3.2 Analysis of the results

Paragraph 3.3.1 presented a comparison of the results yielded by different energy management strategies. These results allowed drawing a first conclusion on the convenience of the two local optimal energy management strategies.
It is of sure interest to go deeper in the analysis and to find an explanation for the results presented in Table 3.1. Therefore, in this paragraph, an efficiency analysis for the energy management strategies is presented, on two levels: first, the engine efficiency is considered. Then, the whole powertrain efficiency is analysed.

ENGINE EFFICIENCY

The first step in the analysis consists in looking at the utilisation profile of the engine, understanding which operating points are favoured by each strategy. The analysis is carried out on one single driving cycle as plotting the engine operating points for 100 driving cycles on the same figure would make the interpretation of results just impossible. However, it is important to state that, even if the profile of utilisation of the engine that will be shown refers to one single driving cycle, the pattern in engine utilisation is general. In fact, all the 100 random driving cycles present a similar engine utilisation, with only limited differences due to the different cycle types.
The driving cycle, pictured in Figure 3.17, was chosen among the sample of 100 random driving cycles. The interest for this particular cycle lies in its mixed profile, partly urban and partly sub-urban, which gives place to a variety of engine operating points.

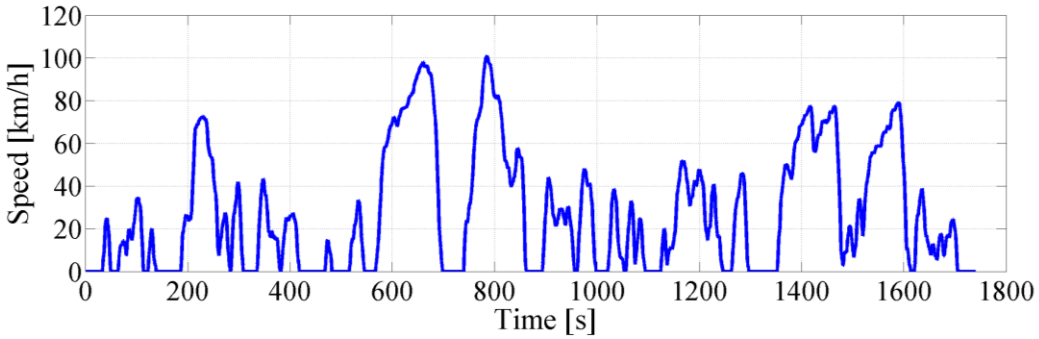

Figure 3.17 – Speed profile of the considered random driving cycle

The engine operating points for different strategies on the driving cycle presented above are illustrated in Figure 3.18. In order to provide clear results, only the two local optimal energy management strategies, in their constrained form, and the PMP strategy are considered in this step of the analysis.

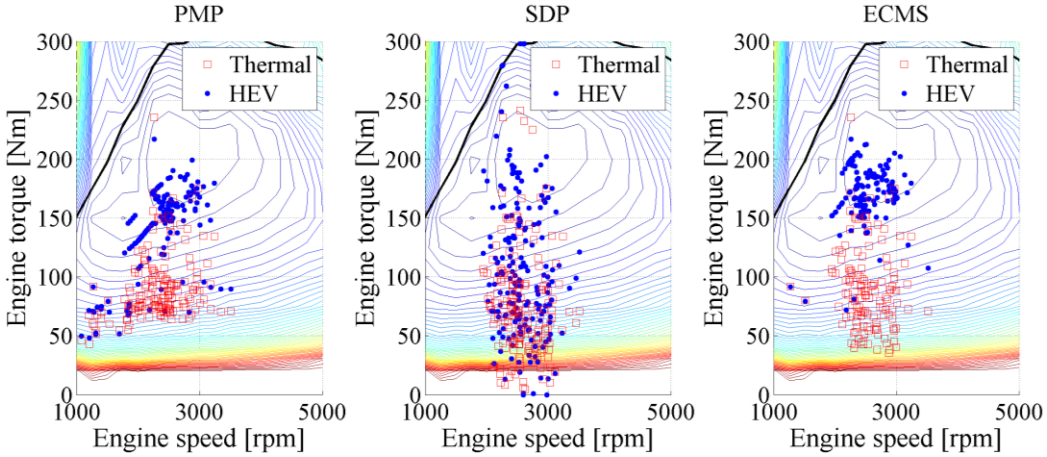

Figure 3.18 – Engine utilisation points for the considered random driving cycle

The first consideration that can be made regards the difference in torque utilisation between the engine of a purely thermal powertrain, presented in red, and the same engine in a hybrid powertrain, presented in blue[20]. Hybridisation, for all strategies, shifts the engine operating points towards higher torque values, thus entailing a more efficient utilisation of the engine. This is the main reason

[20] Engine operating points for the thermal powertrain (points in red) differ for the three considered strategies. This is because each plot shows, for illustrating the shift in engine operating points, only the engine operating points for the thermal powertrain that correspond to the time steps with the engine turned on for the hybrid powertrain.

for the reduction in fuel consumption due to hybridisation, presented in Table 3.1.
Furthermore, it is possible to observe distinct approaches to engine utilisation for different strategies. In fact, the ECMS strategy employs the engine almost uniquely in its optimal operating area, at high levels of torque. On the contrary, the SDP strategy uses the engine in a multitude of operating points, also including lower efficiency areas. The PMP strategy places itself in between the two local optimal strategies, employing the engine in higher efficiency regions than the SDP but not showing such a concentration of points in the optimal zone as the ECMS.
When one considers the two local optimal strategies, the engine utilisation pattern appears to confirm the results presented in Table 3.1. In fact, it is easy to understand how the ECMS strategy translates its more optimal engine utilisation profile into a better fuel consumption than the SDP strategy. However, the same cannot be said when ECMS and PMP are being compared. In Figure 3.18, the engine utilisation profile of ECMS appears being more efficient than the one of PMP, while the theory of optimal control, and results in Table 3.1, state that PMP produces the optimal solution to the control problem. This implies that the engine utilisation profile, even if relevant, is not the sole factor to take into account for understanding results of fuel consumption. In fact, even if in the considered hybrid architecture all the energy delivered to the wheels originates from the engine, it is also of primary importance to consider the energy transformations taking place in the powertrain.

POWERTRAIN EFFICIENCY

In order to better understand and justify the results presented in Table 3.1, the global efficiency of the powertrain operation needs to be analysed.
The parallel hybrid architecture allows two possible pathways to the wheels for the energy produced by the engine: a direct pathway, going directly from the engine to the wheels, and an indirect pathway, passing through the battery and the electric motor. The two pathways are illustrated in Figure 3.19 below.

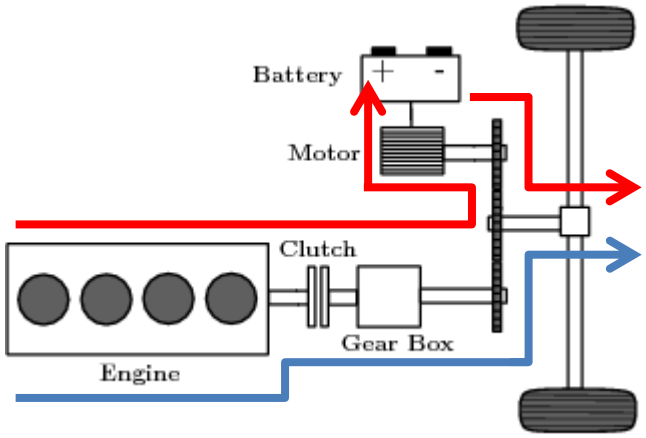

Figure 3.19 – The two pathways to the wheels – The direct pathway is presented in blue and the indirect pathway is in red

The efficiency of each pathway is defined by multiplying the efficiencies of single components in the pathway. The efficiency of a single component at the generic time step k is defined as

$$\eta_{component,k} = \frac{E_{out,component,k}}{E_{in,component,k}} \tag{3.1}$$

where $E_{out,component}$ and $E_{in,component}$ are, respectively, the energy output and the energy input of the component in the considered time step.
The efficiencies of components of the powertrain are known, either as design parameters or by means of experimental characterisation. These efficiencies are expressed with a map depending on several parameters (engine, motor, battery) or with static values (clutch, gears, differential).
It is possible to compute the efficiency of the entire driveline, by joining the single efficiency values of the components. The efficiency of the direct pathway at time k writes:

$$\eta_{direct,k} = \eta_{engine,k} \cdot \eta_{clutch} \cdot \eta_{gearbox,k} \cdot \eta_{differential} \tag{3.2}$$

It is reminded that the efficiencies of the clutch and of the differential are static values, independent from time. Conversely, $\eta_{gearbox}$ presents a dependence on time because of the possibly different efficiencies corresponding to different gears engaged at different times along the driving cycle.

The efficiency of the indirect pathway is distinguished into two alternative efficiencies, one associated to the instants of time when the battery is being recharged and the other when the battery is being discharged. In order to avoid redundancies, the efficiency of the battery is conventionally considered only when the battery is being discharged.

$$\eta_{indirect,rech,k} = \eta_{engine,k} \cdot \eta_{clutch} \cdot \eta_{gearbox,k} \cdot \eta_{motor,k} \tag{3.3}$$

$$\eta_{indirect,disch,k} = \eta_{battery,k} \cdot \eta_{motor,k} \cdot \eta_{differential} \tag{3.4}$$

Expressions (3.3) and (3.4) can be joined in order to obtain a single expression for the efficiency of the indirect pathway:

$$\begin{aligned}\eta_{indirect,k} = \eta_{indirect,rech,k} \cdot \left(P_{batt,k} < 0\right) \\ + \eta_{indirect,disch,k} \cdot (P_{batt,k} > 0)\end{aligned} \tag{3.5}$$

where P_{batt} is the power absorbed or produced by the battery[21]. The relational operators $(P_{batt,k} < 0)$ and $(P_{batt,k} > 0)$ are used for switching to the appropriate definition of efficiency for the considered instant of time. The case in which the battery power is null is not defined as in such case, corresponding to the vehicle standing still, the pathway efficiency is not defined.
Aside from the times the vehicle is standing still, the pathway efficiencies presented above are defined for each time step in the driving cycle. In order to yield a single parameter to describe the operation of the powertrain, an average value of the pathway efficiency is calculated. This is done through the computation of cumulative lost energy in each pathway, which starts from the calculation of the quantity of energy contained in the fuel flow:

$$E_{fuel,k} = Q_{fuel,k} \cdot \rho_{fuel} \cdot LHV \tag{3.6}$$

where Q_{fuel} is the fuel flow, ρ_{fuel} is the fuel density and LHV is the fuel lower heating value.
Then, the quantity of energy passing through each driveline can be computed:

[21] According to the convention presented in Chapter 1, the power absorbed by the battery is attributed a negative sign, the power produced by the battery a positive sign.

$$E_{direct,k} = E_{fuel,k} \cdot ES_k \tag{3.7}$$

$$E_{indirect,k} = E_{fuel,k} \cdot (1 - ES_k) \tag{3.8}$$

where ES is the energy split, a parameter defined as in (3.9) and known as soon as the control variable, presented in (2.8), is known[22].

$$ES_k = \frac{E_{direct,k}}{E_{direct,k} + E_{indirect,k}} \tag{3.9}$$

Once the quantity of energy passing through each driveline during one time step is computed, the cumulative energy input to each driveline for the entire driving cycle is easily found as in (3.10) and (3.11).

$$E_{input,direct} = \sum_{k=1}^{N} E_{direct,k} \tag{3.10}$$

$$E_{input,indirect} = \sum_{k=1}^{N} E_{indirect,k} \tag{3.11}$$

where it is reminded that N is the final time step of the considered driving cycle. Similarly, the cumulative lost energy in each pathway for the driving cycle is computed:

$$E_{lost,direct} = \sum_{k=1}^{N} \left[\left(1 - \eta_{direct,k}\right) \cdot E_{direct,k} \right] \tag{3.12}$$

$$E_{lost,indirect} = \sum_{k=1}^{N} \left[\left(1 - \eta_{indirect,k}\right) \cdot E_{indirect,k} \right] \tag{3.13}$$

[22] In Chapter 2, it was demonstrated that determining the control variable is enough to define all torques and powers in the powertrain. Once all powers for one given time step are known, the energy transiting each driveline in that time step can be calculated by multiplying the power on each driveline times the time step duration.

The drivelines' average efficiency is then obtained with the following expressions, equivalent to the efficiency definition (3.1):

$$\eta_{avg,direct} = 1 - \frac{E_{lost,direct}}{E_{input,direct}} \tag{3.14}$$

$$\eta_{avg,indirect} = 1 - \frac{E_{lost,indirect}}{E_{input,indirect}} \tag{3.15}$$

Another useful parameter in the analysis of the powertrain operation is the fraction of energy that passes through the direct pathway, defined as:

$$Z_{direct} = \frac{E_{input,direct}}{E_{input,direct} + E_{input,indirect}} \tag{3.16}$$

It is interesting to note that Z_{direct} is the averaged version, as it employs cumulative values of energy, of the energy split ES, defined in (3.9).
It is then possible to compute the average powertrain efficiency, which writes:

$$\eta_{avg,powertrain} = \eta_{avg,direct} \cdot Z_{direct} + \eta_{avg,indirect} \cdot (1 - Z_{direct}) \tag{3.17}$$

Powertrain efficiency, opposed to engine efficiency, constitutes a more appropriate indicator for interpreting the results of fuel consumption of hybrid vehicles. This is motivated by the fact that, for powertrain efficiency, the entire powertrain operation is taken into account. Conversely, engine efficiency only focuses on the behaviour of one single component of the powertrain.
The results of the efficiency analysis for the sample of 100 random driving cycles are presented in Table 3.2 below[23]. The impact of regenerative braking on the overall powertrain efficiency is here neglected.

[23] The results for the efficiency analysis omit the unconstrained local optimal strategies (unconstrained SDP and unconstrained ECMS) in order to provide fewer, clearer data for interpretation. In addition, the efficiency analysis, due to its dependence on an average, is not able to explain small differences in fuel consumption (for instance, between SDP and unconstrained SDP).

Table 3.2 – Efficiency analysis for the different energy management strategies

Strategy name	$\eta_{avg,direct}$ **[%]**	$\eta_{avg,indirect}$ **[%]**	Z_{direct} **[%]**	$\eta_{avg,powertrain}$ **[%]**
Pure thermal	22.8	-	100	22.8
PMP	33.1	21.4	67.7	29.3
SDP	31.2	21.7	67.9	28.2
ECMS	33.9	22.4	56.2	28.9

The first conclusion it is possible to draw from results above is that the hybridisation of the powertrain greatly increases the efficiency of the direct pathway, eventually leading to improved powertrain efficiency. As already explained, this is an effect of the decoupling between the torque demand at the wheels and the torque provided by the engine, which enables a more efficient utilisation of the engine.

Focusing on the hybrid powertrain, it is noted that the indirect pathway has, in all cases, a significantly lower efficiency than the direct pathway. This result appears straightforward when considering the number of components in each pathway. In fact, as illustrated by Figure 3.19, when energy produced in the engine is routed to the wheels through the direct pathway, it only needs to pass through the clutch, the gearbox, and the differential. Instead, when energy from the engine is routed to the wheels through the indirect pathway, it needs to pass through the afore mentioned components, through the motor, twice, and through the battery. Since every component presents an efficiency generally different from 1, the longer chain of components will reasonably present the lower overall efficiency. The conclusion is that it is preferable to route a great part of the energy through the direct pathway. As a result, the direct pathway should be employed especially when the required power at the wheels is huge, i.e. at high vehicle speed and during steep accelerations. Conversely, the indirect pathway should be used only as a support, to modify the engine operating point and to power the vehicle when low power at the wheels is requested.

Comparing now the energy management strategies, it is interesting to note how the pathway efficiency figures reflect quite closely the pattern of utilisation of the engine presented in Figure 3.18. In fact, thanks to the high engine efficiency, the ECMS strategy presents the best results in both direct and indirect pathway efficiency, even higher than the results of the optimal PMP strategy. However, this does not translate into the best results for powertrain efficiency owing to the

huge dependence of ECMS on the indirect pathway, where more than 43 % of the total energy is routed.
Conversely, the SDP strategy presents significantly lower figures for pathway efficiencies, but manages to yield a powertrain efficiency, and thus a fuel consumption, close to the one of ECMS thanks to its heavier utilisation of the direct pathway.
The PMP strategy reaches the best results of powertrain efficiency and of fuel consumption by achieving a satisfactory efficiency in the pathways, especially in the direct pathway, and by routing the greatest part of energy through the direct pathway, similarly to the SDP strategy.
To conclude, it is important to remark again how the powertrain efficiencies presented in Table 3.2 reflect well the results of fuel consumption presented in Table 3.1, which have now been justified through the efficiency analysis.

Further insights regarding the different energy routing operated by energy management strategies are provided by Figure 3.20, presenting the engine torque for the SDP and ECMS strategies along an excerpt from the driving cycle pictured in Figure 3.17.

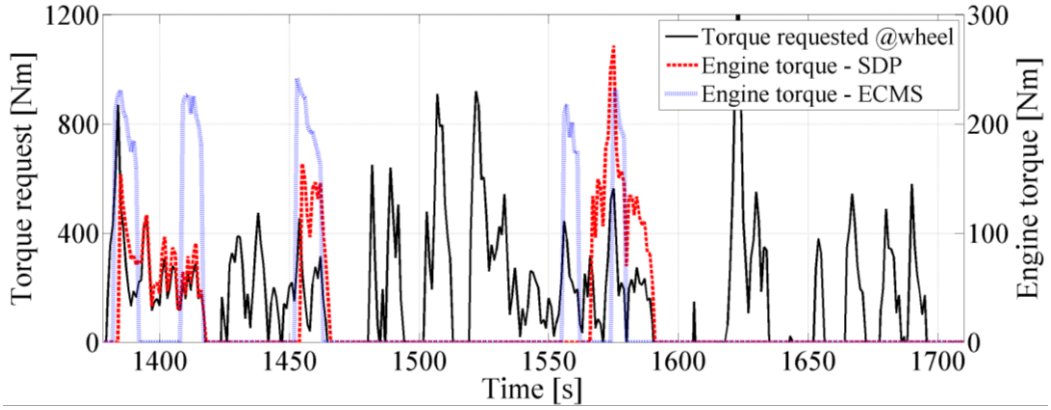

Figure 3.20 – Comparison of engine torque for SDP and ECMS strategies

It is interesting to note the pattern of utilisation of the engine for the ECMS strategy. The engine is, in fact, operated for short periods of time and always at very high torque, corresponding to the best operating efficiency. This behaviour yields a high value for the engine efficiency but imposes transiting a big share of energy through the indirect path. In fact, ECMS operates the engine at high

torque even if the required torque at the wheels is low, meaning that the torque request at the wheels and the torque output by the engine are not related.
On the contrary, the SDP strategy employs the engine at a variety of torque values, following the driver's request more closely. This implies a reduced efficiency for the engine operation but also a lower share of energy passing through the more inefficient indirect pathway.
Eventually, these two factors compensate each other, yielding not too distant results for the powertrain efficiency of SDP and ECMS strategies.

3.4 Conclusion

The chapter has presented a comparison of the performances of different energy management strategies, simulated on a sample of 100 random driving cycles.
Firstly, the methodology of the study was explained, pointing out the aspects intended at granting the fairness of the comparison
In the following section, a calibration procedure was presented for the local optimal strategies and the impact of the relevant parameters was illustrated. Two parameters needed to be calibrated for both strategies: one determining the level of control on the SOC profile, the other limiting the number of engine events. The calibration was carried out with the goal of minimising fuel consumption while ensuring the respect of system constraints in terms of control on the SOC and of number of engine events.
Then, results of fuel consumption for the local optimal energy management strategies thusly calibrated were presented, alongside with results from other strategies, useful for comparison. The conclusion that can be drawn is that the ECMS strategy outperforms the SDP strategy in terms of fuel consumption, yielding a result that is fairly close to the optimal one.
The results of fuel consumption were later interpreted and explained by means of a powertrain efficiency analysis, showing that the high operating efficiency of the engine when controlled by the ECMS strategy does not translate into the best fuel consumption results because of its heavy reliance on the inefficient indirect pathway to the wheels. Conversely, the SDP strategy is able to compensate its relatively low engine operating efficiency by employing more the direct pathway to the wheels, yielding a result not too distant from the one of ECMS.

To conclude the chapter, the bottom line of the analysis is repeated. When the strategies alone are considered, only with a limit on the number of engine events, the ECMS strategy outperforms the SDP strategy in terms of fuel consumption. However, notwithstanding the significantly more efficient engine utilisation associated to the ECMS strategy, the difference in fuel consumption is limited because the SDP strategy manages better the energy routing from the engine to the wheels. In fact, in hybrid vehicles, it is of pivotal importance to optimise the entire powertrain operation, as the optimisation of the engine operation alone is not enough for yielding the best results of fuel consumption.

Chapter 4

Driveability considerations

The classical approach in studies dealing with HEV energy management strategies considers the aspect of fuel consumption alone. Chapter 3 of the study followed a similar approach, presenting a comparison of energy management strategies geared on fuel consumption results, only introducing a limit on the number of engine events in order to carry out a fair comparison.
Anyway, if fuel economy is a decisive parameter for the development of an energy management strategy, it is most certainly not the only one. Another matter of great importance is to provide the driver with a smooth and pleasant driving experience. In fact, the feeling the powertrain gives to the driver is one of the most evident factors in determining customer satisfaction, considering that the driver has a direct impression of how the powertrain responds to their commands.
Consequently, a significant part of the study was dedicated to the analysis and the intervention on vehicle driveability issues. A multitude of aspects can be employed to define the broad concept of driveability. The analysis here presented mainly considers three of them: the dwell time, the engine utilisation profile, and the noise produced by the engine.
Considering that the driveability issue constitutes a real-world problem, the analysis carried out in this chapter is relevant only for on-line energy management strategies. The results of the PMP strategy will be still presented for comparison purposes, but the driveability impositions will not be applied to the strategy, which would otherwise lose its optimality.

4.1 Dwell time

4.1.1 The issue

In Chapter 3, a limit on the number of engine events per minute was introduced. Even if significant for components fatigue reasons, such a limit is not able to significantly improve the driver's comfort. In fact, as presented in [25], drivers

tend to notice engine events only when they take place at short time distances from each other and, instead, bear no sensitivity towards the average number of engine events along the driving cycle.
As a result, the average number of engine events per minute is not a particularly helpful parameter for determining the driving comfort. In order to better represent the driver's sensitivity to engine events, a new indicator, the dwell time, is introduced. The dwell time (DT) is defined as the time passed between two consecutive engine events, i.e. the time spent consecutively with the engine in the same state (turned on or off), before a change in engine state is made. The number of short dwell times in a driving cycle will then constitute a more representative parameter for capturing the discomfort caused to the driver by engine events while driving.
Regarding the definition of short dwell time, the matter becomes fairly subjective and depends on the positioning of the manufacturer with respect to driving comfort. The study follows the assertions of [25], stating that drivers are annoyed by dwell times shorter than 10-20 seconds.
It is now clear that short dwell times need to be avoided in order not to annoy the driver. What is still to be understood is how the energy management strategies behave with respect to the dwell time. This is clarified by Figures 4.1 and 4.2, presenting the experimental probability density function of the dwell times for the local optimal strategies, resulting from the analysis of the strategies simulated over the sample of 100 random driving cycles. The strategies were tuned as illustrated in Chapter 3.

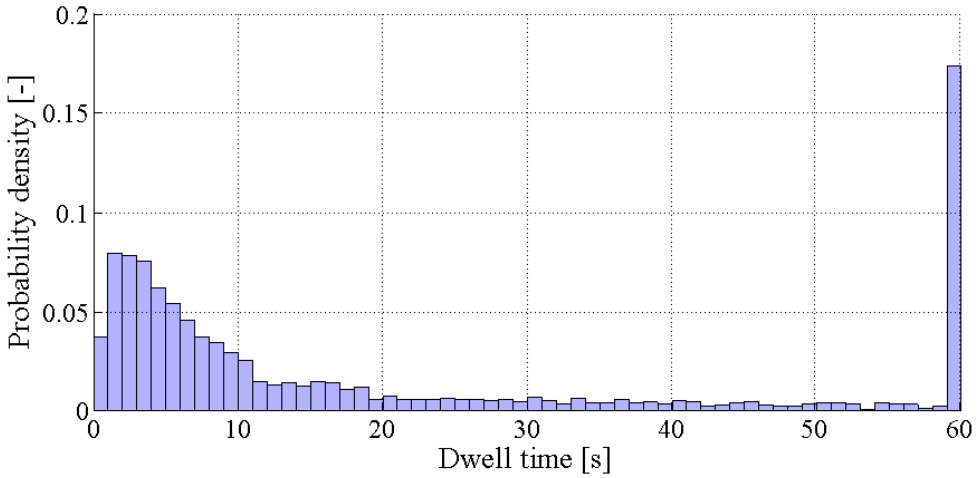

Figure 4.1 – Experimental probability density function of the dwell times for SDP – Dwell times ≥ 60 seconds have been grouped into the 60 seconds bar

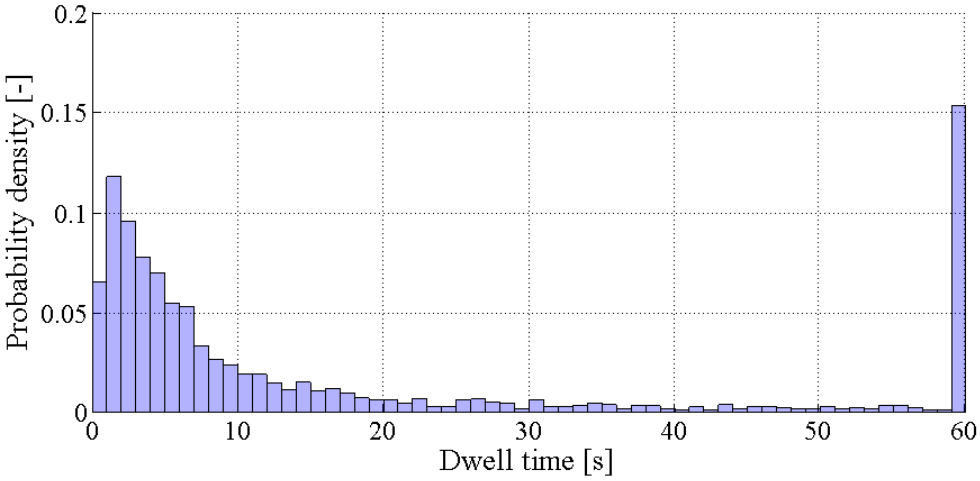

Figure 4.2 – Experimental probability density function of the dwell times for ECMS – Dwell times ≥ 60 seconds have been grouped into the 60 seconds bar

Looking at the two figures above, it is now clear that both considered energy management strategies naturally yield a great number of short dwell times. Even if the limit on engine events, 2 events per minute, dictates an average dwell time of 30 seconds, this is obtained through many very short dwell times and several much longer dwell times.
It is evident that such a behaviour of the energy management strategy cannot be tolerated as the driver would be seriously bothered by the series of engine events taking place a few seconds one from the other. Therefore, this behaviour needs to be corrected. In principle, there are two possibilities for addressing the problem of short dwell times: prevention and removal.

4.1.2 Prevention of short dwell times

In Section 2.3, two parameters were introduced in order to limit the number of engine events along the driving cycle: β for the SDP strategy and ψ for the ECMS strategy. In section 3.2, the strategies were calibrated and it was shown how, once one of the two parameters is defined, also the other is univocally defined, owing to the imposition of the same number of engine events for the two local optimal strategies. Consequently, all references in following paragraphs are centred on only one of the two parameters, more specifically parameter β coming from the SDP strategy.

Parameter β was introduced in order to weigh the cost of engine events and, by doing so, to limit their number along the driving cycle. Even if not affecting dwell times directly, the impact of parameter β on the number of engine events entails a modification in dwell times yielded by the strategy. This impact is on two levels.

First off, parameter β impacts the quantity of dwell times in the cycle. In fact, it was explained how the number of engine events along the driving cycle is reduced when parameter β assumes a high value. Few engine events in the cycle yield few dwell times, no matter their duration. Then, it is clear that a small number of dwell times of any duration also implies, on average, a small number of problematic short dwell times.

Secondly, parameter β also affects the percentage of dwell times that are below the imposed threshold. This can be understood by considering the impact of parameter β on the probability density function of dwell times. The results for the local optimal strategies for two values of β (0 and 0.001) are presented in Figures 4.3 and 4.4 below.

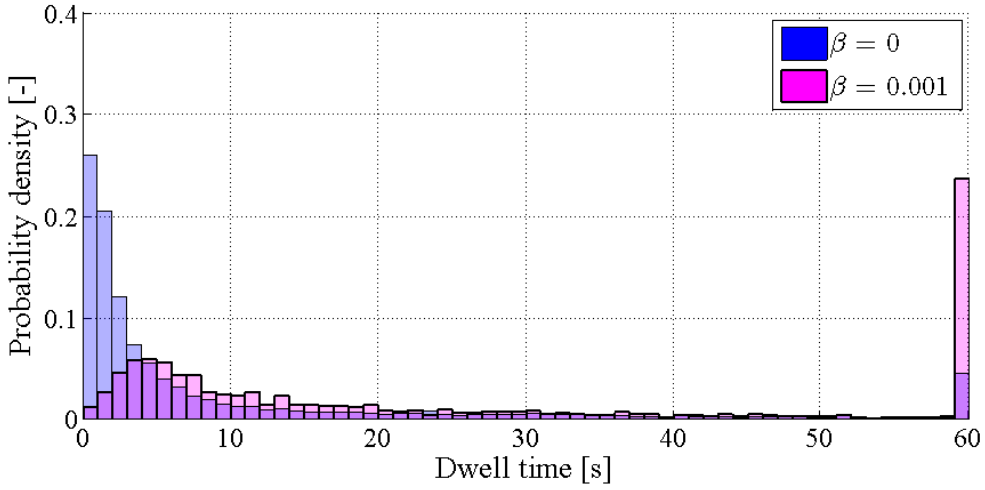

Figure 4.3 – Impact of β on the experimental probability density function of dwell times for SDP – Dwell times ≥ 60 seconds have been grouped into the 60 seconds bar

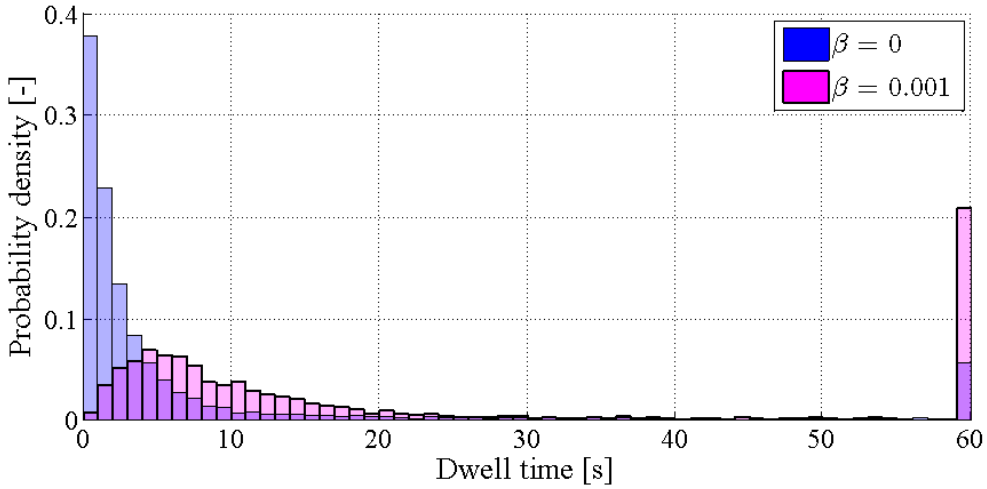

Figure 4.4 – Impact of β on the experimental probability density function of dwell times for ECMS – Dwell times ≥ 60 seconds have been grouped into the 60 seconds bar

The impact of β on the probability density function of dwell time is clear: when β is big, dwell times tend to be shifted towards the right, meaning that longer, and more acceptable, dwell times are yielded. This effect is to be attributed to the increase of the average dwell time due to the bigger β, which manages to alter the shape of the probability density function.

Tables 4.1 and 4.2 below provide a support for the conclusions regarding the way β affects the short dwell time in the cycle. An analysis of dwell times in the 100 random driving cycle sample for different values of β is there presented.

Table 4.1 – Dwell time analysis – SDP strategy

Beta [-]	Engine events [nb/min]	Number of dwell times < 20 seconds [nb]	Percentage of dwell times < 20 seconds [%]
0	5.22	8016	81.9
0.0005	2	2293	65.3
0.001	1.34	1288	55.3

Table 4.2 – Dwell time analysis – ECMS strategy

Beta [-]	Engine events [nb/min]	Number of dwell times < 20 seconds [nb]	Percentage of dwell times < 20 seconds [%]
0	5.25	9487	87.9
0.0005	1.99	3024	75.7
0.001	1.32	1767	66.9

In order to understand whether the reduction of the overall number of dwell times or the reduction of the percentage of short dwell times has the greatest impact on the number of short dwell times, a further step into the analysis is required. Attention is limited to the SDP strategy and to values of β equal to 0.0005 and 0.001. Table 4.1 shows that, in the considered case, both the number of short dwell times and their percentage see a decrease for the greater value of β. The decrease in the number of short dwell times is much steeper than the decrease in the percentage of short dwell times. In fact, the number of short dwell times is almost halved, while the percentage is decreased by 10 %. The more significant reduction in the number of short dwell times rather than the one in the percentage of short dwell times indicates that the predominant factor in reducing the number of short dwell times is the reduction of the overall number of dwell times. Instead, the reduction of the percentage of short dwell times constitutes a secondary factor in reducing the number of short dwell times. Reasonably, similar considerations apply to other values of β and to the ECMS strategy.

Tables 4.1 and 4.2 and Figures 4.3 and 4.4 also present a first comparison of the behaviour of the two local optimal strategies towards the dwell time. It is interesting to see that the SDP strategy is naturally advantaged over the ECMS strategy when it comes to short dwell times. In fact, SDP presents significantly fewer short dwell times than ECMS, for any value of β, thus yielding smaller values for the percentage of short dwell times. In addition, the probability density function of dwell times yielded by SDP naturally tends to be shifted to the right with respect to the probability density function yielded by ECMS. This is true for any value of β, yet the difference is more evident when β is small.

4.1.3 Removal of short dwell times

Even if beneficial, a high value of β is not enough to completely prevent short dwell times along the driving cycle. As a result, these short dwell times need to be removed in other ways. Since the local optimal strategies are blind to the temporal horizon, it is necessary to impose a rule on top of the strategy preventing to change the engine state before a given amount of time in present state has passed. The rule is suspended in case of major force reasons, namely the SOC close to its boundary, the vehicle having zero speed, and the motor alone not being able to provide enough power to follow the driver's request. In addition, the engine is imposed to turn off in case of a steep deceleration, overriding the minimum dwell time prescription. This last imposition was added in order not to disadvantage too much the strategies during braking.
The effect of the imposition of a minimum dwell time is presented in Figures 4.5 through 4.8, showing the engine state over a random driving cycle for the local optimal strategies when the dwell time is not imposed and when it is imposed. The strategies are calibrated as in Chapter 3 and the minimum dwell time imposed is equal to 20 seconds.

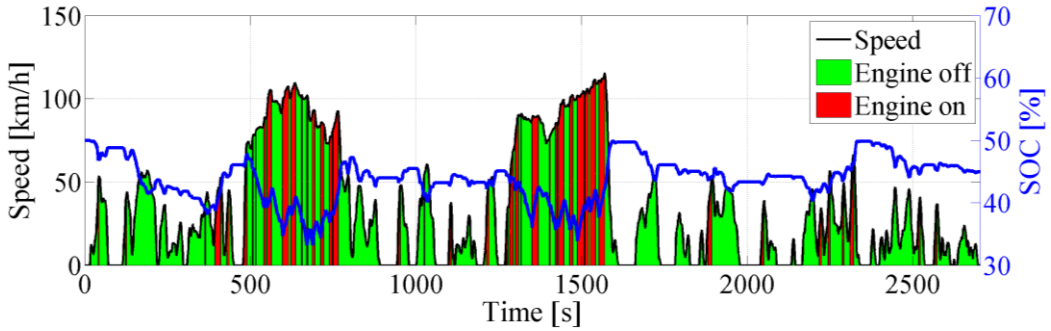

Figure 4.5 – Engine state over a random driving cycle for the SDP strategy - minimum dwell time not imposed

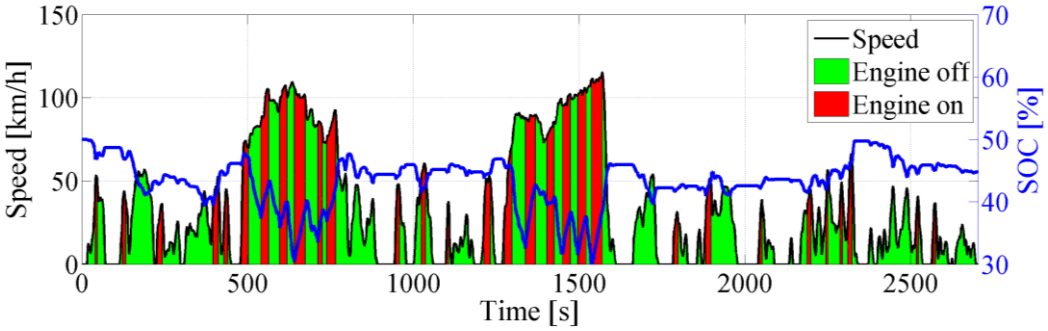

Figure 4.6 – Engine state over a random driving cycle for the SDP strategy - minimum dwell time of 20 seconds

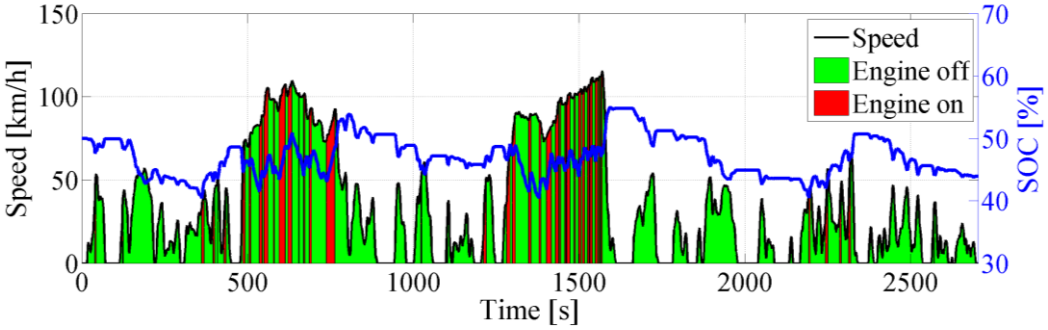

Figure 4.7 – Engine state over a random driving cycle for the ECMS strategy - minimum dwell time not imposed

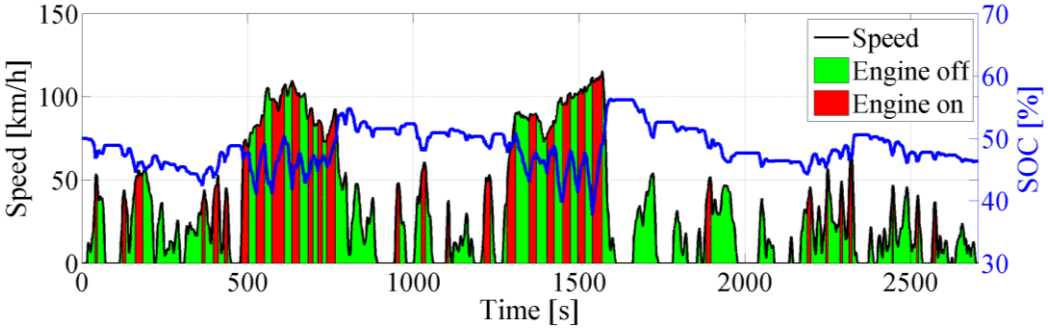

Figure 4.8 – Engine state over a random driving cycle for the ECMS strategy - minimum dwell time of 20 seconds

The impact of a minimum dwell time imposition is clear: all the short time oscillations in the engine state are removed and the behaviour of the powertrain becomes fairly more regular for both strategies.

But the imposition of a minimum dwell time affects the SOC profile too. In fact, when the engine is shut down, the minimum dwell time imposes to employ the

powertrain in the electric only mode for at least 20 seconds. This entails a greater depletion of the battery, especially when such electric only periods take place at high speeds, and makes it more difficult to ensure the control on the SOC required by constraints in (2.19). In particular, the respect of SOC boundaries along the driving cycle is affected.

This can have an impact on the strategies calibration. However, the SDP strategy manages to ensure the respect of SOC boundaries with the same calibration even when a minimum dwell time is imposed, mainly thanks to the quadratic dependence of the cost function on the distance from the target SOC in (2.40). The same cannot be said for the ECMS strategy. In fact, for high-speed driving profiles, a value of the proportional gain k_p equal to 1, as chosen in the calibration procedure of Chapter 3, yields a SOC profile that at times goes below the lower boundary of 30 %. Hence, it is necessary to recalibrate parameter k_p, which is now chosen equal to 5.

Due to the significant change in powertrain utilisation, the imposition of a minimum dwell time has a considerable impact on fuel consumption results. Figures 4.9 and 4.10 below show the impact of the imposition of a minimum dwell time, 10 or 20 seconds, on fuel consumption. The results are presented for different values of β (0, 0.0001, 0.0005, 0.001, 0.01) in order to illustrate the interaction between parameter β and the imposition of a minimum dwell time.

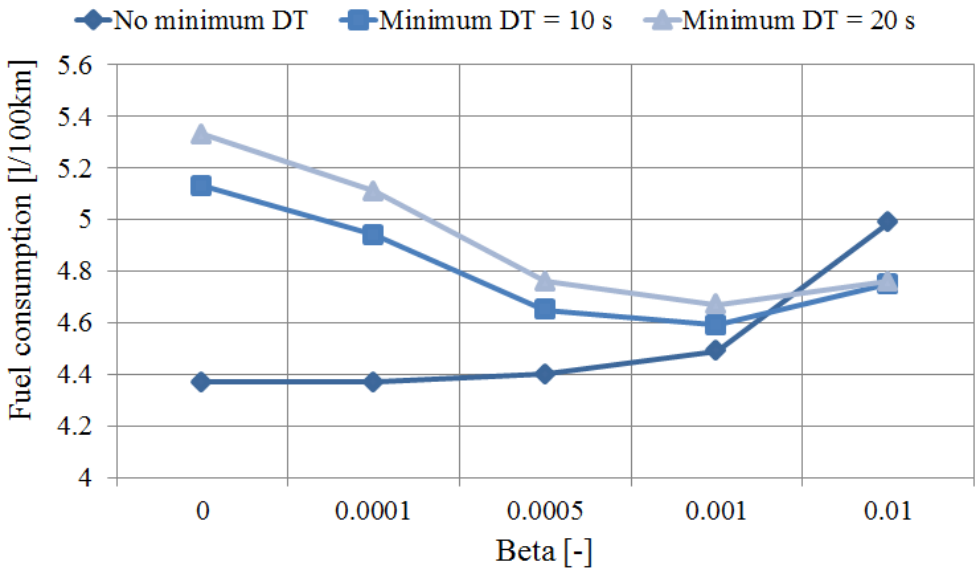

Figure 4.9 – Impact on fuel consumption of the imposition of a minimum dwell time for the SDP strategy

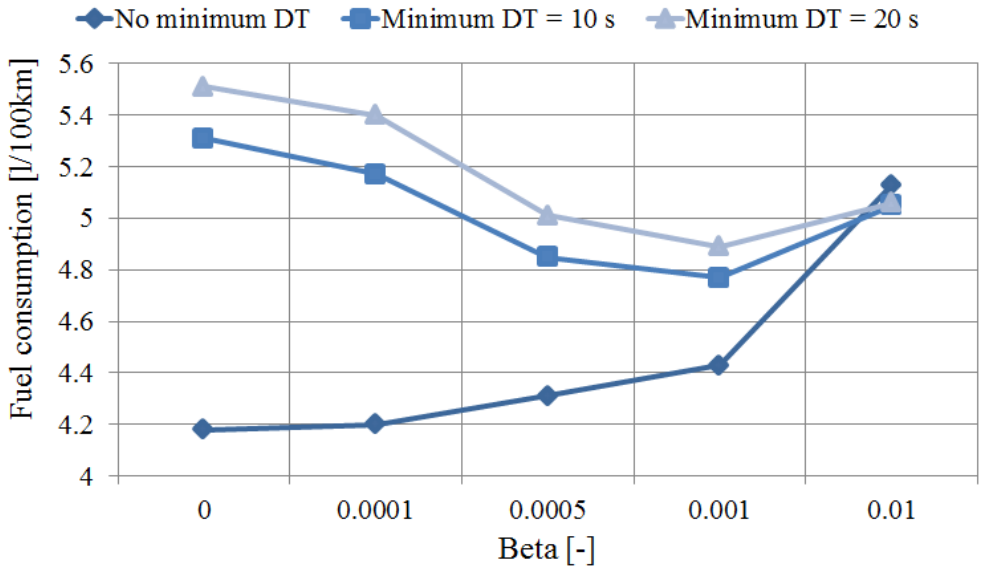

Figure 4.10 – Impact on fuel consumption of the imposition of a minimum dwell time for the ECMS strategy

The first thing one can observe is that the imposition of a minimum dwell time causes a significant increase in fuel consumption, for both values of the minimum dwell time and for both strategies. This is true for any considered value of β, with the sole exception of the case where β is equal to 0.01. In this case the strategy, greatly constrained because of the high value of β, benefits from the imposition of turning off the engine during steep decelerations. This increases the overall number of engine events, leading to a less constrained and more efficient strategy.

For all other cases, the higher fuel consumption associated to the imposition of a minimum dwell time is due to the suboptimal management of the powertrain in such situations. In fact, local optimal strategies optimise the functioning of the powertrain, in terms of engine state and power split. When the minimum dwell time imposition forces an engine state different from the one suggested by the local optimal control strategy, the utilisation of the powertrain is not optimal anymore. This eventually comports a substantial increase in fuel consumption of the vehicle.

It is also particularly interesting to notice the impact of parameter β on results of fuel consumption when a minimum dwell time is imposed. The observed trend is the opposite with respect to the case where there is no minimum dwell time. In fact, when no minimum dwell time is imposed, fuel consumption is increased for bigger values of β; instead, when a minimum dwell time is imposed, fuel

consumption decreases for greater values of β. This is true up to a given extent since, if the chosen value of β is too high, the strategy is so constrained that it yields an unsatisfactory result of fuel consumption, whether or not the minimum dwell time is imposed.

As explained in Paragraphs 3.2.1 and 3.2.2, the trend of fuel consumption for the cases where no minimum dwell time is imposed is due to the stricter constraints imposed on the strategy corresponding to greater values of β. Conversely, the reason for the trend of fuel consumption when a minimum dwell time is imposed is to be found in Section 4.1.2. There, it was explained how a high value of β manages to significantly reduce the number of short dwell times yielded by the strategy. Fuel consumption benefits from this effect of β since, if short dwell times are reduced, the minimum dwell time imposition needs to intervene fewer times. In this way, the powertrain operates longer in the conditions dictated by the local optimal strategy and relies less on the engine state impositions due to the respect of the minimum dwell time, which are clearly non-optimised.

Further insights in the analysis are provided by Figure 4.11, which presents the percentage difference in fuel consumption due to the imposition of a minimum dwell time with respect to the baseline strategy (respectively, SDP or ECMS without the minimum dwell time imposition).

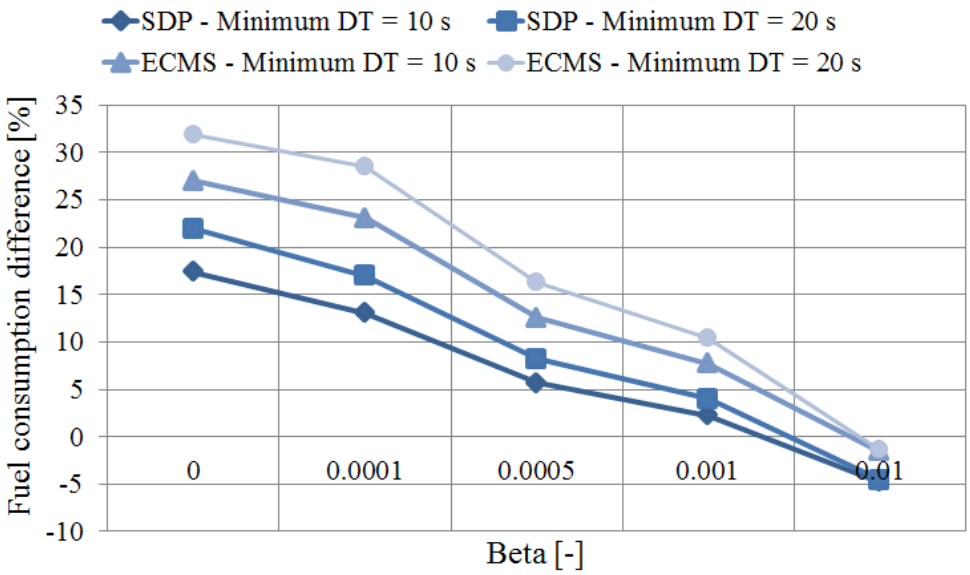

Figure 4.11 – Percentage difference in fuel consumption due to the imposition of a minimum dwell time

Results of Figure 4.11 are interesting under several aspects and allow pointing out different conclusions. First off, the increase in fuel consumption due to the minimum dwell time imposition has been quantified, showing a difference that is very relevant in almost any case and that can exceed 30 % in particular cases.
Secondly, results show that the difference between the imposition of a minimum dwell time of 10 seconds and of a minimum dwell time of 20 seconds is quite limited for both strategies, with the maximum difference being around 5 %. This means that the very imposition of a minimum dwell time, rather than the minimum dwell time duration, causes the greatest increase in fuel consumption. This conclusion appears reasonable after analysing the experimental probability density functions presented in Figures 4.3 and 4.4, which show that the majority of dwell times is clustered around very low values, generally lower than 5-10 seconds. As a result, it is advisable to employ sufficiently high values of minimum dwell time for improving the comfort of the driver, since degradation in fuel consumption due to longer minimum dwell time values is limited.
Figure 4.11 also allows drawing a comparison of the response of the two local optimal strategies to the imposition of a minimum dwell time. The conclusion is that, when a minimum dwell time is imposed, the SDP strategy responds to the constraint much better than the ECMS strategy, in all considered cases.
This result is primarily due to the different approach of the mentioned strategies to engine state management. In fact, the SDP strategy is based on a stochastic engine state management, while the ECMS relies on the instantaneous conditions for determining the engine state. This means that, when making a decision about engine state, the SDP strategy also takes into account the probability of needing or not the engine turned on in the following instants of time. As a result, the strategy decides to turn off the engine if it is convenient for current powertrain conditions and if it is likely that in the immediate future the engine will not be used[24]. This eventually yields a strategy that is naturally robust with respect to the engine state decision and that does not suffer too much from minimum dwell time impositions.
Conversely, the ECMS strategy is completely blind to future conditions, even the near future, and decides whether or not to use the engine only basing on present powertrain conditions. As a result, the strategy tends to shut down the engine as soon as the driver brakes, even if slightly. If, afterwards, the driver accelerates again, the strategy will probably command to turn the engine on. In case a minimum dwell time is imposed, this imposition will prevent the engine

[24] The same reasoning also applies to the case of turning on the engine.

from being turned on, causing a far from the optimal and inefficient utilisation of the powertrain. The result is a strategy that suffers greatly from the dwell time imposition because of its non-robust approach to engine state management[25].

The more robust attitude of SDP strategy towards the minimum dwell time imposition is confirmed by results of Paragraph 4.1.2, in particular the ones in Tables 4.1 and 4.2. There, it was shown how SDP was naturally better predisposed than ECMS for avoiding short dwell times. In fact, SDP presented fewer short dwell times along the 100 random driving cycles than ECMS, for any considered value of β. This determines a smaller need for corrections when a minimum dwell time is imposed and, consequently, an advantage in terms of fuel consumption.

Contrarily to what one could reasonably believe, the imposition of a minimum dwell time does not alter greatly engine operating points, which are only slightly different from the ones yielded by the strategies when no minimum dwell time is imposed. Figures 4.12 and 4.13 below present a comparison between engine operating points for the local optimal strategies with no minimum dwell time imposed and with a minimum dwell time of 20 seconds. Similarly to what was done previously, the presented results refer to one single random driving cycle, illustrated in Figure 3.17. However, results can be considered general as all the 100 random driving cycles present a similar engine operation pattern.

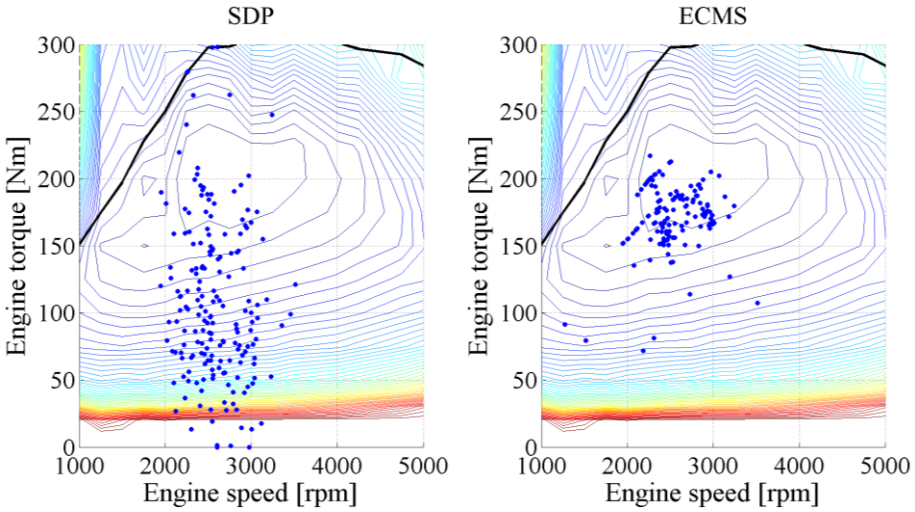

Figure 4.12 – Engine utilisation points for the considered random driving cycle – Minimum dwell time not imposed

[25] This applies to the state-of-the-art ECMS strategy and is not a structural defect of it. In fact, it is possible to imagine implementing a stochastic state machine on top of the control strategy, in order to manage the engine state in a more robust fashion.

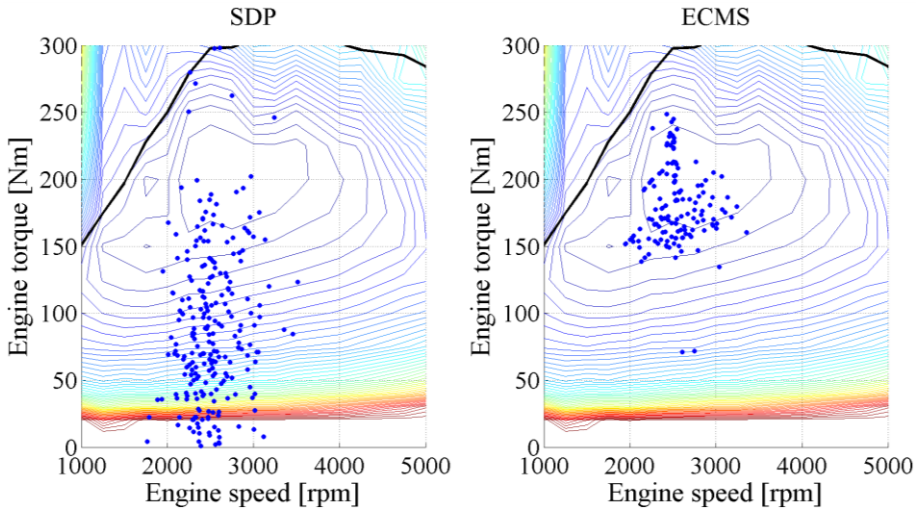

Figure 4.13 – Engine utilisation points for the considered random driving cycle – Minimum dwell time of 20 seconds

Differences in engine operating points in the two cases are limited and do not cause a significant change in engine operating efficiency. As a result, it is possible to conclude that the degradation in fuel economy yielded by the imposition of a minimum dwell time primarily depends on the different engine state management imposed by the constraint, rather than on engine utilisation.
As a result, it is possible to conclude that the engine state management is an issue of the greatest importance in the definition of an energy management strategy, with a huge impact on fuel consumption results. The state-of-the-art SDP strategy presents a more robust approach in this sense than the state-of-the-art ECMS strategy, giving to SDP a significant edge when a minimum dwell time is imposed.

4.1.4 Recalibration and fuel consumption results

The imposition of a minimum dwell time alters significantly the results of fuel consumption for both local optimal strategies. A particular interaction is observed between parameter β and the minimum dwell time, with a big change in the trend of fuel consumption with respect to the situation where no minimum

dwell time is imposed. As a consequence, in order to select the most appropriate value of β, a recalibration of the strategies is made necessary[26].
Figure 4.14 below constitutes a support for the choice of β, presenting the trend of fuel consumption results for both strategies in case a minimum dwell time is or is not imposed. The minimum dwell time value is set equal to 20 seconds in order to provide the driver with a smooth driving experience. In addition, it has been previously shown that the increase in fuel consumption between minimum dwell times of 10 and 20 seconds is limited.

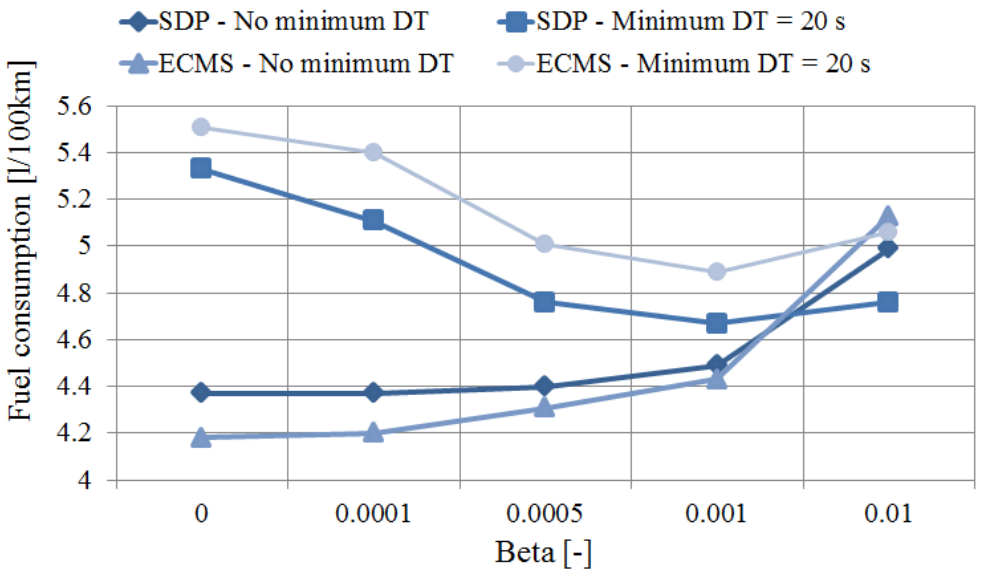

Figure 4.14 – Impact of parameter β on fuel consumption results for both strategies when a minimum dwell time is or is not imposed

Since the limit on the average number of engine events per minute was substituted by the minimum dwell time imposition and the strategies were already adapted to follow the constraints on the control of the SOC, the re-calibration process is based only on the results of fuel consumption. Hence, the procedure is straightforward: the selected value of β for each strategy is the one that minimizes fuel consumption. When a minimum dwell time is imposed, both strategies see a minimum in their results of fuel consumption for a value of β equal to 0.001, which is then the selected value for the recalibration procedure.

[26] The recalibration procedure deals uniquely with β, and not with α and k_p. This is because α and k_p primarily impact on the control of the SOC and the fulfilment of the constraints related to the SOC profile was already discussed in Paragraph 4.1.3.

Results of simulation over 100 random driving cycles for the recalibrated local optimal strategies are presented in Table 4.3 below. For comparison purposes, the table also presents the results of the thermal case and the optimal results yielded by PMP, on which no minimum dwell time was imposed.

Table 4.3 – Results for simulation over 100 random driving cycles of the different energy management strategies – Minimum dwell time of 20 seconds for local optimal strategies

Strategy name	Fuel consumption [l/100km]	Engine events [nb/min]	Final SOC [%]	Gain /pure thermal [%]
Pure thermal	9.35	-	-	-
PMP	3.97	5.14	50	57.5
SDP	4.67	1.1	44.26	50.1
ECMS	4.89	1.1	49.43	47.7

The results presented in Table 4.3 and in Figure 4.14 highlight the superiority of SDP in terms of fuel economy when a minimum dwell time is imposed. In fact, the SDP strategy outperforms the ECMS strategy for the selected calibration and in all other considered cases.
The results presented in Table 3.1 are then overturned. If the ECMS strategy proved its greater efficiency when no driveability constraint was imposed, the SDP strategy takes an edge when a real-life driveability constraint, such as the minimum dwell time, is taken into account. As a result, the stochastic approach of the SDP strategy appears being particularly suitable for the energy management of a real vehicle, where a satisfactory driveability needs to be ensured.

4.2 Engine utilisation

A great deal of attention should be given also to how the engine is employed, considering that the engine utilisation profile impacts both the durability of the engine and the driving comfort of the vehicle.
In fact, the decoupling between the torque request at the wheels and the torque provided by the engine introduced through hybridisation of the powertrain can lead to a multitude of engine utilisation profiles. Then, the utilisation profile of

the engine can be quite unusual and distant from a normal utilisation profile for an internal combustion engine.

A comparison of the utilisation of the engine for local optimal strategies is presented in Figure 4.15, which constitutes a subset of Figure 3.18. In order to outline the differences in engine utilisation introduced by the powertrain hybridisation, the plot presents two sets of data: the engine utilisation points for the hybrid powertrain are presented in blue, the utilisation points for the same powertrain employing only the thermal driveline are presented in red.

The comparison presents engine points from one single random driving cycle, the one portrayed in Figure 3.17. However, also in this case the conclusion is general as the presented utilisation pattern is common to all the 100 random driving cycles.

In addition, the engine utilisation points for the hybrid powertrain are for the case of minimum dwell time not enforced. The conclusion can be extended also to the case of a minimum dwell time enforced, considering that in Section 4.1.3 it was shown how the imposition of a minimum dwell time does not alter significantly the engine operating points.

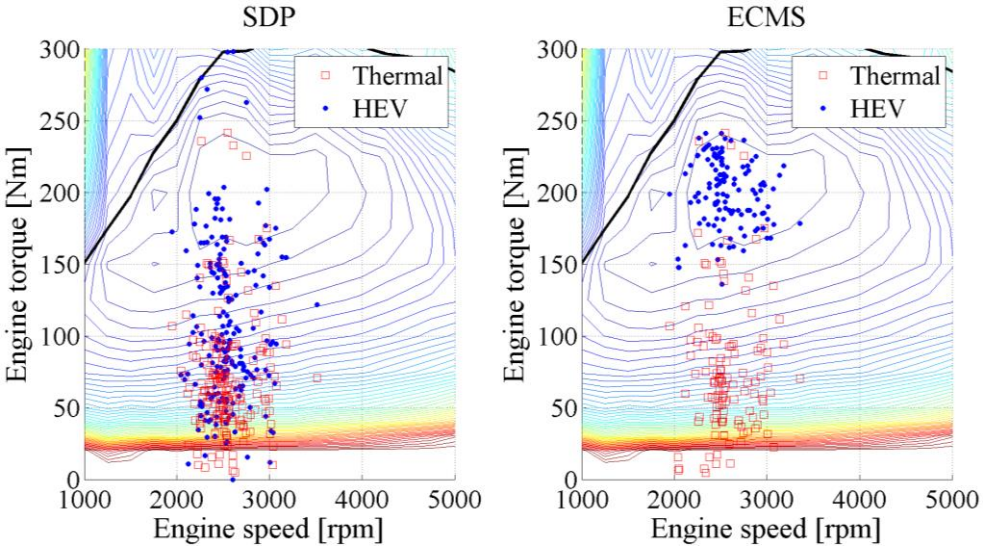

Figure 4.15 – Engine utilisation points for the considered random driving cycle in case of hybrid and thermal powertrain

Both strategies displace the original engine operating points towards higher torque areas, increasing in this way the engine efficiency. However, the difference between engine operating points for the thermal and the hybrid cases

for the SDP strategy is fairly limited, with the engine being used at a multitude of torque levels even in the hybrid case. On the contrary, the difference introduced by the ECMS strategy is much more pronounced, considering that in the hybrid case all engine operating points are displaced to the highest efficiency area.

This different engine utilisation profile entails consequences on two levels: the adaptation of the engine to the powertrain and the driving comfort.

First off, it is immediate to notice that engine utilisation, when ECMS is the governing strategy, is more reminiscent of the way a range extender in a series hybrid is employed rather than of the normal utilisation of a thermal engine. In fact, the ECMS strategy shifts all engine operating points to the highest efficiency area, independently from the current torque request at the wheels. This imposes a rethinking of the engine design as the engine is being used in a fairly different way with respect to its usual operation. Hence, it is possible to imagine reducing the engine size and optimising the highest efficiency area as much as possible, strengthening at the same time some key components, which have to endure the continuous utilisation at very high torque. However, such modifications to the engine design are probably undesired by the manufacturer, in view of the fact that the parallel hybrid architecture is considered the first step into the hybrids' domain and that it can usually accommodate previously designed engines without inconveniences.

On the contrary, modifications in engine operation introduced by the SDP strategy are far more limited, with the engine points in the hybrid case presenting only a slightly higher torque than those in the full thermal case. This limited difference, together with the fact that the engine is employed in a multitude of zones and not in one single area, would probably not require any modification in the engine design. In this way, an easy and immediate adaptation of an already available engine to the hybrid architecture is possible.

Aside from impacting the engine design, the engine utilisation pattern also has an impact on the driveability of the vehicle. In fact, the driver expects a correlation between the pedal position and the response of the engine. Countless hours of driving have taught drivers that pushing on the pedal causes the acceleration of the vehicle and, at the same time, more noise and vibration coming from the engine. Hybrid electric vehicles are capable of decoupling the torque request, defined by the pedal position, and the torque produced by the engine, one of the main factors determining the noise and vibration produced by the engine. As a result, this decoupling might cause the loss of the correlation

between pedal position and engine response in terms of noise and vibration, resulting in a nuisance for the driver.

In the case of the SDP strategy, the proximity between the engine operating points for the hybrid powertrain and the points for the thermal powertrain, as illustrated in Figure 4.15, indicates that a correlation between pedal position and engine noise and vibration is maintained. The same cannot be said for the ECMS case. In fact, for said strategy, the engine points for the hybrid powertrain are fairly distant from the ones for the thermal case and no correlation between the two groups of points can be observed.

This evidence is better explained by observing Figure 3.20, presenting the profile of the torque request at the wheels and the torque produced by the engine for both local optimal strategies over an excerpt of a random driving cycle. For the convenience of the reader, Figure 3.20 is repeated below.

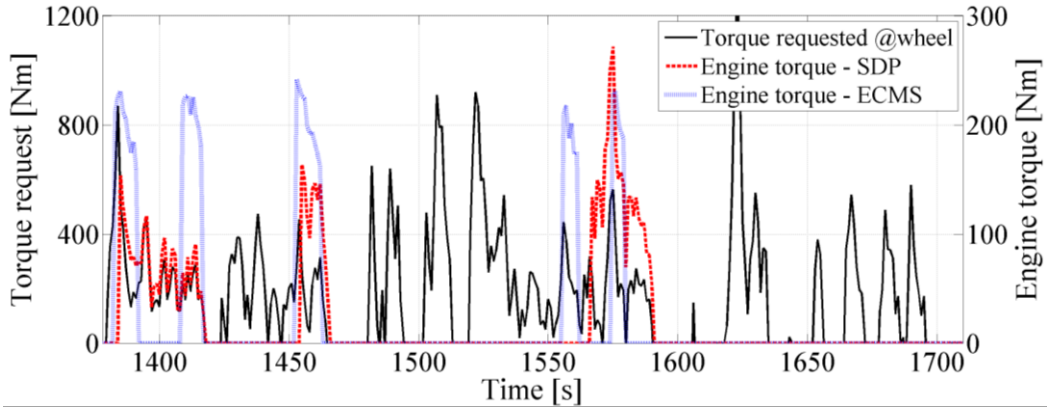

Figure 3.20 – Comparison of the engine torque for the SDP and ECMS strategies

When SDP is the governing strategy, the engine torque approximately follows the torque request at the wheels. In fact, even if the torque produced in the engine is generally in excess with respect to the needed torque for powering the wheels, variations in the torque request are followed by corresponding, even if shifted, variations in the engine torque. This means that the driver will hear the expected noise feedback from the engine while acting on the pedal.

The situation is opposite for the ECMS strategy, as no significant correlation is observed between the torque trace of the engine and the torque requested at the wheels. In fact, the engine, while switched on, is constantly operated at the same (high) torque level. As a result, the driver will not hear a feedback noise from the engine corresponding to the action on the pedal, but a steady and fairly loud

noise. Eventually, the frustration of the driver's expectation will probably result in an odd, if not distressing, driving experience.

4.3 Engine noise

Aside from being important as a feedback to the driver's action on the pedal, engine noise constitutes a fundamental aspect of vehicle driveability per se. In fact, one of the primary factors for providing the driver with a comfortable driving experience is the reduction of the perceived noise while driving. A great attention is thus dedicated by manufacturers to understanding and addressing the issue.

The main sources of noise perceived in the vehicle are the powertrain, the interaction between road and tyres, and the interaction between vehicle and air. The relative importance of such sources depends on the vehicle speed, with powertrain noise being dominant at low speeds, road-tire interaction noise dominant at medium speeds, and vehicle-air interaction noise dominant at high speeds. The noise share versus the speed is presented in Figure 4.16 below.

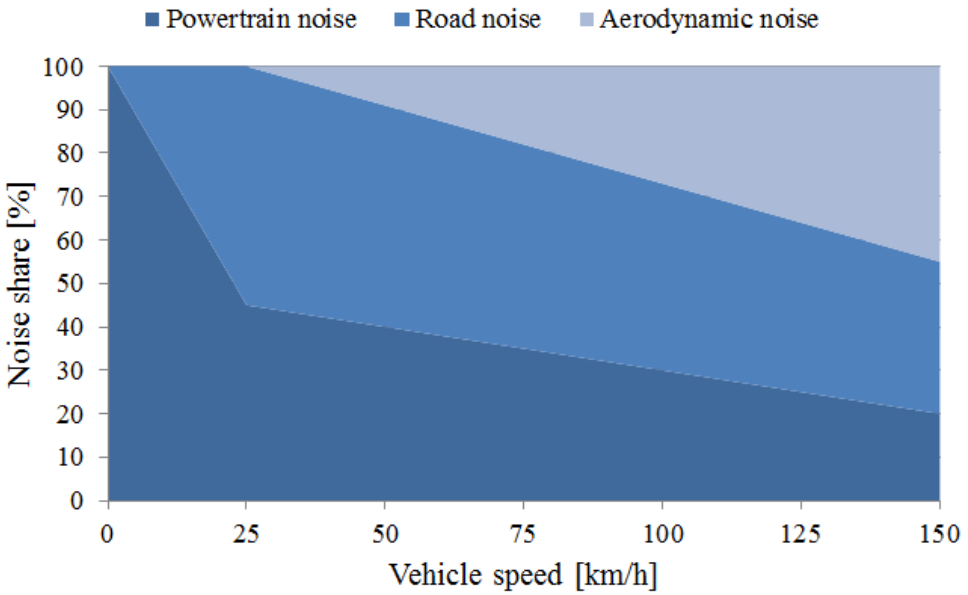

Figure 4.16 – Composition of noise perceived in the vehicle with respect to vehicle speed [66]

Focusing the attention on the noise originating from the powertrain, its magnitude is essentially depending on two parameters: the engine rotating speed and the engine torque [66]. Since in the study the speed profile and the gearshift law are imposed, the engine rotating speed is fixed. Hence, the only degree of freedom on which the strategies can act in order to improve the acoustic comfort of the vehicle, aside from the engine state, is here the engine torque.
As already explained, the possibility of decoupling the torque request at the wheels from the torque provided by the engine in hybrid electric vehicles comes with a great advantage, the improvement of fuel economy, and a few issues. Among them lies the possibility of producing a distressing engine noise. In fact, the new freedom in engine utilisation enabled by hybridisation can lead to a weird production of noise. Most notably, the driver expects to hear a limited amount of noise from the engine while cruising at low speed. In a hybrid powertrain, instead, it is possible to imagine having the engine working at full load even while cruising at low speed, probably in order to quickly recharge the battery. This would cause an incongruous and unexpected amount of noise perceived by the driver, who might think that there is something wrong with their engine.
The scenario described above, and other similar ones, can be avoided by imposing two rules on top of the strategy:

- *Rule 1*. For vehicle speeds below 20 km/h, the engine must be switched off;

- *Rule 2*. For vehicle speeds between 20 km/h and 50 km/h, the maximum engine torque must be below a given threshold. The torque limit consists of a line joining the engine torque necessary to drive the vehicle at a speed of 20 km/h with an acceleration of 1 m/s^2 and the torque necessary at 50 km/h with the same acceleration.

Similarly to what was done with the dwell time imposition, the rules regarding noise limitations are suspended in case of major force reasons, for instance the SOC level being close to exceeding its boundaries, or the limited powertrain torque being insufficient to cover the torque request at the wheels.
The limits on engine noise were chosen to cover only the speed range from 0 km/h to 50 km/h since, as shown by Figure 4.16, powertrain noise is the dominant source of noise in this speed area. In addition, this is a particularly

sensitive area as the driver expects a limited noise production while moving at low speeds. Therefore, efforts aimed at limiting the perceived powertrain noise should be primarily addressed to vehicle operation at low speed.

The impact of the rules introduced above on engine operation is shown in Figures 4.17 through 4.20, presenting the engine operating points versus the vehicle speed for the whole sample of 100 random driving cycles before and after the imposition of the noise rules.

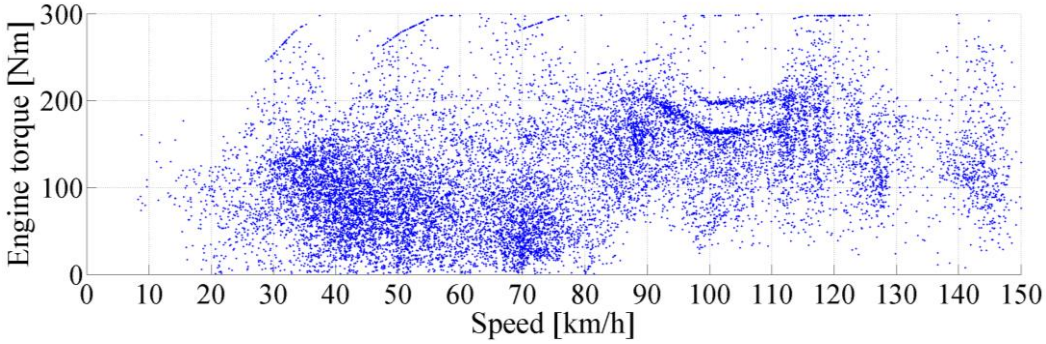

Figure 4.17 – Engine utilisation points with respect to vehicle speed for the SDP strategy when noise rules are not enforced

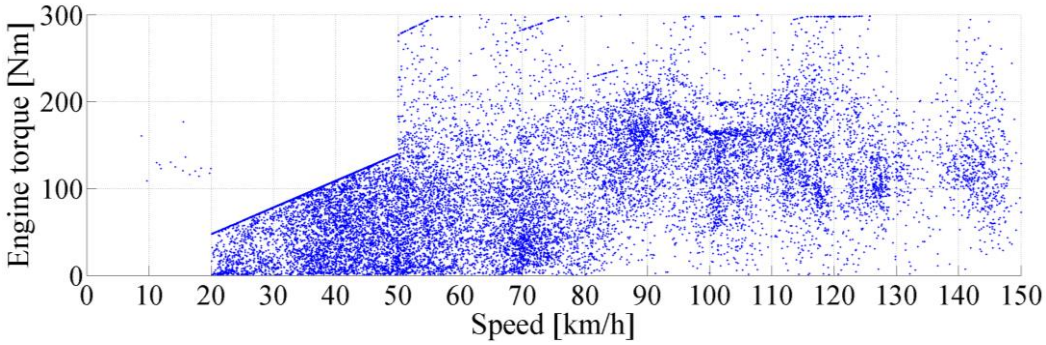

Figure 4.18 – Engine utilisation points with respect to vehicle speed for the SDP strategy with noise rules enforced

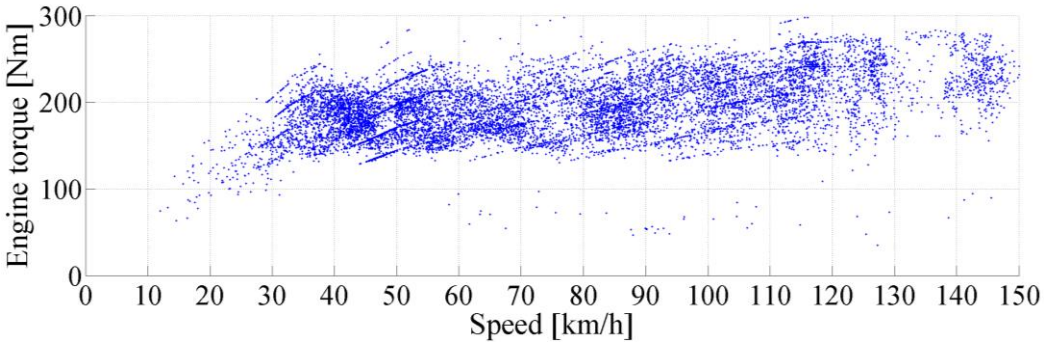

Figure 4.19 – Engine utilisation points with respect to vehicle speed for the ECMS strategy when noise rules are not enforced

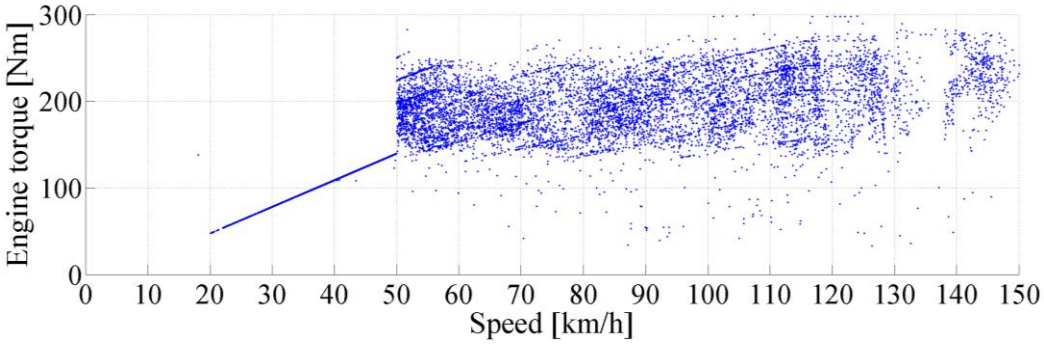

Figure 4.20 – Engine utilisation points with respect to vehicle speed for the ECMS strategy with noise rules enforced

The impact of noise limiting impositions appears being massive for both strategies in figures above. In fact, a significant number of engine operating points is displaced or eliminated.

Therefore, it is of great interest to analyse the impact of the two noise limiting impositions on results of fuel consumption, which are reported in Table 4.4. Noise limiting rules are implemented in local optimal strategies alongside the minimum dwell time imposition.

Comparing the results of Table 4.4 with those of Table 4.3, where only the minimum dwell time rule was imposed, it is possible to see that the noise limiting impositions comport a slight increase in the result of fuel consumption for the SDP strategy and a slight reduction for the ECMS strategy.

First off, it is interesting to point out the magnitude of the change, which is hardly noticeable for both strategies. This indicates that the variations in engine utilisation depicted in Figures 4.17 through 4.20 do not affect fuel consumption

in sensible measure. As a result, it is possible to state that both local optimal strategies are robust to noise limiting impositions and can smoothly accept on top of them rules apt to modify their behaviour regarding noise emissions.

Table 4.4 – Results for simulation over 100 random driving cycles of the different energy management strategies – Minimum dwell time of 20 seconds and noise limiting impositions applied to the local optimal strategies

Strategy name	Fuel consumption [l/100km]	Engine events [nb/min]	Final SOC [%]	Gain /pure thermal [%]
Pure thermal	9.35	-	-	-
PMP	3.97	5.14	50	57.5
SDP	4.7	1.16	44.12	49.7
ECMS	4.82	1.16	49.24	48.4

Secondly, particular attention is dictated by the direction of the change of fuel consumption. In fact, the imposition of noise constraints causes an increase in fuel consumption for the SDP strategy, while the fuel consumption yielded by the ECMS strategy presents a decrease. If the result of SDP appears quite reasonable, the result of ECMS at first appears puzzling and against common sense, since logic dictates that a more constrained strategy should yield worse results in terms of fuel consumption. However, the explanation for the result lies in the interaction between the dwell time imposition and Rule 1 for noise limitation. In fact, the dwell time imposition might lead to periods of time with the engine forced to be on while the vehicle speed is low, without the possibility of shutting it down since the minimum dwell time of 20 seconds has not passed yet. Such a situation would clearly result in poor fuel consumption during the period. This issue is addressed through the imposition that the engine must be off for speeds below 20 km/h, with the eventual result of an improvement in fuel consumption.

The beneficial effect of the interaction between Rule 1 and the dwell time imposition is observed only in the case of the ECMS strategy and not for the SDP strategy. This difference is due to the fact that, as shown in Section 4.1, the ECMS strategy is much more affected by the imposition of a minimum dwell time, due to its engine state management based solely on present conditions. Conversely, the SDP strategy manages the engine state considering also the probabilities for future vehicle utilisation, turning on the engine only when it is

needed for prolonged periods of time. Hence, the strategy is already robust to the dwell time imposition and does not benefit particularly from Rule 1.
Instead, due to the imposition of Rule 2, fuel consumption yielded by the SDP strategy shows a small increase when noise limiting rules are enforced.

4.4 Additional impositions

In the previous sections, driveability of the vehicle has been improved by imposing some constraints on the minimum dwell time and on the noise produced by the engine. In addition, the engine utilisation profile has been analysed in order to understand which strategy presents the most favourable engine utilisation pattern. Many other driveability aspects can be taken into account for improving vehicle behaviour, especially in order to tweak the vehicle response in particular situations. The remainder of the chapter discusses two of them, the imposition of engine turned on for high vehicle speeds and the imposition of engine turned off during long decelerations.
However, it is important not to implement too many rules on top of the energy management strategy and to limit their impact to a few, circumscribed vehicle operating conditions. In fact, by adding rule over rule, the local optimal energy management strategy will tend to become more and more like a heuristic strategy, thus losing its optimal trait and incurring into the problems associated with heuristic strategies that were described in paragraph 2.3.1.

4.4.1 Engine on for high vehicle speeds

When the vehicle is moving at high speed, for instance while cruising on a highway, the power request at the wheels is very high. Then, the energy management strategy will naturally tend to keep the engine switched on, in order to ensure a good powertrain operating efficiency. However, there exist some cases, in particular during braking, when the engine is turned off by the strategy even if vehicle speed is pretty high. This comports the need for turning on the engine again as soon as the driver resumes pushing on the accelerator pedal, eventually yielding a distressful oscillating behaviour of the engine state. In such conditions even the dwell time imposition is often powerless, considering that switching on the engine is allowed at all times if the torque request at the

wheels exceeds the maximum torque that can be provided by the electric motor alone.
As a result, it is good practice to implement a rule detecting highway driving conditions and imposing the engine to be on at all times in such cases. It is also recommended to include a hysteresis in the rule, in order to avoid oscillatory behaviour for the engine state while cruising at a speed close to the threshold speed. The two rules for managing the engine state at high speed are then the following:

- *Rule 1*. The engine must be turned on at all times when vehicle speed is above 100 km/h;

- *Rule 2*. Once triggered, the engine on imposition is deactivated when vehicle speed goes below 80 km/h.

The impact of rules above on the engine state over one random driving cycle is presented in Figures 4.21 through 4.24. The baseline figures (Figures 4.21 and 4.23) present the results for the local optimal strategies with a minimum dwell time of 20 seconds and the noise limiting impositions discussed in the previous section. The two other figures (Figures 4.22 and 4.24) show the results for the strategies with the rules apt to manage the engine state at high speed implemented alongside the dwell time and the noise limiting impositions.

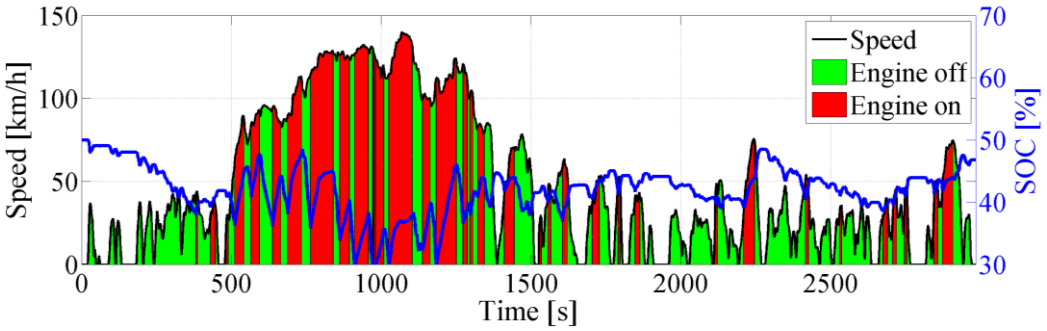

Figure 4.21 – Engine state over a random driving cycle for the SDP strategy before the high speed imposition

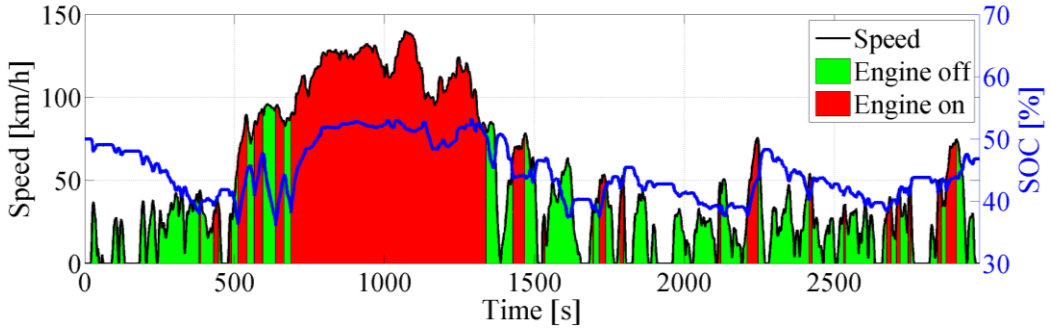

Figure 4.22 – Engine state over a random driving cycle for the SDP strategy after the high speed imposition

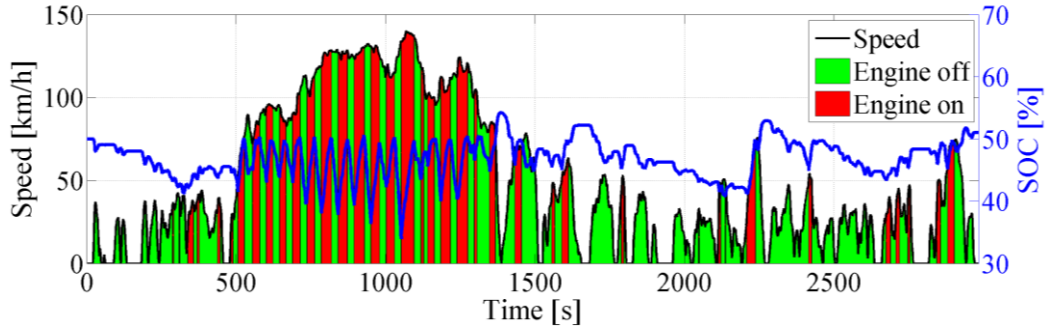

Figure 4.23 – Engine state over a random driving cycle for the ECMS strategy before the high speed imposition

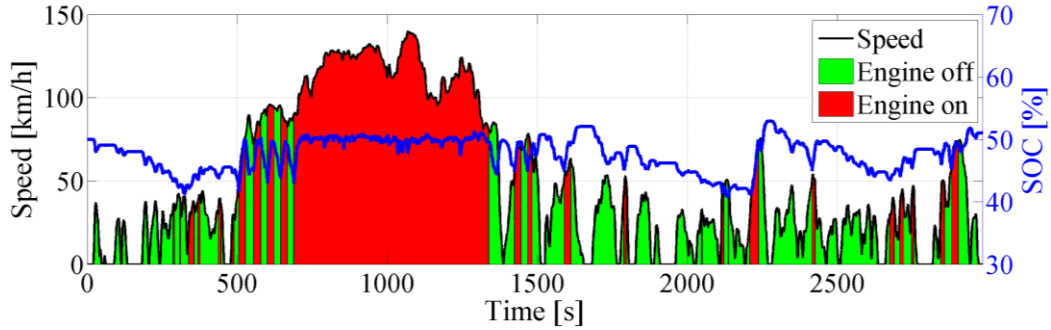

Figure 4.24 – Engine state over a random driving cycle for the ECMS strategy after the high speed imposition

As shown by figures above, the two rules described previously manage to identify highway driving conditions effectively and impose to keep the engine on during these periods, leaving the rest of the cycle substantially unaffected. This imposition produces a more regular profile of the engine state, with the removal of oscillatory behaviour at high speed. As a result, the new engine state

profile will prove more comfortable for the driver thanks to the steadier utilisation of the engine when the vehicle is moving at high speed.
A second beneficial impact of the rules discussed in the paragraph is the improved management of the SOC level along the driving cycle. In fact, long periods of time spent with the vehicle moving at high speed constitute a great challenge for local optimal strategies, which struggle to keep the SOC level in the proximity of target SOC in such conditions. The imposition of keeping the engine turned on during these high-speed periods is helping greatly the strategy in this sense, by preventing that the huge amount of energy required to power the vehicle during such periods is provided by the battery alone. As a result, after the imposition of the high-speed rules, control on the SOC is more robust and the SOC profile stays well clear of the boundaries suggested by the battery manufacturer.
It is reasonable to believe that the rules presented in the paragraph have an impact on fuel consumption results, owing to the modification of the engine state suggested by the local optimal strategy. Then, fuel consumption results yielded by the strategies incorporating also the high-speed impositions are presented in Table 4.5 below.

Table 4.5 – Results for simulation over 100 random driving cycles of the different energy management strategies – Minimum dwell time of 20 seconds, noise limiting and high vehicle speed impositions applied to local optimal strategies

Strategy name	Fuel consumption [l/100km]	Engine events [nb/min]	Final SOC [%]	Gain /pure thermal [%]
Pure thermal	9.35	-	-	-
PMP	3.97	5.14	50	57.5
SDP	4.71	1.04	44.38	49.6
ECMS	4.84	1.04	49.31	48.2

The conclusion that can be drawn from fuel consumption results is that the high-speed engine state imposition does not have a sensible impact on fuel consumption. In fact, the results show a very small increase in fuel consumption for both SDP and ECMS. This is because the modifications brought to the strategies are limited to a particular operating area and force an overall efficient behaviour of the powertrain (engine on at high speeds). In this way, the negative

impact of not following the optimised engine state prescribed by the strategy at all times is limited.
As a result, it is possible to state that both strategies are robust to the imposition of the high-speed rules. Hence, it is suggested to implement these rules on top of on-line energy management strategies, as the advantages in terms of vehicle driveability and of control on the SOC are countered only by a negligible increase in fuel consumption.

4.4.2 Engine off for prolonged decelerations

As already explained, drivers expect a correlation between some of their actions and the vehicle response. One such correlation that has not been addressed yet is the response of the powertrain to the depression of the brake pedal. In fact, if the general behaviour for the local optimal strategies, especially for the ECMS, is to turn off the engine when the torque request at the wheels is negative, this does not happen every single time. In some cases, the strategy considers that the cost of an engine shut-down outweighs the lost gain in regenerated power caused by the engine being kept turned on. As a result, the strategy will sometimes keep the engine on even during vehicle braking. While this behaviour is not unfavourable a priori, as the vehicle might accelerate again after a few seconds, it is preferable to provide the driver with a consistent response when braking.
It is then advisable to introduce a rule to define the behaviour of the powertrain while braking. Keeping in mind the importance of modifying the local optimal strategies as little as possible, the imposed rule is the following:

- *Rule 1*. The engine is turned off after 3 seconds of consecutive negative torque request at the wheels.

The impact of the rule presented above on results of fuel consumption is shown in Table 4.6.
Similarly to what happened for the high-speed impositions in Paragraph 4.4.1, fuel consumption is not affected in noticeable measure by the imposition of the rule for prolonged braking. Actually, a small decrease in fuel consumption is observed for both strategies, by virtue of the more power regenerated during braking.

Table 4.6 – Results for simulation over 100 random driving cycles of the different energy management strategies – Minimum dwell time of 20 seconds, noise limiting, high vehicle speed and prolonged deceleration impositions applied to local optimal strategies

Strategy name	Fuel consumption [l/100km]	Engine events [nb/min]	Final SOC [%]	Gain /pure thermal [%]
Pure thermal	9.35	-	-	-
PMP	3.97	5.14	50	57.5
SDP	4.68	1.14	44.32	49.9
ECMS	4.83	1.15	49.11	48.3

As a result, it is suggested to implement a rule on top of the energy management strategy to address the behaviour of the powertrain while braking. In fact, even if not as significant as the high-speed impositions, this rule helps improving the vehicle driveability at no cost.

4.5 Conclusion

The chapter has discussed the issue of driveability of the vehicle, illustrating its relevance and its impact on local optimal energy management strategies.
First off, the driveability issue was introduced and it was pointed out how it constitutes a primary factor in the satisfaction of the customer. Then, some driveability aspects were defined and their impact on local optimal energy management strategies was analysed.
The minimum dwell time is the first of such aspects. Its imposition entailed a substantial change in simulation results, with a significant increase of fuel consumption for both local optimal strategies. However, the ECMS strategy is the most affected, with the consequence that the results for the optimal calibration of Chapter 3 were overturned. In fact, when a minimum dwell time is imposed, the SDP strategy yields the best results in terms of fuel consumption, outperforming the ECMS strategy in any case analysed.
The second aspect of driveability analysed is the engine utilisation pattern, which is important both for the engine adaptation and for the feedback noise delivered to the driver. Also in this case the SDP strategy outperforms the ECMS strategy, showing an engine utilisation pattern not too distant from the

one of pure thermal engines. As a result, the SDP strategy would not require any redesign of the engine and would overall feel quite natural to the driver. On the contrary, the ECMS strategy would probably need a redesign of the engine, at least partial, and it would sound quite weird to the driver.
Successively, it was shown how it is possible to tweak local optimal strategies by imposing simple rules apt to address the powertrain behaviour in particular situations. Rules limiting engine noise at low speed, imposing the engine to be turned on at high speed, and shutting off the engine for prolonged decelerations were introduced. Results showed that the impact on fuel consumption of such rules is practically negligible, while the improvement to the comfort of the driver is substantial. Yet, it is important to keep the number of rules imposed on top of the strategy at a minimum, in order not to turn the local optimal energy management strategy into a heuristic energy management strategy, with all the ensuing problems.

To conclude the chapter, it is intended to highlight how the SDP strategy has proven the better strategy in terms of robustness and adaptability to driveability constraints. In fact, its stochastic approach to the energy management problem results in being more appropriate than the instantaneous optimisation of the ECMS strategy for integrating driveability constraints, in particular the dwell time. This results in better fuel consumption when some real-world driveability constraints are applied to the strategy. In addition, the SDP strategy presents an engine utilisation that is closer to the one of pure thermal vehicles, entailing decisive advantages in terms of engine adaptation and of driveability.
As a result, Stochastic Dynamic Programming appears as the strongest candidate for responding to the challenge of energy management in charge-sustaining hybrid electric vehicles for the near future.

Chapter 5

Conclusion and future perspectives

5.1 Summary

The thesis has presented the problem of energy management in charge-sustaining hybrid electric vehicles and has proposed a solution that is considered answering in the best way to the challenge.
In the introduction, the centrality of HEVs in today's automotive scenario was discussed. The advantages with respect to purely thermal vehicles introduced by HEVs, leading to an improvement of fuel consumption, were presented. Then, the problem of energy management in hybrids was introduced, presenting the challenges the energy management strategy needs to address.
In Chapter 1, the considered vehicle architecture was illustrated and a few relevant data about the vehicle were given. Then, the models employed for simulation were presented and the vehicle model was validated. Finally, the sample of random driving cycles employed in simulations was introduced and the methodology for its generation was presented.
In Chapter 2, the energy management controller position in the framework of the entire powertrain control architecture was illustrated and its duties were explained. The energy management problem was defined formally and some possible solutions to it were presented. A few energy management strategies were introduced from a theoretical standpoint and their advantages and disadvantages were discussed. A distinction between heuristic strategies, global optimisation strategies, and local optimisation strategies was made. The concept of on-line and off-line controllers was also illustrated, highlighting how an on-line controller is needed to address the power split on real HEVs.
In Chapter 3, the tuning procedure for local optimal strategies was explained and the impact of proportionality coefficients was detailed. Then, the results for simulation of the strategies were presented, showing how ECMS outperforms SDP in case the only driveability constraint is a limit on the maximum number of engine events. The results were analysed and justified by means of a powertrain efficiency analysis, showing how it is of pivotal importance to

optimise the whole powertrain operation and not the engine operating points alone.
In Chapter 4, the issue of driveability was introduced to the analysis, explaining its centrality for customer's satisfaction. A few driveability parameters were discussed: the dwell time, the engine utilisation, the engine noise, and other minor ones. It was explained how impositions on the minimum dwell time greatly affect fuel consumption results, overturning the results of Chapter 3. In fact, when a minimum dwell time was imposed, SDP had an edge over ECMS in terms of fuel consumption. In addition, it was explained how SDP is also advantaged by its engine utilisation profile, which is closer to the one of purely thermal vehicles, and the deriving implications in terms of engine adaptation and driveability were illustrated.

5.2 Conclusion

The goal of the study was to identify the most appropriate control strategy for taking up the challenge of energy management in hybrid electric vehicles. In this way, the study was intended to suggest an alternative to heuristic strategies currently employed by manufacturers on production HEVs. Two particularly promising local optimal energy management strategies were compared: the Equivalent Consumption Minimisation Strategy (ECMS) and the Stochastic Dynamic Programming (SDP).
The simulation results, carried out on a sample of 100 random driving cycles, show that ECMS has a clear advantage over SDP in terms of fuel consumption when the "naked" strategies, only with a limit on the number of engine events, are considered. This result is primarily due to the significantly more efficient engine utilisation in ECMS. However, this more efficient engine utilisation comports a greater reliance on the indirect path to the wheels, which reduces the overall efficiency of the powertrain. As a result, the difference between fuel consumption of ECMS and SDP is contained.
In order to improve the vehicle driving pleasure and move towards a more realistic situation, a few driveability aspects were introduced to the analysis. The study allowed to understand that, when a real-life driveability imposition, such as the minimum dwell time, is integrated to local optimal strategies, the results of fuel consumption for both strategies are significantly increased. Furthermore, conclusions presented above are overturned as, when a minimum dwell time is

imposed, SDP proves better than ECMS in terms of fuel consumption. The reason for this primarily lies in the more robust engine state management operated by SDP, by virtue of its stochastic approach to energy management. Moreover, SDP presents an engine utilisation profile that is reminiscent of that of purely thermal vehicles, entailing decisive advantages in the adaptation of previously designed engines and in the feeling given to the driver.
To conclude, SDP appears more suitable than ECMS for managing the energy flow in a real vehicle. As a result, Stochastic Dynamic Programming, by virtue of its close-to-optimal fuel consumption and its adaptability to real-world constraints, proposes itself as the natural candidate for relieving the challenge of energy management in the transition from conventional to hybrid electric vehicles.

5.3 Future perspectives

In the last few months, the SDP energy management strategy has been adapted to the architecture of Flex Hybrid, the research vehicle of IFP Energies nouvelles, and has been calibrated for the new application. At the moment of redaction of this chapter, the SDP strategy was compiled and run in parallel to the current energy management strategy equipped on Flex Hybrid. The next step is constituted by the utilisation of the torque set points yielded by the SDP strategy for determining the power split in the test vehicle. This would constitute a major milestone in the energy management field as, to the author's knowledge, SDP has never been equipped on an actual vehicles previously.
Future work regarding SDP should be addressed to the improvement of compatibility of the SDP strategy to production vehicles requirements. In fact, at the moment, the SDP strategy employs four dimensional maps for determining the torque split on-line. This can constitute a problem for production vehicles, whose limited memory capacity would probably be insufficient for containing four dimensional maps. Hence, it would be greatly beneficial to find a strategy to interpolate, at least partially, the maps and reduce their number of dimensions or to extract a set of rules from them. In addition, it would be of sure interest to develop a simple way to tune the SDP strategy after generation, in order to provide the repair shop with an effective tool to alter the strategy behaviour in case of problems, without needing to go back to the design department of the vehicle manufacturer.

Moreover, it could be interesting to dedicate some attention to the evaluation of other objectives and constraints, aside from fuel consumption and vehicle driveability, for both local optimal strategies. For instance, it would be of sure interest to evaluate the impact of the different profiles of engine utilisation on pollutants emissions. Another development worth of notice is the analysis of the possibility of integrating in both local optimal strategies additional states to control, alongside the battery SOC. This would prove most useful, for instance, for the control of the engine temperature, especially in the first few minutes of vehicle operation.

Finally, another aspect worth exploring is the application of local optimal energy management strategies to the plug-in hybrid case. In such context, a comparison similar to the one carried out in the thesis would prove most useful for indicating the direction academic institutions and manufacturers should address their efforts in coming years.

Annex 1

Complete vehicle specifications

Vehicle	Mass	m	1930 kg
	Wheel radius	r_{wheel}	0.317 m
	Wheel inertia	J_{wheel}	1.1 kg·m^2
	Drag area	$A_f \cdot c_d$	0.835 m^2
	First rolling friction coefficient	$f_{r,1}$	0.0069
	Second rolling friction coefficient	$f_{r,2}$	$9.48 \cdot 10^{-5}$ 1/(m/s)
	Mechanical brakes limit torque	$T_{brake,limit}$	- 4000 N·m
Engine	Typology		4 cylinders in line, turbocharged
	Displacement		2.0 l
	Maximum power	$P_{eng,max}$	150 kW
	Maximum torque	$T_{eng,max}$	304 N·m
	Maximum speed	$N_{eng,max}$	6300 rpm
	Idle speed	$N_{eng,idle}$	750 rpm
Motor	Maximum power	$P_{mot,max}$	42 kW
	Maximum torque	$T_{mot,max}$	140 N·m
	Minimum torque	$T_{mot,min}$	-140 N·m
Battery	Typology		NiMH
	Capacity	Q_{batt}	5 Ah, 1.9 kWh
	Upper SOC limit		70 %
	Lower SOC limit		30 %
	Initial SOC for simulations		50 %
	Target SOC		50 %
Transmission	Ratio gear 1	$i_{g,1}$	3.9091
	Ratio gear 2	$i_{g,2}$	2.1053
	Ratio gear 3	$i_{g,3}$	1.3871
	Ratio gear 4	$i_{g,4}$	1.0233

	Ratio gear 5	$i_{g,5}$	0.814
	Ratio gear 6	$i_{g,6}$	0.6739
	Efficiency gears 1 to 6	$\eta_{g,m}$	97 %
	Ratio differential	i_{diff}	3.8421
	Efficiency differential	η_{diff}	98 %
	Ratio electric driveline coupling gear	$i_{g,mot}$	2.863
	Efficiency electric driveline coupling gear	$\eta_{g,mot}$	100 %
Various parameters	Air density	ρ_{air}	1.226 kg/m^3
	Fuel (petrol) density	ρ_{fuel}	0.745 kg/l
	Fuel (petrol) lower heating value	LHV	42,23 MJ/kg

Annex 2

The gear shifting rule

MATLAB CODE

```
% Gear shift based on heuristic law
Gear_Number = 0;
Engine_Speed = 0;

for ii = 2:Cycle_Length-1
    Engine_Speed(ii) = (Gear_Number(ii-1) ~= 0) *
    Vehicle_Speed(ii-
    1)/Tyre_Radius*Ratio_primary_to_wheel(max(Gear_Number(ii-
    1),1))*30/pi;

    if Torque_Wheels(ii) > 0 && Gear_Number(ii-1) == 0

        Gear_Number(ii) = 1;

    elseif Engine_Speed(ii) >
    Engine_Speed_max(max(Gear_Number(ii-1),1)) &&
    Gear_Number(ii-1) < 6

        Gear_Number(ii) = Gear_Number(ii-1)+1;

    elseif Engine_Speed(ii) <
    Engine_Speed_min(max(Gear_Number(ii-1),1)) &&
    Gear_Number(ii-1) > 1

        Gear_Number(ii) = Gear_Number(ii-1)-1;

    elseif V_veh_sp(ii) == 0

        Gear_Number(ii) = 0;

    else

        Gear_Number(ii) = Gear_Number(ii-1);

    end
end

Gear_Number(end+1) = 0;
Engine_Speed(end+1) = 0;
```

ENGINE SPEED LIMIT VECTORS

Gear Number [-]	**Minimum engine speed (Engine_Speed_min) [rpm]**	**Maximum engine speed (Engine_Speed_max) [rpm]**
1	750	3000
2	1500	3000
3	1500	3000
4	1500	3000
5	1500	3000
6	1500	5000

Annex 3

Estratto in Italiano

Il presente estratto è volto a fornire un'introduzione al problema della gestione dell'energia nei veicoli ibridi elettrici, affrontato dalla tesi, e ad illustrare i principali risultati ottenuti. Considerato che figure e tabelle nell'estratto sono riprese dal testo della tesi, anche la numerazione originale è riportata al fine di agevolare la ricerca della sezione corrispondente nel corpo della tesi.

A3.1 Introduzione

Gli ultimi anni hanno visto sviluppi sostanziali nell'ambito dei veicoli ibridi elettrici, che hanno dimostrato di essere una soluzione particolarmente efficace e conveniente per ridurre i consumi di carburante e le emissioni di CO_2 dei veicoli per passeggeri. I veicoli ibridi elettrici portano notevoli vantaggi, ma comportano anche una complicazione dell'architettura del propulsore, a causa dell'aggiunta di un sistema di propulsione elettrico (costituito, nella sua versione più semplice, da batteria, motore elettrico e convertitori di corrente).
Una delle criticità più rilevanti introdotte dall'ibridazione del propulsore è la gestione dell'energia, ovvero la decisione, fatta in tempo reale sul veicolo, su come soddisfare la richiesta di coppia alle ruote. Difatti, l'introduzione di un sistema di propulsione elettrico porta ad una nuova flessibilità nell'adempimento della richiesta di coppia alle ruote, che può essere soddisfatta in diversi modi: con il solo motore termico, con il solo motore elettrico, oppure con entrambi i motori allo stesso tempo. La decisione su quale di questi organi utilizzare per soddisfare la richiesta alle ruote è effettuata da una strategia di gestione dell'energia, il cui studio costituisce l'argomento principale della tesi.

Diverse strategie di controllo sono state sviluppate negli ultimi anni per rispondere al problema della gestione dell'energia. Limitando l'analisi agli ibridi di tipo charge-sustaining, è possibile riscontrare due direzioni differenti seguite dalle case produttrici di veicoli ibridi e dal mondo accademico.

Difatti, le case automobilistiche hanno perlopiù sviluppato strategie di controllo euristiche, costituite da un insieme di regole determinanti il comportamento del propulsore in ogni situazione e basate sull'intuizione e l'esperienza degli sviluppatori. Queste strategie sono caratterizzate da un'ottima affidabilità, tanto che ogni veicolo ibrido attualmente in produzione le utilizza, e da risultati dei consumi sufficientemente soddisfacenti [34]. Nonostante ciò, le strategie euristiche presentano notevoli svantaggi in termini di tempi e costi di sviluppo, a causa dell'ingente lavoro di calibrazione che è necessario effettuare, e presentano uno svantaggio strutturale in termini di consumo di carburante rispetto alle strategie basate su un'ottimizzazione [36].

Al contrario, il mondo accademico si è maggiormente focalizzato su strategie ottimizzate, ovvero strategie basate su un'ottimizzazione globale o locale.

Le strategie di ottimizzazione globale ottimizzano il comportamento del propulsore sull'intero ciclo di guida, che deve essere conosciuto per intero a priori, escludendo quindi l'applicazione di tali strategie su veicoli reali (da cui la definizione di strategie off-line). Queste strategie sono utili come riferimento, in virtù della garanzia di ottimalità dei risultati da esse prodotti. Due strategie di ottimizzazione globale hanno ricevuto una particolare attenzione nell'ambito dei veicoli ibridi, il Principio del minimo di Pontryagin (PMP) [38], [39], e la Programmazione Dinamica (DP) [45], [46].

Le strategie di ottimizzazione locale, invece, ottimizzano il comportamento del propulsore sull'istante di tempo corrente. Di conseguenza, nessuna informazione relativa al comportamento futuro del veicolo è richiesta e le strategie possono essere implementate in tempo reale sul veicolo (da cui l'inclusione di tali strategie nelle gruppo delle strategie on-line). Due strategie di ottimizzazione locale hanno suscitato un particolare interesse negli ultimi anni: la Strategia di Minimizzazione del Consumo Equivalente (ECMS), nelle sue varie declinazioni [38], [51], [53], e la Programmazione Dinamica Stocastica (SDP), [58], [63].

L'obiettivo dello studio risiede nell'effettuare una comparazione rigorosa tra le strategie ECMS ed SDP, al fine di comprendere quale strategia di controllo dell'energia sia più adeguata per venire implementata sui veicoli di produzione del prossimo futuro. L'attenzione è rivolta sia all'aspetto classico del consumo di carburante che all'aspetto, più innovativo, della guidabilità del veicolo. Alla fine dello studio verrà proposta una strategia capace di unire risultati di consumo di carburante soddisfacenti ad un buon comfort di guida del veicolo.

A3.2 Dati ed architettura del veicolo

Il veicolo considerato per lo studio è una Renault Scenic, equipaggiata con un propulsore ibrido elettrico parallelo, rappresentato nella Figura A3.1.

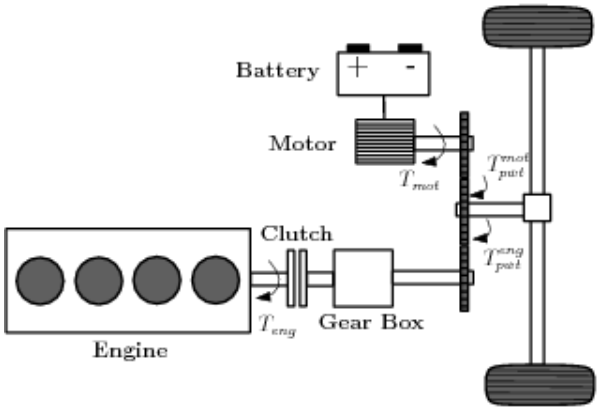

Figura A3.1 (1.1) – L'architettura del propulsore (ibrido parallelo)

Il propulsore è un ibrido parallelo post-trasmissione, considerato che la congiunzione tra il motore termico ed il motore elettrico è effettuata a valle del cambio. Questa congiunzione è effettuata per mezzo di un ingranaggio fisso, mentre il cambio è un cambio robotizzato. Le più rilevanti specifiche del veicolo sono riportate nella Tabella A3.1.

Tabella A3.1 (1.1) – Specifiche del veicolo

Motore termico	4 cilindri, 2.0 L, 150 kW / 5000 rpm
Motore elettrico	42 kW
Trasmissione	Cambio robotizzato
Batteria	NiMH, 5 Ah
Massa del veicolo	1930 kg

A3.3 Strategie di gestione dell'energia

Lo studio si propone di analizzare le strategie di controllo che possono venire equipaggiate su un veicolo reale. Di conseguenza, l'attenzione sarà rivolta alle strategie di ottimizzazione locale, ECMS ed SDP.

A3.3.1 Il problema di gestione dell'energia

Il funzionamento della strategia di controllo è illustrato dalla Figura A3.2. Sostanzialmente, il compito della strategia di gestione dell'energia consiste nel determinare il valore della variabile di controllo u_k. Per far ciò, la strategia utilizza degli input esterni al propulsore (v_k, velocità del veicolo, e a_k, accelerazione del veicolo, entrambi considerati all'istante di tempo corrente k) e degli input interni ad esso (x_k, stato di carica della batteria, e $e_{on,k}$, stato del motore termico).

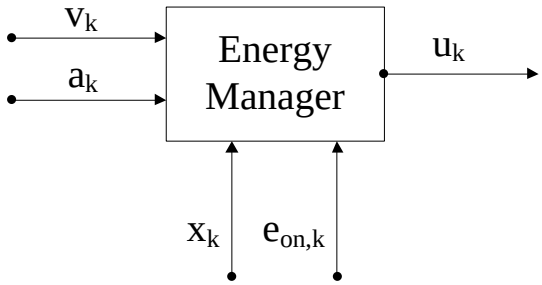

Figura A3.2 (*2.2*) – *Rappresentazione di input ed output della strategia di gestione dell'energia*

La variabile di controllo u_k definisce la suddivisione della coppia tra il motore elettrico ed il motore termico. Nello studio questa variabile è scelta come segue:

$$u_k = T_{eng,k} \tag{A3.1}$$

con $T_{eng,k}$ coppia prodotta dal motore termico.
La scelta della coppia del motore termico (piuttosto che la coppia del motore elettrico) come variabile di controllo è arbitraria visto che, una volta definita una delle due coppie, l'altra è immediatamente identificata grazie alla relazione

$$T_{pwt,k} = T_{eng,k} \cdot i_{tr,th,k} \cdot \eta_{tr,th,k} + T_{mot,k} \cdot i_{tr,el} \cdot \eta_{tr,el} \tag{A3.2}$$

dove $T_{pwt,k}$ è la coppia richiesta alle ruote, $T_{mot,k}$ è la coppia prodotta dal motore elettrico, $i_{tr,th,k}$ ed $\eta_{tr,th,k}$ sono il rapporto e l'efficienza delle trasmissioni dal motore termico alle ruote, e $i_{tr,el}$ ed $\eta_{tr,el}$ sono il rapporto e l'efficienza delle trasmissioni dal motore elettrico alle ruote. La coppia richiesta alle ruote è un input della strategia di controllo, derivato dalla posizione del pedale dell'acceleratore tramite una mappa. Il rapporto e l'efficienza delle trasmissioni nel propulsore sono, invece, parametri di design. Di conseguenza,

le uniche due incognite in A3.2 sono i valori di coppia del motore termico e del motore elettrico. Quando uno dei due è determinato, anche l'altra variabile è conosciuta.

Utilizzando una terminologia più propria, gli input della strategia di controllo vengono definiti stati del sistema e, per convenienza, gli stati sono raggruppati nel vettore $\boldsymbol{X_k}$

$$\boldsymbol{X_k} = \begin{Bmatrix} x_k \\ v_k \\ a_k \\ e_{on,k} \end{Bmatrix} \tag{A3.3}$$

La dinamica del sistema può dunque venire espressa come

$$\boldsymbol{X_{k+1}} = F(\boldsymbol{X_k}, u_k) \tag{A3.4}$$

Il costo associato ad uno stato del sistema $\boldsymbol{X_k}$ ed ad una variabile di controllo u_k è definito come

$$C(\boldsymbol{X_k}, u_k) = Q_{fuel}(\boldsymbol{X_k}, u_k) + \gamma \cdot \left(e_{on,k+1} - e_{on,k}\right)^2 \tag{A3.5}$$

dove Q_{fuel} è il flusso di carburante nel motore all'istante di tempo k e γ è un coefficiente di proporzionalità che determina il costo di ogni evento del motore termico (spegnimento o accensione).
Il problema di gestione dell'energia può dunque essere formulato come segue:

$$\begin{gathered} u^* = \arg\min_{u \in U} \left[\sum_{k=1}^{N} C(\boldsymbol{X_k}, u_k) \right] \\ \text{soggetto a} \begin{cases} \boldsymbol{X_{k+1}} = F(\boldsymbol{X_k}, u_k) \\ G(\boldsymbol{X_k}, u_k) \leq 0 \\ x_N = \overline{x} \end{cases} \end{gathered} \tag{A3.6}$$

dove *N* è l'ultimo istante nel ciclo di guida.
Essenzialmente, (A3.6) è un problema di ottimizzazione vincolata. Dunque, risolvere (A3.6) significa individuare il valore della variabile di controllo u^* che

minimizzi il costo totale dell'operazione del veicolo sull'intero ciclo di guida. Perché la soluzione sia accettabile, il valore scelto della variabile di controllo u^* deve essere incluso nell'insieme U di valori che possono essere assunti dalla variabile di controllo.
Inoltre, la minimizzazione è soggetta ad alcune limitazioni, raggruppate nella parentesi graffa. Innanzi tutto, il sistema è soggetto alla propria dinamica. In secondo luogo, è necessario rispettare le imposizioni riguardanti lo stato corrente del sistema, che vengono raggruppate nella disuguaglianza $G(\boldsymbol{X_k}, u_k) \leq 0$. Esempi di tali imposizioni sono la coppia massima che può essere trasmessa alle ruote o i limiti imposti allo stato di carica della batteria. La terza imposizione riguarda lo stato di carica della batteria alla fine del ciclo di guida, che deve essere pari al valore $\overline{x}$. L'imposizione di questa regola è necessaria al fine di garantire all'inizio del ciclo di guida successivo una carica della batteria sufficiente perché il motore elettrico possa trasmettere coppia alle ruote.
La teoria del controllo ottimo ha sviluppato diversi approcci alla soluzione di (A3.6), da cui derivano diverse strategie di gestione dell'energia. In questo estratto, l'attenzione è posta sulle due strategie di ottimizzazione locale: la Strategia di Minimizzazione del Consumo Equivalente e la Programmazione Dinamica Stocastica.

A3.3.2 Strategia di Minimizzazione del Consumo Equivalente

La strategia ECMS risolve il problema (A3.6) dividendolo in una serie di sotto-problemi, uno per ogni passo temporale, che vengono risolti on-line, durante la marcia del veicolo.
Innanzi tutto, è necessario ridefinire la funzione di costo (A3.5) come segue:

$$C_{ecms}(\boldsymbol{X_k}, u_k) = Q_{fuel}(\boldsymbol{X_k}, u_k) + \psi \cdot \left(e_{on,k+1} - e_{on,k}\right)^2 \qquad \text{(A3.7)}$$

dove ψ è un coefficiente di proporzionalità specifico per la strategia ECMS, equivalente a γ di (A3.5).
La funzione Hamiltoniana del sistema è dunque definita come

$$H(\boldsymbol{X_k}, u_k, s_k) = C_{ecms}(\boldsymbol{X_k}, u_k) + \frac{s_k}{LHV} \cdot P_{batt}(\boldsymbol{X_k}, u_k) \qquad \text{(A3.8)}$$

dove LHV è il potere calorifico inferiore del carburante, P_{batt} è la potenza prodotta o assorbita dalla batteria e s_k è il fattore di equivalenza, un coefficiente utilizzato per convertire l'energia elettrica nel flusso di carburante equivalente [38].
Per ogni passo temporale la strategia sceglie il valore della variabile di controllo che minimizza l'Hamiltoniana del sistema, scegliendo tra i valori possibili della variabile di controllo e garantendo sempre il rispetto dei vincoli in (A3.6):

$$u_k^* = \arg\min_{u \in U}[H(\boldsymbol{X_k}, u_k, s_k)] \tag{A3.9}$$

Il rispetto della terza imposizione in (A3.6) è ottenuto tramite l'adattamento on-line del fattore di equivalenza s_k, per mezzo di un controllore proporzionale:

$$s_k = s_0 - k_p \cdot (x_k - \overline{x}) \tag{A3.10}$$

dove s_0 è il valore iniziale del fattore di equivalenza, uguale per ogni ciclo di guida, e k_p è il guadagno del controllore proporzionale. Quando lo stato di carica della batteria è inferiore allo stato di carica desiderato al termine del ciclo di guida, il valore di s_k viene aumentato. In questo modo, l'energia elettrica ha un costo relativo maggiore in (A3.8), con il risultato che la strategia tende a privilegiare un utilizzo maggiore del motore termico. Così, lo stato di carica della batteria può aumentare. La situazione diametralmente opposta si verifica quando lo stato di carica della batteria è superiore allo stato di carica desiderato al termine del ciclo di guida. In questo modo la strategia di gestione dell'energia riesce a garantire il sostegno della carica della batteria in ogni condizione, come richiesto in (A3.6).

A3.3.3 Programmazione Dinamica Stocastica

Un'altra soluzione per il problema (A3.6) è fornita dalla Programmazione Dinamica Stocastica [43]. Il fondamento della strategia risiede nel vedere il ciclo di guida come una catena di Markov, secondo cui lo stato del veicolo nel prossimo passo temporale, in termini di velocità ed accelerazione, dipende unicamente dallo stato corrente del veicolo:

$$\begin{cases} v_{k+1} = v_k + a_k \cdot \Delta t \\ a_{k+1} \sim P(a_{k+1}|a_k, v_k) \end{cases} \tag{A3.11}$$

dove Δt è il passo temporale. Se la velocità del veicolo nel prossimo passo temporale è conosciuta deterministicamente, l'accelerazione del veicolo nel prossimo passo temporale è invece espressa in termini probabilistici, come spiegato in [63]. La densità di probabilità associata al valore dell'accelerazione nel prossimo passo temporale è identificata tramite l'analisi statistica di un campione di cicli di guida di riferimento.
L'utilità di modellizzare il ciclo di guida come una catena di Markov risiede nell'eliminazione della dimensione temporale dal problema di ottimizzazione (A3.6), con la conseguenza di ridurre il problema globale in una serie di problemi locali.
Anche per la strategia SDP la funzione di costo (A3.5) viene ridefinita:

$$C_{sdp}(\boldsymbol{X_k}, u_k) = Q_{fuel}(\boldsymbol{X_k}, u_k) + \beta \cdot \left(e_{on,k+1} - e_{on,k}\right)^2 \tag{A3.12}$$

dove β è il coefficiente di proporzionalità specifico per la strategia SDP, equivalente a γ di (A3.5).
La variabile di controllo u^* è trovata risolvendo il problema del percorso minimo stocastico:

$$\begin{aligned} u^*(\boldsymbol{X_k}) = \arg\min_{u \in U} \mathbb{E}\Bigg[& \sum_{n=1}^{\infty} C_{sdp}(\boldsymbol{X_n}, u^*) \\ & + \alpha \cdot (x_k - \overline{x})^2 \cdot P(V_{on,k+1} = 0) \Bigg] \end{aligned} \tag{A3.13}$$

La variabile di controllo ottimale u^* è quella che minimizza il valore atteso del costo, ovvero il costo di uno stato del sistema per la probabilità che tale stato si verifichi, su un orizzonte infinito a partire dalle condizioni attuali $\boldsymbol{X_k}$ del sistema. Il rispetto dell'imposizione sul valore finale della carica della batteria, introdotto in (A3.6), è ottenuto per mezzo di un costo aggiuntivo che penalizzi i valori della carica differenti dal valore finale prefissato $\overline{x}$. L'importanza di questo costo è determinata dal valore di α, un altro coefficiente di proporzionalità. E' importante notare come anche questo costo sia un costo

probabilistico, essendo moltiplicato per la probabilità di spegnere il veicolo e terminare il ciclo di guida nel passo temporale successivo ($V_{on,k+1} = 0$).
In pratica, la strategia viene definita risolvendo (A3.13) off-line, in maniera ricorsiva, per tutte le possibili combinazioni dei valori del vettore $\boldsymbol{X_k}$, propriamente discretizzati. Il risultato è una mappa a 4 dimensioni, con gli stati del sistema sugli assi e contenente i valori ottimizzati della variabile di controllo u^*. Durante l'utilizzo del veicolo, questa mappa indica il valore della coppia del motore termico (e, conseguentemente, anche del motore elettrico) da adottare, risolvendo così il problema di ripartizione dell'energia on-line.

A3.4 Risultati della simulazione

Le strategie illustrate nella Sezione A3.3 presentano una serie di parametri per cui è necessaria una calibrazione: α e β per la strategia SDP, k_p e ψ per la strategia ECMS. Nello studio, il parametro ψ non necessita di calibrazione visto che, al fine di effettuare un paragone equo, viene imposto che entrambe le strategie basate sull'ottimizzazione locale presentino lo stesso numero di accensioni e spegnimenti del motore termico, qua limitato a 2 eventi al minuto. Di conseguenza, quando il parametro β è determinato, anche il parametro ψ è determinato univocamente. La calibrazione degli altri parametri è invece effettuata cercando di ottenere i consumi di carburante più bassi, ottemperando al tempo stesso ai vincoli in (A3.6).
Il valore scelto per gli stati di carica iniziale e finale della batteria è uguale a 50 %. Considerato che le strategie di controllo on-line non riescono a garantire il rispetto esatto della condizione sul valore finale dello stato di carica, tale condizione non è imposta strettamente. Invece, viene richiesto che il valore finale dello stato di carica sia superiore a 40 % per tutti i cicli di guida considerati. Successivamente, i valori di consumo di carburante vengono aggiustati al fine di compensare la distanza dello stato di carica finale da 50 %.
Le strategie di gestione energetica sono state simulate su un campione di 100 cicli di guida casuali, rappresentanti diverse condizioni di guida (urbane, suburbane, miste) e generati come spiegato in [63]. La diversità e la dimensione del campione permettono di ottenere risultati realistici, rappresentativi delle condizioni di utilizzo reali di un veicolo.
I risultati della simulazione, presentati nella Tabella A3.2, includono anche la strategia PMP, per quanto si tratti di una strategia prettamente off-line e non

applicabile su un veicolo reale. Difatti, i risultati della strategia PMP sono presentati in virtù della loro ottimalità, al fine di fornire un metro di paragone per le altre strategie.

Tabella A3.2 (3.1) – Risultati della simulazione su 100 cicli di guida casuali

Nome della strategia	Consumo di carburante [l/100km]	Eventi del motore [no/min]	Stato di carica finale [%]	Guadagno/ propulsore termico [%]
Propulsore termico	9.35	-	-	-
PMP	3.97	5.14	50	57.5
SDP	4.4	2	43.93	52.9
ECMS	4.15	1.99	47.43	55.6

E’ possibile osservare nei risultati presentati sopra come la strategia ECMS presenti un consumo di carburante decisamente migliore rispetto a quello della strategia SDP. In aggiunta, il consumo di carburante della strategia ECMS è particolarmente vicino al risultato ottimale della strategia PMP, per quanto svantaggiato dal limite imposto al numero di eventi del motore termico.

A3.5 Considerazioni sulla guidabilità

Se il consumo di carburante è uno dei parametri principali da tenere in conto per lo sviluppo di una strategia di gestione dell’energia, non è certamente il solo parametro. Infatti, è altrettanto importante fornire al guidatore un’esperienza di guida confortevole e piacevole, considerato che l’esperienza di guida costituisce un fattore immediato nella soddisfazione del cliente.
Diversi aspetti possono venire considerati per definire meglio il concetto di guidabilità del veicolo. Questo estratto si focalizza sui due aspetti più rilevanti, ovvero il tempo di stazionamento ed il profilo di utilizzo del motore termico.

A3.5.1 Tempo di stazionamento

Nella Sezione A3.4 un limite al numero di eventi del motore termico è stato introdotto. Questo limite è utile a ridurre lo sforzo sui componenti del

propulsore, ma non è efficace per migliorare il comfort di guida del veicolo. Difatti, come sostenuto in [25], non è un grande numero di eventi del motore termico lungo il ciclo di guida ad infastidire il guidatore, quanto la ripetizione di accensioni e spegnimenti a poca distanza di tempo gli uni dagli altri, ovvero ad una distanza temporale inferiore ai 10-20 secondi.
Di conseguenza, per migliorare la guidabilità del veicolo, è più interessante studiare gli intervalli di tempo tra due eventi del motore termico. E' dunque necessario introdurre un nuovo parametro: viene definito tempo di stazionamento il tempo trascorso tra due eventi consecutivi del motore termico, ovvero il tempo passato continuativamente con il motore termico nel medesimo stato (acceso o spento).
Al fine di migliorare il comfort di guida è necessario evitare i tempi di stazionamento troppo brevi. In teoria, ciò può essere realizzato in due modi: prevenendoli od eliminandoli.

PREVENZIONE

Nella Sezione A3.4 è stato mostrato come, una volta definito il parametro β della strategia SDP, anche il parametro ψ della strategia ECMS è definito. Di conseguenza, tutti i riferimenti nella sezione corrente sono fatti al valore di β.
L'obiettivo di questo parametro β consiste nel ridurre il numero di accensioni e spegnimenti del motore termico durante la guida. E' quindi ragionevole che il parametro abbia un impatto sul comportamento della strategia nei riguardi del tempo di stazionamento, impatto che si rivela essere duplice.
Innanzi tutto, il parametro β, riducendo il numero di eventi del motore lungo il ciclo di guida, riduce il numero assoluto dei tempi di stazionamento per un dato ciclo, qualunque sia la loro durata. Un minor numero di tempi di stazionamento implica, in media, un minor numero di brevi tempi di stazionamento, con il risultato di un migliore comfort di guida per il guidatore.
In secondo luogo, β ha anche un impatto sulla distribuzione di probabilità dei tempi di stazionamento, come illustrato nelle Figure A3.3 ed A3.4. Difatti, il valore di β più alto sposta la distribuzione di probabilità verso destra, ovvero verso valori di tempo di stazionamento più accettabili, per entrambe le strategie di ottimizzazione locale.

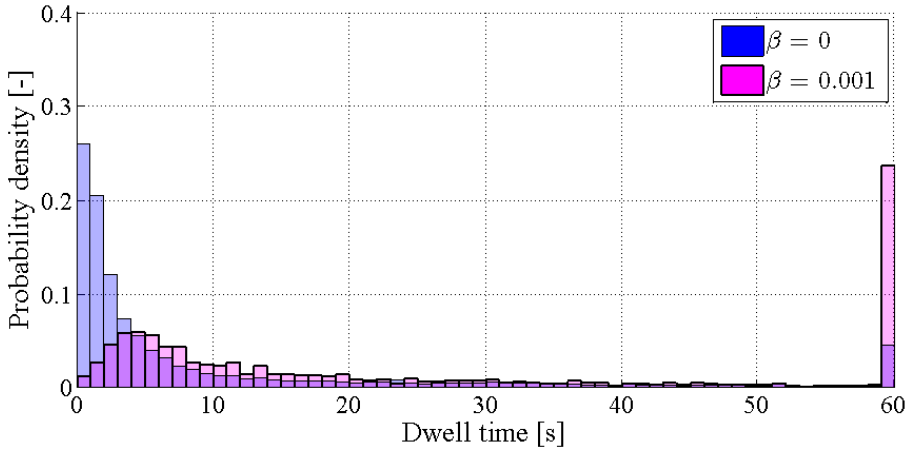

Figura A3.3 (4.3) – Impatto di β sulla distribuzione di probabilità dei tempi di stazionamento per la strategia SDP – I tempi di stazionamento ≥ 60 secondi sono stati raggruppati nella colonna corrispondente a 60 secondi

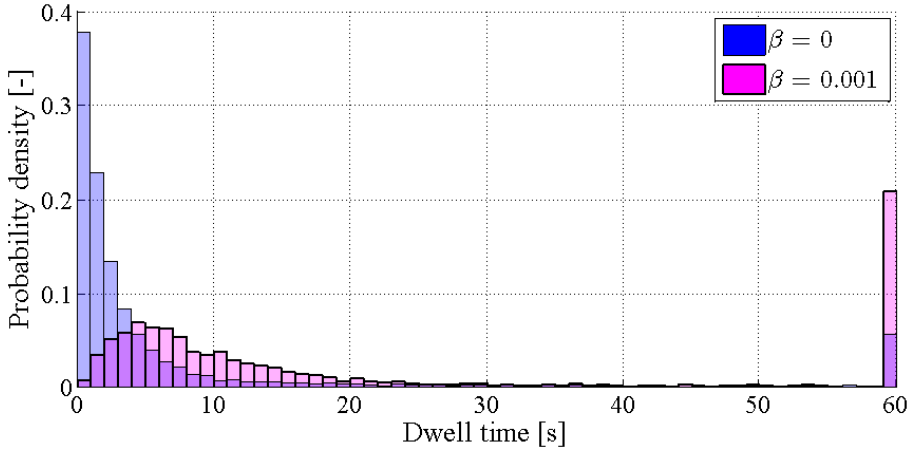

Figura A3.4 (4.4) – Impatto di β sulla distribuzione di probabilità dei tempi di stazionamento per la strategia ECMS – I tempi di stazionamento ≥ 60 secondi sono stati raggruppati nella colonna corrispondente a 60 secondi

RIMOZIONE

Il parametro β riesce a ridurre il numero di brevi tempi di stazionamento lungo il ciclo, ma non è abbastanza per evitarli completamente. Di conseguenza, è necessario imporre una regola che costringa la strategia di controllo del propulsore a produrre tempi di stazionamento di almeno 20 secondi. Questa

imposizione è sospesa nei casi di forza maggiore, per esempio quando lo stato di carica della batteria è vicino ai limiti prefissati o quando il motore da solo non è sufficiente per provvedere all'intera richiesta alle ruote. In aggiunta, al fine di non svantaggiare troppo la strategia durante i periodi di frenata, viene anche imposto di spegnere il motore termico durante le forti decelerazioni.
L'impatto dell'imposizione di un tempo di stazionamento minimo di 20 secondi sui consumi di carburante di entrambe le strategie e per valori di β differenti è mostrato nella Figura A3.5.

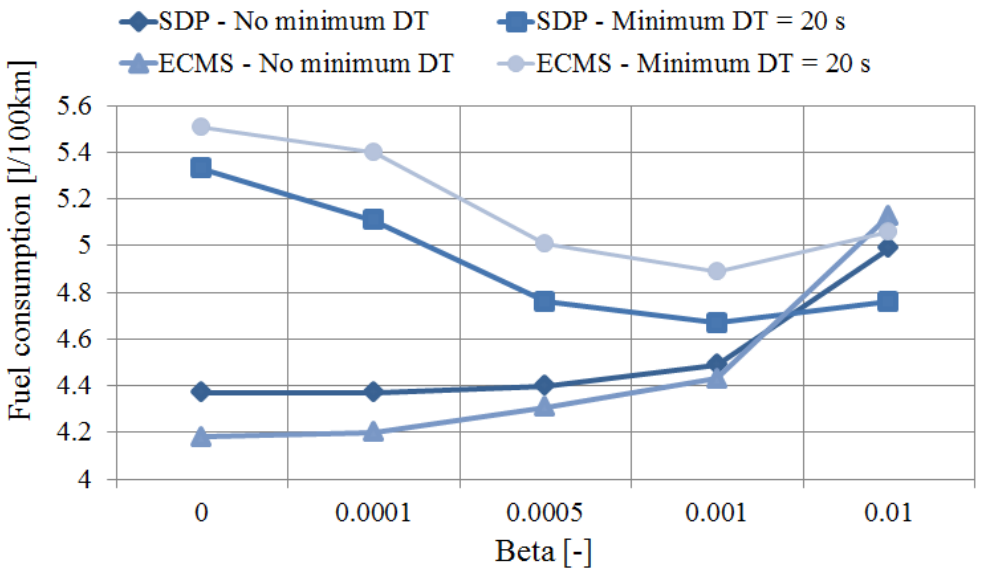

Figura A3.5 (4.14) – Impatto dell'imposizione di un tempo minimo di stazionamento di 20 secondi per valori diversi di β

Innanzi tutto, il consumo di carburante è fortemente aumentato dall'imposizione di un tempo minimo di stazionamento, per entrambe le strategie[27]. L'unico caso che non segue questo trend è il caso di $\beta = 0.01$. Infatti, questo valore di β produce una strategia di controllo per cui il numero degli eventi del motore permessi è fortemente limitato. L'applicazione delle regole descritte in precedenza risulta essere vantaggiosa grazie all'imposizione di spegnere il motore termico durante le forti decelerazioni, che aumenta il numero di eventi

[27] L'imposizione di un minimo tempo di stazionamento impone la ricalibrazione della strategia ECMS, al fine di mantenere un controllo adeguato sul profilo dello stato di carica della batteria. Il valore del parametro k_p è dunque più elevato di quello utilizzato per ottenere i risultati della Tabella A3.2, da cui scaturisce un aumento del consumo di riferimento nella Figura A3.5.

del motore lungo il ciclo di guida e dà luogo ad un migliore risultato di consumo di carburante.

Assodato che β riduce l'occorrenza dei brevi tempi di stazionamento, è possibile osservare che, quando un minimo tempo di stazionamento è imposto, ad un aumento di β corrisponde una diminuzione dei consumi. Questo è vero fino ad un certo punto visto che, se β è troppo grande, il risultato del consumo di carburante è insoddisfacente che il minimo tempo di stazionamento venga imposto o meno.

Quando un tempo minimo di stazionamento viene imposto, la strategia SDP ha un chiaro vantaggio sulla strategia ECMS in tutti i casi considerati. La ragione di questo risultato risiede principalmente nella differente gestione degli eventi del motore termico. Infatti, quando decide se spegnere o meno il motore, la strategia SDP tiene in conto anche la probabilità di avere bisogno del motore nell'immediato futuro. In questo modo, il motore viene spento solo quando non ve ne sarà bisogno per un periodo di tempo prolungato. Lo stesso avviene per la decisione di accendere il motore, producendo così una strategia che non soffre eccessivamente a causa dell'imposizione di un minimo tempo di stazionamento. Al contrario, la strategia ECMS determina lo stato del motore termico solo in base alle condizioni correnti. Di conseguenza, la strategia tende a spegnere il motore non appena il guidatore agisce sul pedale del freno, anche se lievemente. Nel caso che, poi, il guidatore acceleri di nuovo, l'imposizione di un minimo tempo di stazionamento impedisce di accendere il motore termico, causando così un comportamento non ottimale del propulsore. Il risultato finale è che la strategia ECMS soffre particolarmente le imposizioni legate al minimo tempo di stazionamento.

Un'altra ragione volta a giustificare il migliore comportamento della strategia SDP può essere individuata nella distribuzione di probabilità dei tempi di stazionamento per le due strategie, mostrata nelle Figure A3.3 ed A3.4. La distribuzione di probabilità della strategia SDP, a parità di β, tende ad essere spostata sulla destra rispetto a quella della strategia ECMS. Questo indica che la strategia SDP propende naturalmente a produrre dei tempi di stazionamento più lunghi, con una necessità minore di intervento dell'imposizione del minimo tempo di stazionamento.

L'interazione osservata tra β ed i risultati di consumo di carburante impone una ricalibrazione del parametro quando un minimo tempo di stazionamento viene imposto. La ricalibrazione è effettuata seguendo le linee guida spiegate nella Sezione A3.4. Dunque, i risultati per le strategie ricalibrate, con un tempo

minimo di stazionamento di 20 secondi imposto alle strategie di ottimizzazione locale, sono mostrati nella Tabella A3.3.

Tabella A3.3 (4.3) – Risultati della simulazione su 100 cicli di guida casuali – Tempo minimo di stazionamento di 20 secondi per le strategie di ottimizzazione locale

Nome della strategia	Consumo di carburante [l/100km]	Eventi del motore [no/min]	Stato di carica finale [%]	Guadagno/ propulsore termico [%]
Propulsore termico	9.35	-	-	-
PMP	3.97	5.14	50	57.5
SDP	4.67	1.1	44.26	50.1
ECMS	4.89	1.1	49.43	47.7

A3.5.2 Profilo di utilizzo del motore termico

Un altro aspetto di grande interesse nei propulsori ibridi è rappresentato dal profilo di utilizzo del motore termico, la cui analisi è rilevante sia per la guidabilità del veicolo che per la progettazione del propulsore. La Figura A3.6 presenta i punti di utilizzo del motore termico per un ciclo di guida casuale per le due strategie basate sull'ottimizzazione locale. I punti in blu rappresentano i punti di utilizzo del motore nel propulsore ibrido; i punti in rosso rappresentano l'utilizzo dello stesso motore nel caso di un propulsore puramente termico.
Innanzi tutto, è bene sottolineare che, per quanto nella Figura A3.6 sia presentato un solo ciclo di guida, il profilo di utilizzo del motore termico è generale, visto che si ripete in tutti i 100 cicli di guida casuali analizzati.
Entrambe le strategie di gestione dell'energia spostano i punti di utilizzo del motore termico verso zone caratterizzate da valori di coppia più elevati, aumentando in questo modo l'efficienza di utilizzo del motore. Se questa variazione è contenuta per la strategia SDP, la variazione introdotta dalla strategia ECMS è ben più drastica. Questo comporta conseguenze su due livelli.

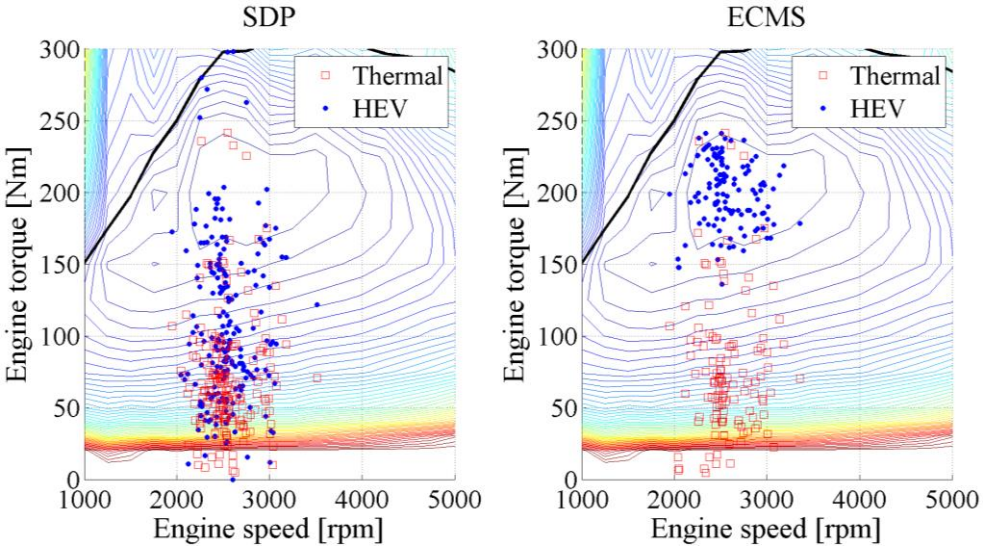

Figura A3.6 (4.15) – I punti di utilizzo del motore per un ciclo di guida casuale nei casi di propulsore ibrido e propulsore termico

Per prima cosa, la progettazione del motore termico deve tenere in conto il profilo di utilizzo del motore stesso. La strategia ECMS utilizza il motore in modo non dissimile da quello di un ibrido serie. Considerando che il motore termico degli ibridi serie risponde a dei criteri di progettazione ben differenti da quelli di un ibrido parallelo, è probabile che l'applicazione della strategia ECMS al caso sotto esame imponga un adattamento significativo del design del motore. Ciò è particolarmente svantaggioso per il caso di un ibrido parallelo, architettura che è considerata il primo passo nell'ibridazione del veicolo e che, generalmente, adatta motori progettati per applicazioni puramente termiche. Al contrario, il profilo di utilizzo del motore per la strategia SDP è abbastanza prossimo a quello del propulsore termico da non richiedere alcuna modifica sostanziale al design del motore.

In secondo luogo, il guidatore è solito aspettarsi una correlazione tra la posizione del pedale dell'acceleratore e la risposta del motore termico, innanzi tutto in termini di rumore e vibrazioni. Per la strategia SDP, la vicinanza dei punti di utilizzo del motore termico del propulsore ibrido a quelli del propulsore termico indica che questa correlazione è mantenuta. Al contrario, per la strategia ECMS tale correlazione è persa, visto che i punti di utilizzo del motore termico sono cambiati fortemente. Queste affermazioni sono giustificate dall'analisi di Figura A3.7, che presenta l'utilizzo del motore termico da parte delle due strategie su un estratto di uno dei 100 cicli di guida casuali.

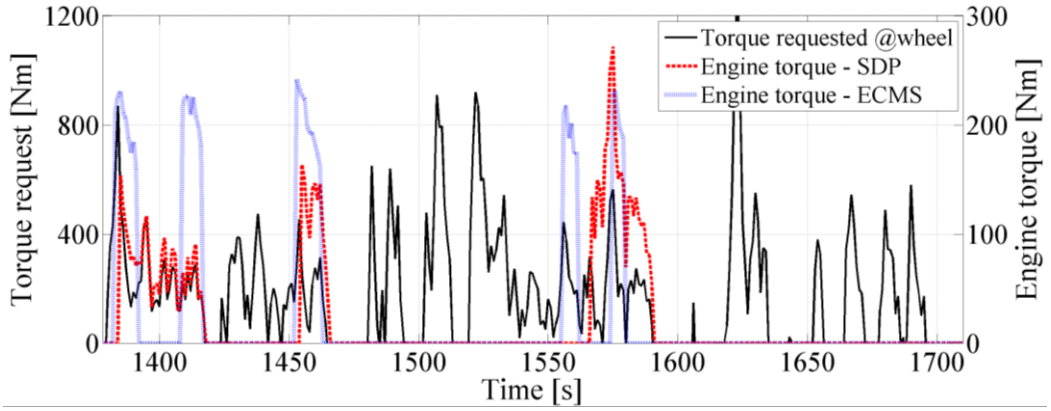

Figura A3.7 (3.20) – Comparazione della coppia per le strategie SDP ed ECMS

La strategia SDP produce un profilo di coppia del motore termico che segue, approssimativamente, il profilo di coppia richiesto alle ruote. In questo modo, il guidatore riceve il feedback atteso rispetto alla sua azione sul pedale dell'acceleratore. Questo feedback non è invece più presente per la strategia ECMS, il cui profilo di utilizzo del motore termico è completamente disgiunto dal profilo di coppia richiesto alle ruote.

A3.6 Conclusione

In questo estratto il problema della gestione dell'energia nei propulsori ibridi è stato introdotto e formalizzato. Sono state presentate due possibili soluzioni al problema, la Programmazione Dinamica Stocastica (SDP) e la Strategia di Minimizzazione del Consumo Equivalente (ECMS). Una comparazione tra queste due strategie è stata effettuata, focalizzandosi sugli aspetti di consumo del carburante e di guidabilità del veicolo.
I risultati dell'analisi mostrano che, nel caso le strategie vengano considerate senza imposizioni di guidabilità, la strategia ECMS appare essere più conveniente della strategia SDP in virtù del suo inferiore consumo di carburante. La situazione è ribaltata quando un vincolo di guidabilità realistico, come il tempo minimo di stazionamento, viene imposto alle due strategie. Infatti, in tale caso, la strategia SDP risulta essere più efficiente della strategia ECMS, grazie ad una più robusta gestione degli eventi del motore termico. In aggiunta, la strategia SDP presenta un utilizzo del motore termico piuttosto prossimo a

quello di un veicolo puramente termico, portando così dei vantaggi in termini di facilità di adattamento di un motore già in produzione ed in termini di guidabilità del veicolo.
Per concludere, è stato mostrato come la strategia basata sulla Programmazione Dinamica Stocastica riesca a coniugare un consumo di carburante soddisfacente ad una buona adattabilità a delle imposizioni di guidabilità realistiche e ad un utilizzo del motore termico particolarmente vantaggioso. Di conseguenza, la strategia SDP appare essere la soluzione più appropriata per risolvere il problema della gestione dell'energia nei veicoli ibridi elettrici di tipo charge-sustaining.

Acronyms

AMT	Automated Manual Transmission
ANN	Artificial Neural Networks
BSFC	Brake Specific Fuel Consumption
DP	Dynamic Programming
DT	Dwell Time
ECMS	Equivalent Consumption Minimisation Strategy
HEV	Hybrid Electric Vehicle
ICE	Internal Combustion Engine
OOL	Optimal Operating Line
PCM	Powertrain Control Module
PHEV	Plug-in Hybrid Electric Vehicle
PMP	Pontryagin's Minimum Principle
SDP	Stochastic Dynamic Programming
SOC	State Of Charge
WLTC	Worldwide harmonized Light duty Test Cycle
ZEV	Zero-Emissions Vehicle

List of Symbols

α	Weighing coefficient for distance from target SOC – Specific to SDP
β	Weighing coefficient for engine events cost – Specific to SDP
γ	Weighing coefficient for engine events cost
η	Efficiency
ϑ	Slope of the road
ρ	Density
ψ	Weighing coefficient for engine events cost – Specific to ECMS
ω	Rotating speed
a	Vehicle acceleration
c_d	Aerodynamic drag coefficient
c_{on}	Clutch state
e_{on}	Engine state
f_r	Rolling friction coefficient
g	Gravity acceleration
i	Reduction ratio
k	General time step
k_p	Controller's proportional gain
m	Mass of the vehicle

p_{tyre}	Tyre pressure
r_{wheel}	Radius of the wheel
s	Equivalence factor
t	Time
u	Control variable
v	Vehicle speed
x	Battery state of charge
A_f	Frontal area of the vehicle
$BSFC$	Brake specific fuel consumption
C	Cost
E	Energy
ES	Energy split
F	Force
H	Hamiltonian function
HR	Hybridisation ratio
J_u	Cost-to-go matrix
J_{wheel}	Moment of inertia of the wheel
I_{batt}	Battery current
LHV	Fuel lower heating value
N	Final time step of the driving cycle
P	Power
PS	Power split ratio

Q_{batt}	Battery capacity
Q_{fuel}	Fuel flow
R	Resistance
T	Torque
U	Set of acceptable values of the control variable
V_{oc}	Open circuit voltage
V_{on}	Position of the vehicle key
$\boldsymbol{X}$	States of the system
Z_{direct}	Fraction of energy passing through the direct pathway

Bibliography

[1] J. Fuglestvedt, T. Berntsen, G. Myhre, K. Rypdal, and R. Bieltvedt Skele, "Climate forcing from the transport sectors," in *Proceedings of the National Academy of Sciences*, 2008, vol. 105, no. 2, pp. 454–8.

[2] N. Nakicenovic, J. Alcamo, G. Davis, B. de Vries, J. Fenhann, S. Gaffin, K. Gregory, A. Grubler, T. Y. Jung, T. Kram, E. L. La Rovere, L. Michaelis, S. Mori, T. Morita, W. Pepper, H. M. Pitcher, L. Price, K. Riahi, A. Roehrl, H.-H. Rogner, A. Sankovski, M. Schlesinger, P. Shukla, S. J. Smith, R. Swart, S. van Rooijen, N. Victor, and Z. Dadi, *Special Report on Emissions Scenarios : a special report of Working Group III of the Intergovernmental Panel on Climate Change*. Cambridge University Press, New York, NY (US), 2000.

[3] T. Takaishi, A. Numata, R. Nakano, and K. Sakaguchi, "Approach to High Efficiency Diesel and Gas Engines," *Mitsubishi Heavy Industries, Ltd. Technical Review*, vol. 45, no. 1, 2008.

[4] P. Leduc and B. Dubar, "Downsizing of Gasoline Engine: an Efficient Way to Reduce CO2 Emissions," *Oil & Gas Science and Technology*, vol. 58, no. 1, pp. 115–127, 2003.

[5] T. Katrašnik, "Hybridization of powertrain and downsizing of IC engine – A way to reduce fuel consumption and pollutant emissions – Part 1," *Energy Conversion and Management*, vol. 48, no. 5, pp. 1411–1423, May 2007.

[6] V. Wouk, "Hybrids: then and now," *Spectrum, IEEE*, vol. 32, no. 7, pp. 16–21, 1995.

[7] K. Morita, "Automotive power source in 21st century," *JSAE Review*, vol. 24, no. July 2002, pp. 3–7, 2003.

[8] H. Yeo and H. Kim, "Hardware-in-the-loop simulation of regenerative braking for a hybrid electric vehicle," in *Proceedings of the Institution of Mechanical Engineers, Part D: Journal of Automobile Engineering*, 2002, vol. 216, no. 11, pp. 855–864.

[9] O. Bitsche and G. Gutmann, “Systems for hybrid cars,” *Journal of Power Sources*, vol. 127, no. 1–2, pp. 8–15, Mar. 2004.

[10] C. Mercier, *Advanced powertrain controls - Lecture at IFP School*. PSA Peugeot Citroën, 2012.

[11] J. Chen, Y. Li, and J. Wang, “Simultaneous optimisation of fuel consumption and emissions for a parallel hybrid electric SUV using fuzzy logic control,” *International journal of vehicle design*, vol. 46, no. 2, pp. 204–218, 2008.

[12] J. Vetter, P. Novák, M. R. Wagner, C. Veit, K.-C. Möller, J. O. Besenhard, M. Winter, M. Wohlfahrt-Mehrens, C. Vogler, and a. Hammouche, “Ageing mechanisms in lithium-ion batteries,” *Journal of Power Sources*, vol. 147, no. 1–2, pp. 269–281, Sep. 2005.

[13] G. Paganelli, M. Tateno, A. Brahma, G. Rizzoni, and Y. Guezennec, “Control development for a hybrid-electric sport-utility vehicle: strategy, implementation and field test results,” in *American Control conference*, 2001, vol. 6, pp. 5064–5069.

[14] O. Sundström, L. Guzzella, and P. Soltic, “Optimal hybridization in two parallel hybrid electric vehicles using Dynamic Programming,” in *Proceedings of the 17th IFAC world congress*, 2008, pp. 4642–4647.

[15] J. J. Valera, I. Iglesias, A. Peña, A. Martin, and J. Sánchez, “Integrated Modeling Approach for Highly electrified HEV. Virtual Design and Simulation Methodology for Advanced Powertrain Prototyping,” in *Proceedings of International Battery, Hybrid and Fuel Cell Electric Vehicle Symposium (EVS 24)*, 2009, vol. 3.

[16] L. Guzzella and A. Sciarretta, *Vehicle propulsion systems: introduction to modeling and optimization*. Springer Verlag, 2005.

[17] Bosch, *Bosch Automotive Handbook*. Robert Bosch GmbH, 2007.

[18] J. Heywood, *Internal combustion engine fundamentals*. McGraw-Hill, 1988.

[19] L. E. Unnewehr and S. A. Naser, *Electric vehicle technology*. John Wiley and Sons, New York, NY, 1982, p. 256.

[20] UNECE, “WLTC methodology,” 2011.

[21] P. Bremaud, *Markov Chains: Gibbs Fields, Monte Carlo Simulation, and Queues*. Springer, 1999.

[22] D. Kum, H. Peng, and N. Bucknor, “Optimal Energy and Catalyst Temperature Management of Plug-in Hybrid Electric Vehicles for Minimum Fuel Consumption and Tail-Pipe Emissions,” in *IEEE Transactions on Control Systems Technology*, 2013, pp. 14–26.

[23] L. Thibault, O. Grondin, C. Querel, and G. Corde, “Energy Management Strategy and Optimal Hybridization Level for a Diesel HEV,” *SAE International Journal of Alternative Powertrains*, vol. 1, no. 1, pp. 260–271, Jul. 2012.

[24] D. Opila, X. Wang, R. McGee, R. Gillespie, and J. W. Grizzle, “Incorporating drivability metrics into optimal energy management strategies for hybrid vehicles Part 1: Model, methods, and government drive cycles,” *IEEE Transactions on Control Systems Technology*, 2010.

[25] D. Opila, X. Wang, R. McGee, R. Gillespie, and Grizz, “Incorporating Drivability Metrics into Optimal Energy Management Strategies for Hybrid Vehicles Part 2: Real-World Robustness and Constraint Implementation,” in *IEEE Transactions on Control Systems Technology*, 2010.

[26] L. Serrao, S. Onori, A. Sciarretta, Y. Guezennec, and G. Rizzoni, “Optimal energy management of hybrid electric vehicles including battery aging,” in *American Control Conference*, 2011, pp. 2125–2130.

[27] S. Ebbesen, P. Elbert, and L. Guzzella, “Battery State-of-Health Perceptive Energy Management for Hybrid Electric Vehicles,” *IEEE Transactions on Vehicular Technology*, vol. 61, no. 7, pp. 2893–2900, Sep. 2012.

[28] L. Serrao, “A comparative analysis of energy management strategies for hybrid electric vehicles,” Ohio State University, 2009.

[29] N. Jalil, N. A. Kheir, and M. Salman, “A Rule-Based Energy Management Strategy for a Series Hybrid Vehicle,” in *American Control Conference*, 1997, no. June, pp. 689–693.

[30] E.-S. Koo, H.-D. Lee, S.-K. Sul, and J.-S. Kim, “Torque control strategy for a parallel hybrid vehicle using fuzzy logic,” in *Conference Record of 1998 IEEE Industry Applications Conference*, 1998, vol. 3, pp. 1715–1720.

[31] H.-D. Lee and S.-K. Sul, “Fuzzy-logic-based torque control strategy for parallel-type hybrid electric vehicle,” *IEEE Transactions on Industrial Electronics*, vol. 45, no. 4, pp. 625–632, 1998.

[32] N. J. Schouten, M. A. Salman, and N. A. Kheir, “Energy management strategies for parallel hybrid vehicles using fuzzy logic,” *Control Engineering Practice*, vol. 11, no. 2, pp. 171–177, Feb. 2003.

[33] F. R. Salmasi, “Control Strategies for Hybrid Electric Vehicles: Evolution, Classification, Comparison, and Future Trends,” *IEEE Transactions on Vehicular Technology*, vol. 56, no. 5, pp. 2393–2404, Sep. 2007.

[34] B. Glenn, G. Washington, and G. Rizzoni, “Operation and Control Strategies for Hybrid Electric Automobiles,” *SAE Paper*, 2000.

[35] A. Sciarretta and L. Guzzella, “Rule-based and optimal control strategies for energy management in parallel hybrid vehicles,” in *6th International Conference on Engines for Automobile (ICE 2003)*, 2003.

[36] D. F. Opila, X. Wang, R. McGee, J. A. Cook, and J. W. Grizzle, “Fundamental structural limitations of an industrial energy management controller architecture for hybrid vehicles,” in *ASME Dynamic Systems and Control Conference*, 2009.

[37] L. Pontryagin, V. Boltyanskii, R. Gamkrelidze, and E. Mishchenko, *Mathematical theory of optimal processes*. New York: Interscience Publishers, 1962.

[38] A. Chasse and A. Sciarretta, “Supervisory control of hybrid powertrains: An experimental benchmark of offline optimization and online energy management,” *Control Engineering Practice*, vol. 19, no. 11, pp. 1253–1265, Nov. 2011.

[39] L. Serrao, S. Onori, and G. Rizzoni, “ECMS as a realization of Pontryagin’s minimum principle for HEV control,” in *American Control Conference*, 2009, pp. 3964–3969.

[40] G. Paganelli, T. Guerra, S. Delprat, J. . Santin, M. Delhom, and E. Combes, “Simulation and assessment of power control strategies for a parallel hybrid car,” in *Proceedings of the Institution of Mechanical Engineers, Part D: Journal of Automobile Engineering*, 2000, pp. 705–717.

[41] A. Sciarretta, L. Guzzella, and C. H. Onder, “On the power split control of parallel hybrid vehicles: from global optimization towards real-time control,” *Automatisierungstechnik*, vol. 51, no. 5, pp. 195–203, 2003.

[42] A. Sciarretta, L. Guzzella, and M. Back, “A real-time optimal control strategy for parallel hybrid vehicles with on-board estimation of the control parameters,” in *IFAC Symposium on Advances in Automotive Control*, 2004, pp. 19–23.

[43] D. Bertsekas, *Dynamic programming and optimal control*, 3rd editio. Athena Scientific, 2005.

[44] R. Bellman, *Dynamic Programming*. Princeton University Press, 1957.

[45] A. Brahma, Y. Guezennec, and G. Rizzoni, “Optimal energy management in series hybrid electric vehicles,” in *Proceedings of the 2000 American Control Conference*, 2000, vol. 1, no. 6, pp. 60–64.

[46] L. V. Pérez, G. R. Bossio, D. Moitre, and G. O. García, “Optimization of power management in an hybrid electric vehicle using Dynamic Programming,” *Mathematics and Computers in Simulation*, vol. 73, no. 1–4, pp. 244–254, Nov. 2006.

[47] C.-C. Lin, H. Peng, J. W. Grizzle, and J.-M. Kang, “Power management strategy for a parallel hybrid electric truck,” in *Control Systems Technology , IEEE Transactions on*, 2003, vol. 11, no. 6, pp. 839–849.

[48] H.-J. Yoon and S.-J. Lee, “An optimized control strategy for parallel hybrid electric vehicle,” *SAE transactions*, vol. 112, no. 7, pp. 579–586, 2003.

[49] G. Paganelli, G. Ercole, A. Brahma, Y. Guezennec, and G. Rizzoni, “General supervisory control policy for the energy optimization of charge-sustaining hybrid electric vehicles,” *JSAE review*, vol. 22, no. 4, pp. 511–518, Oct. 2001.

[50] J. Won, R. Langari, and M. Ehsani, “An energy management and charge sustaining strategy for a parallel hybrid vehicle with CVT,” *Control Systems Technology , IEEE Transactions on*, vol. 13, no. 2, pp. 313–320, Mar. 2005.

[51] S. Jeon, S. Jo, Y. Park, and J. Lee, “Multi-mode driving control of a parallel hybrid electric vehicle using driving pattern recognition,” *ASME Journal of dynamic systems, measurement, and control*, vol. 124, no. 1, pp. 141–149, 2002.

[52] M. Koot, J. T. B. A. Kessels, B. de Jager, W. P. M. H. Heemels, P. P. J. Van den Bosch, and M. Steinbuch, “Energy Management Strategies for Vehicular Electric Power Systems,” *IEEE Transactions on Vehicular Technology*, vol. 54, no. 3, pp. 771–782, May 2005.

[53] C. Musardo, G. Rizzoni, and B. Staccia, “A-ECMS: An adaptive algorithm for hybrid electric vehicle energy management,” in *44th IEEE Conference on Decision and Control, 2005 European Control Conference*, 2005, vol. 11, no. 4–5, pp. 1816–1823.

[54] A. Sciarretta and L. Guzzella, “Control of hybrid electric vehicles,” *IEEE Control Systems Magazine*, vol. 27, no. 2, pp. 60–70, Apr. 2007.

[55] A. Sciarretta, M. Back, and L. Guzzella, “Optimal Control of Parallel Hybrid Electric Vehicles,” *IEEE Transactions on Control Systems Technology*, vol. 12, no. 3, pp. 352–363, May 2004.

[56] S. Delprat, J. Lauber, T. M. Guerra, and J. Rimaux, “Control of a Parallel Hybrid Powertrain: Optimal Control,” *IEEE Transactions on Vehicular Technology*, vol. 53, no. 3, pp. 872–881, May 2004.

[57] L. Buie, M. Fry, P. Fussey, and C. Mitts, “An application of cost based power management control strategies to hybrid fuel cell vehicles,” *SAE Technical Paper*, 2004.

[58] E. D. Tate, J. W. Grizzle, and H. Peng, “Shortest path stochastic control for hybrid electric vehicles,” *International Journal of Robust and Nonlinear Control*, vol. 18, no. 14, pp. 1409–1429, Sep. 2008.

[59] R. Howard, *Dynamic Programming and Markov Processes*. Technology Press of Massachusetts Institute of Technology, 1960.

[60] C. Lin, H. Peng, and J. Grizzle, “A stochastic control strategy for hybrid electric vehicles,” in *American Control Conference*, 2004, pp. 4710 – 4715.

[61] E. D. Tate and J. W. Grizzle, “SP-SDP for Fuel Consumption and Tailpipe Emissions Minimization in an EVT Hybrid,” *IEEE Transactions on Control Systems Technology*, vol. 18, no. 3, pp. 673–687, May 2010.

[62] D. F. Opila, X. Wang, R. McGee, R. B. Gillespie, J. A. Cook, and J. W. Grizzle, “An Energy Management Controller to Optimally Trade Off Fuel Economy and Drivability for Hybrid Vehicles,” *IEEE Transactions on Control Systems Technology*, vol. 20, no. 6, pp. 1490–1505, Nov. 2012.

[63] T. Leroy, J. Malaize, and G. Corde, “Towards real-time optimal energy management of HEV powertrains using Stochastic Dynamic Programming,” in *2012 IEEE Vehicle Power and Propulsion Conference*, 2012, pp. 383–388.

[64] Y. Wang and Z. Sun, “SDP-based extremum seeking energy management strategy for a power-split hybrid electric vehicle,” in *American Control Conference (ACC), 2012*, 2012, pp. 553 – 558.

[65] K. Aouchiche, F. Bonnans, G. Granato, and H. Zidani, “A stochastic dynamic principle for hybrid systems with execution delay and decision lags,” in *IEEE Conference on Decision and Control and European Control Conference*, 2011, pp. 6788–6793.

[66] L. Gavric, *Anti-vibration Technology, Automotive Acoustics and Engine Noise - Lecture at IFP School*. PSA Peugeot Citroën, 2012.

[67] T. Barlow, S. Latham, I. McCrae, and P. Boulter, *A reference book of driving cycles for use in the measurement of road vehicle emissions*. 2009.